UNIVERSIDADE D
COIMBRA

Natalia Sozza Bernardi

Evaluation of immuntoxicological properties of PCL and PCL/Glucan nanoparticles

Dissertação no âmbito do Mestrado em Biotecnologia Farmacêutica orientada pela Professora Doutora Olga Maria Fernandes Borges Ribeiro e co-orientada por Doutora Sandra Cristina Campos de Jesus e apresentada à Faculdade de Farmácia da Universidade de Coimbra.

Julho de 2019

EVALUATION OF IMMUNOTOXICOLOGICAL PROPERTIES OF PCL AND PCL/GLUCAN NANOPARTICLES

Natalia Sozza Bernardi

Dissertação de Mestrado em Biotecnologia Farmacêutica, orientada pela Professora Doutora Olga Maria Fernandes Borges Ribeiro e co-orientada por Doutora Sandra Cristina Campos de Jesus, e apresentada à Faculdade de Farmácia da Universidade de Coimbra

Julho 2019

The experimental work presented in this thesis was developed under the scientific supervision of Professor Doctor Olga Maria Fernandes Borges Ribeiro from the Pharmaceutical Technology Laboratory of Faculty of Pharmacy, University of Coimbra. This work was funded by FEDER funds through the Operational Programme Competitiveness Factors - COMPETE 2020 and national funds by FCT - Foundation for Science and Technology under the project PROSAFE/0001/2016 and POCI-01-0145-FEDER-030331 and strategic project POCI-01-0145-FEDER-007440.


COMPETE
2020

PORTUGAL
2020

UNIÃO EUROPEIA
Fundo Europeu
de Desenvolvimento Regional

FCT
Fundação para a Ciência e a Tecnologia
MINISTÉRIO DA CIÊNCIA, TECNOLOGIA E ENSINO SUPERIOR

NANOBIOMAT
www.gonanobiomat.eu

Acknowledgment

Com a conclusão desta etapa, gostaria de deixar aqui o meu agradecimento a todos aqueles que de alguma forma contribuíram para a realização deste trabalho.

À minha orientadora, Professora Doutora Olga Maria Fernandes Borges Ribeiro, pela oportunidade de realização deste trabalho no seu laboratório e a orientação e ensinamentos proporcionados e toda consideração e tempo disponibilizados.

Não posso deixar de agradecer também o grande apoio de todos do "Nanolab" a Alana, Jessica, João e Mariana que sempre se mostraram disponíveis a me ajudar e ensinar ao longo deste ano. E também, pela força e pelo carinho que sempre me prestaram ao longo de todo esta jornada. Obrigada pelo ambiente criativo e amigável e por todos os momentos que partilhámos dentro e fora do laboratório.

Agradeço em especial à Doutora Sandra, pelo desempenho dedicado a elaboração deste trabalho, pela ajuda e ideias, e por estimular o meu interesse pelo conhecimento e também por sua disponibilidade sempre. Foi sem dúvida um grande apoio, aqui lhe exprimo a minha gratidão.

Por último, mas não menos importante, gostaria de deixar um agradecimento a minha família, por sempre me apoiar em minhas decisões e por me darem a força necessária para a realização dos meus sonhos.

Enfim, quero demonstrar o meu agradecimento, a todos aqueles que, de um modo ou de outro, tornaram possível a realização deste trabalho.

Table of contents

List of abbreviations

APC	Antigen-presenting cell
BCA	Pierce™ Bicinchoninic acid
BSA	Bovine serum albumin
CMH	Cyanmethemoglobin
CR	Complement receptor
DLS	Dynamic light scattering
DMEM	Dulbecco's Modified Eagle Medium
DMSO	Dimethyl sulfoxide
dTBH	diluted Total Blood Hemoglobin
ELISA	Enzyme-linked immunosorbent assay
EPR	Enhanced permeability and retention
FBS	Fetal bovine serum
FITC	Fluorescein isothiocyanate
HeLa	Human cervix carcinoma
IL	Interleukin
LAL	Limulus amebocyte lysate
LC	Loading capacity
LE	Loading efficacy
LPS	Lipopolysaccharidae
MFI	Mean fluorescence intensity
MTT	3-(4,5-dimethylthiazol-2-yl)-2,5-diphenyltetrazolium bromide
mV	Millivolts
Mw	Molecular weight
NaNO2	Sodium nitrite
NaOH	Sodium hydroxide
NC	Negative control
nm	Nanometer
NO	Nitric oxide
NP	Nanoparticle
PAMP	Pathogen-associated molecular pattern
PBMC	Peripheral blood mononuclear cell
PBS	Phosphate buffer saline

PC	Positive Control
PCL	Polycaprolactone
PDI	Polydispersity index
PI	Propidium iodide
PRR	Pattern recognition receptor
PVA	Polynynyl alcohol
ROS	Oxygen reactive species
RPMI	Roswell Park Memorial Institute cell culture medium
SEM	Standard error of the mean
TEM	Transmission electron microscopy
TFA	Trifluoroacetic acid
THF	Tetrahydrofuran
TLR	Toll-like receptor
TNF	Tumor necrosis factor
VC	Vehicle control (filtrate)
ZP	Zeta Potential

Abstract

Nanotechnology has been used to develop nanomedicines to facilitate the delivery of therapeutic agents. The nanomedicines have demonstrated extraordinary potential due to their properties to improve the therapeutic impact of the drug by diverse mechanisms such as increasing its retention time on target tissues or allowing the controlled release of the drug. Polycaprolactone is a biodegradable polyester that has biocompatibility and low toxicity and a capacity of blending with other polymers. Due to its characteristics, it has been used for a large set of different applications. Curdlan is a neutral polymer consisting of β-1,3-linked glucose residues. It is extracted from *Alcaligenes faecalis* and has many applications in the medical field based on its physicochemical and immunomodulatory properties. Taking this into account, the main objective of this work was to study the *in vitro* immunotoxicity properties of PCL and PCL/Glucan nanoparticles for that secondary objectives were defined.

First the development and characterization of PCL/Glucan and PCL nanoparticles as delivery systems were performed. For that, the PCL NPs were produced according to the optimized PCL/Glucan NPs through nanoprecipitation technique. The nanoparticles have a similar size, 180 nm for PCL/Glucan and 170 nm for PCL, with an almost neutral zeta potentials (-1.59 and - 2.54 mV, respectively) and round shape morphology. In terms of stability, PCL/Glucan and PCL NPs showed great stability up to 3 weeks at room temperature whereas in the cell culture medium the NPs demonstrate a decrease in size in DMEM however remains similar in RPMI. Regarding their capacity of carrying a model protein, among the model proteins tested, myoglobin showed the higher loading efficacy.

Immunotoxicity tests were done in a macrophage cell line, RAW 264.7 and in human primary cells (PBMCs) to evaluate the NPs interaction with immune system cells and also the hemocompatibility of the delivery system was assessed by hemolysis. The two nanoparticles showed few differences. For cell viability tested in RAW 264.7, no statistical difference were observed for both NPs, while in PBMCs the PCL/Glucan NPs revealed to be less cytotoxic than PCL NPs however less hemocompatible when tested in the blood components.

In relation to the immunomodulatory effects, PCL/Glucan and PCL NPs did not induce ROS or NO production, nevertheless in higher concentration the PCL/Glucan showed inhibitory effect of the NO production. Regarding cytokines production, the results are not absolutely conclusive, apparently PCL induced more IL-6 production than PCL/Glucan NPs however, both showed similar ability to induce the TNF-α. Finally, the NPs uptake studies showed that

the presence of glucan in the PCL NPs increases its ability as a delivery system for proteins and also were more efficiently internalized by PBMCs.

Overall, in this work, we reported for the first time, the successful production and characterization of PCL/Glucan NPs. The association of a second polymer (glucan) to PCL NPs resulted in a blend nanoparticle with different cytotoxicity profile and immunomodulatory properties. Both NPs showed to have a good capacity to adsorb therapeutic proteins and to deliver them to immune cells. Therefore, PCL and PCL/Glucan NPs are promising nanomedicines that can be tested to deliver antigens and other therapeutic proteins.

Keywords: PCL; Glucan; nanoparticles; polymeric delivery systems; immunotoxicity.

Resumo

A nanotecnologia tem sido utilizada para o desenvolvimento de nanomedicamentos afim de facilitar a entrega de agentes terapêuticos. Os nanomedicamentos têm demonstrado extraordinário potencial devido às suas propriedades em melhorar a eficácia terapêutica do fármaco por diversos mecanismos, como o aumento do tempo de retenção em tecidos alvos ou permitindo a sua libertação controlada.

A Policaprolactona é um poliéster biodegradável que possui biocompatibilidade e baixa toxicidade e também possui a capacidade de se ligar a outros polímeros. Devido a estas características tem sido utilizado em várias aplicações. Curdlan é um polímero neutro que consiste em resíduos de glicose com ligações β-1,3. É extraído da bactéria não-patogénica *Alcaligenes faecalis* e possui muitas aplicações baseadas nas suas propriedades físico-químicas e imunomoduladoras. Desta forma, o objetivo deste trabalho foi estudar *in vitro* a imunotoxicidade das nanopartículas de PCL/Glucano e PCL, para isso objetivos secundários foram definidos.

Desenvolver um método de preparação e caracterizar as nanopartículas de PCL/Glucano e PCL como sistemas de entrega de fármacos. Para isso, as NPs de PCL e PCL/Glucano foram produzidas pelo método de nanoprecipitação. As nanopartículas possuem tamanhos semelhantes, 180 nm para PCL/Glucano e 170 nm para PCL, com potencial zeta quase neutro (-1.59 mV e - 2.54 mV, respectivamente) e apresentaram forma arredondada. Em termos de estabilidade, PCL/Glucano e PCL NPs mostraram grande estabilidade durante as 3 semanas de ensaio à temperatura ambiente. Por outro lado, em meio de cultura de células as NPs apresentaram uma diminuição no seu tamanho em DMEM, porém permanecem similares em RPMI. Em relação à capacidade de adsorver proteínas à sua superficie, entre as proteínas testadas, a mioglobina mostrou melhor eficácia de adsorção.

Os testes de imunotoxicidade foram feitos em linha celular de macrófagos, RAW 264.7 e em células primárias humanas (PBMC), a fim de se avaliar a interação das NPs com as células do sistema imunitário assim como a hemocompatibilidade do sistema de entrega através do teste da hemólise. Os dois tipos de nanopartículas mostraram algumas diferenças. Para viabilidade celular em RAW 264.7, não foram observadas diferenças com significado estatístico entre as NPs, enquanto que nas PBMCs as NPs de PCL/Glucano se mostraram menos citotóxicas que as de PCL, porém foram menos hemocompatíveis quando testadas nos componentes sanguíneos.

Em relação aos efeitos imunomoduladores, as diferentes NPs não induziram a produção de ROS e NO, porém na maior concentração testada, as nanopartículas PCL/Glucano apresentaram efeito inibitório na produção de NO. Em relação à produção de citocinas, os resultados não são totalmente conclusivos, aparentemente as NPs de PCL induziram uma maior produção de IL-6 que as PCL/Glucano, no entanto, ambas mostraram indução semelhante de TNF-α. Finalmente, estudos de internalização mostraram que a presença de glucano nas PCL NPs aumenta a sua capacidade como sistema de entrega de proteínas e também aumenta a sua internalização em PBMCs.

No geral, neste trabalho, nós demonstramos pela primeira vez, a produção e caracterização de nanopartículas de PCL/Glucano. A associação de um segundo polímero (glucano) às PCL NPs resultou em nanopartículas com perfil citotoxicológico e propriedades imunomodulatórias diferentes do perfil encontrado para as nanopartículas da PCL. Ambas as nanopartículas mostraram uma boa capacidade para adsorver proteínas e fazer a sua entrega às células do sistema imunitário. Assim sendo, podemos afirmar que as nanopartículas de PCL/Glucano e PCL são nanomedicamentos promissores que podem ser testados na entrega de antigéneos e outras proteínas terapêuticas.

Palavras-chave: PCL; Glucano; nanopartículas, Sistema polimérico de entrega, imunotoxicidade.

Chapter 1
Introduction

Chapter I - Introduction

1.1 Nanotechnology

Nanotechnology is a thriving area in the materials science whose multidisciplinary applications comprise distinct fields, as for example computer and biomedical sciences, with a common purpose to improve modern society lifestyles (Porter e Youtie, 2009). Nanoparticles have demonstrated extraordinary potential due to their unique physicochemical properties. In consequence of particular characteristics, such as small size and large surface area, nanoparticles are able to overcome some limitations found in conventional therapeutic medicines and diagnostic agents (Cheng *et al.*, 2015).

The polymeric nanoparticles are made from natural or synthetic polymers (Pawar *et al.*, 2016) and have been attracted considerable interest over the last few years due to their unique and interesting properties (Farokhzad e Langer, 2009). As asserted by different authors, these nanobiomaterials show potential for a wide range of applications in the field of the health sciences, such as diagnostics, medical devices or drug delivery systems (Crucho e Barros, 2017).

The methods used to load the drug onto the nanoparticles include physical adsorption, encapsulation after the formation of the particles, drug entrapment during the preparation and chemical binding of drug molecules on the surface of polymeric nanoparticles (Bhowmik, Khan e Ghosh, 2015). The drug release kinetic and its characteristics depend to a large extent on the drug trapping method polymer chemical structure (Juillerat-Jeanneret, 2007). Thus, the intention of the surface functionalization of polymer is to improve the drug delivery capability. These systems offer low toxicity, high loading capacity, being able to encapsulate both hydrophilic and hydrophobic substances, improves stability of the drug by protecting it from degradation and by modifying its clearance. They offer the possibility to administer the formulation by various routes of administration, including oral and present target capability, for instance to solid tumors due to the enhanced permeability and retention (EPR) effect (Pawar *et al.*, 2016). As drug loaded particles, besides biocompatibility, one of the most important requirements is that the matrix material should be biodegraded within a suitable period which is compatible with the drug release rate (Koleske, 2014). Additionally, the use of nanoparticles as vehicles for drugs may have the ability to enhance the specificity of drug delivery and decreases the minimum amount of drug necessary for attaining and maintaining the therapeutic effect, thereby reducing the eventual toxicity. This is especially important in

the case of highly toxic and short-lived chemo- and radio-therapeutic agents (Jong, De e Borm, 2008).

In addition, nanoparticles based on conjugated polymers are emerging as multifunctional nanoscale materials that promise great potential to offer exciting opportunities in these areas (e.g., drug delivery systems, scaffolds, vaccines). These conjugated polymer nanoparticles are desirable for a number of reasons. Their properties can be tuned easily for desired applications through the choice of the polymers and surface modification. Additionally, their easy synthesis, less toxicity and more biocompatibility compared to the existing inorganic nanoparticles further make these materials highly attractive (Tuncel e Demir, 2010).

In this manner, the polymers that we chose to work were polycaprolactone (PCL) and glucan. PCL is a polymer with low toxicity, hydrophobic and that easily blend to other polymers while glucan is one of the most known polysaccharides for its immunomodulatory effect. The purpose of introducing the glucan into PCL nanoparticles is to use its ability to bind to the dectin-1 receptor, very present in the cells of the immune system, and thereby to develop a polymeric nanoparticulate system capable of vectorizing the drug specifically.

1.2 Polycaprolactone

PCL is synthetic biodegradable polyester that is produced from crude oil. It is a hydrophobic, semi-crystalline polymer; its crystallinity tends to decrease with increasing molecular weight, which generally vary from 3 000 g/mol to 90 000 g/mol. PCL has a glass transition temperature of -60 °C and melting point ranging between 59 and 64 °C, depending upon its crystalline nature (Sinha *et al*., a2004). PCL is known for its slow biodegradation, so it is most suitable for long-term delivery extending over a period of more than 1 year (Sinha *et al*., 2004) and with appropriate blending the delivery can be increased/decreased as desired.

An important characteristic of PCL is its capacity to blend with other polymers; this depends on the ratio chosen and is generally used to have better control over the permeability of the delivery systems. Copolymers (block and random) of PCL can be formed using many monomers, e.g., ethylene oxide, polyvinylchloride, chloroprene, polyethylene glycol, polystyrene, diisocyanates, tetrahydrofuran (THF), among others (Luciani *et al.,* 2008). This ability can affect the degradation kinetics, facilitating tailoring to fulfil desired release profiles (Ávila *et al*., 2017). It should be noted, that several studies exist which exploit the positive properties of PCL and blend these with other materials producing superior copolymers and composites, which may have desirable properties for use in mechanically challenging applications where a more resilient material is needed (Woodruff e Hutmacher, 2010).

Because of its excellent biocompatibility, flexibility and thermoplasticity, PCL and its copolymers have been proposed for use in various biomedical applications (Wu e Liao, 2012) and have been recently approved by Food and Drug Administration (FDA), following this approval, several commercially successful applications have emerged.

PCL has a wide range of application area, such as food packaging, medical implant (Mohamed e Yusoh, 2015), different medical devices application, such as: suture (Dash e Konkimalla, 2012), wound dressings (involved in subdermal delivery of l-methadone from PCL microspheres) (Woodruff e Hutmacher, 2010). It has been utilized as an ultra-thin film for dressing cutaneous wounds (Ng *et al.*, 2007) and also as a release vehicle for the chemical antiseptic chlorohexidine (Woodruff e Hutmacher, 2010). In tissue engineering, is used to repair or replace portions of whole tissues (e.g., blood vessels and bladder) bone and cartilage (tendon and ligament). It is also is associated with used in scaffold fabrication, (Mohamed e Yusoh, 2015) and subdermal contraceptive implants (Woodruff e Hutmacher, 2010).

Due to a high permeability to many drugs and excellent biocompatibility the PCL is also suitable for controlled drug delivery, (Azimi *et al.*, 2018) once the drug-releasing property is able to be managed (Puppi *et al.*, 2012). Various polymeric devices like microspheres, microcapsules, nanoparticles, pellets, implants, and films have been fabricated using this polymer (Azimi *et al.*, 2018).

1.2.1 Production methods for PCL nanoparticles

Different methods have been reported in the literature for the preparation of PCL nanoparticles. Table 1 shows some examples of the production method techniques and the characteristics of the nanoparticle formed.

The simplest method for the preparation of polymeric nanoparticles containing a drug or blend polymers is known as nanoprecipitation method. In Table 1, the first examples utilized this methodology and it is possible to observe that for nanoparticle formation in nanometer size was used different surfactants. In addition, the presence of a stabilizer (normally a surfactant or emulsifier) is very important to avoid the formation of aggregates and to impart stability to nanoparticles during the nanoprecipitation technique (Chin, Azman e Pang, 2014).

In the nanoprecipitation method, the nanoparticles are obtained and form a colloidal suspension, the polymer phase is slowly added to the aqueous phase under moderate stirring. The formation of the NPs is instantaneous and needs only one-step, so it has the advantage of being a rapid and easy operation. The key parameters in the preparation method, such as organic phase injection rate, aqueous phase agitation rate, organic phase/aqueous phase ratio,

polymer concentration and composition of the phases (Mora-Huertas, Fessi e Elaissari, 2010) have a great influence on the characteristics (critical quality attributes) of the particles.

The experimental design developed to obtain PCL nanoparticles showed that the molecular weight (Mw) of the polymer and the type of surfactant used were relevant factors on the average diameter of the nanoparticles obtained, where with the higher Mw the bigger became the nanoparticles (Colmenares-Roldan *et al.*, 2018).

Moreover, PCL microspheres can be prepared by several different methods, including the solvent evaporation method. This method was described by diverse authors, like (Singh *et al.*, 2013), (Mendes *et.al.,* 2011) and (Dhanka, Shetty e Srivastava, 2017). The method is based on the emulsification of the organic solution of the polymer into a water phase, followed by organic solvent evaporation (Wang *et al.*, 2013). Additionally, the double emulsion technique and spray drying techniques are also common techniques for producing PCL microspheres from linear polymers and have been studied by Singh and co-workers (Singh *et al.*, 2013).

Drug release rates from PCL nanoparticles depends on type of formulation, method of preparation, PCL content, size and percent of drug loaded in the nanoparticles (Sinha *et al.*, 2004). Table 1 shows different technics to prepare the particles and the size/ zeta potential results that were obtained, which are probably related to the characteristics of the encapsulated drug and how it behaves concerning possible interaction with the polymer (Sathyamoorthy *et al.*, 2017) (Maaz *et al.*, 2015) (Alex *et al.*, 2016).

Therefore, a large number of block copolymers with different compositions for the delivery of chemotherapeutic agents, genes and molecular-targeted drugs have been developed and the total number is still growing (Alexis *et al.*, 2008). In Table 2, is possible to observe several examples using more than one polymer in order to produce conjugated nanoparticles. The production method is variable and an interesting point is that even using a nanoprecipitation technic, is not easy to produce nanoparticles smaller than 200 nm even for a polymer with lower molecular weight, as is possible to observe in the studies published elsewhere (Vásquez Marcano *et al.*, 2018) (Jesus *et al.*, 2018).

A study conducted by Li and co-workers, tested a production of core-shell nanoparticles using di-block copolymers and tri-block copolymers of PEGylated PCL with different PEG and PCL compositions. The configuration and composition of the copolymers were important for the properties and functions of the nanoparticles. Nanoparticles prepared from the di-block copolymer with a particle size around 300 nm and the hydrophobic composition about 80 % resulted as the most effective drug carrier (Li *et al.*, 2009).

Table 1: Methods of producing PCL nanoparticles and their characterization

Nanoparticles	Production method	Polymer	Surfactant/ emulsifier	Size (nm)	PDI	Zeta potential (mV)	Observations	References
PCL NP	Nanoprecipitation method	Mw 14000 g·mol^{-1}	PVA and Tween 80	175 to 297		-6.86 to -7.07		(Badri *et al.*, 2017)
PCL NP	Nanoprecipitation method	Mw 80000 g·mol^{-1}	Pluronic ® F-68	163.8 ± 1.65	0.07 ± 0.01	-9.3 ± 1.07	PCL concentration: 0.2 %	(Tavares *et al.*, 2017)
				184.3 ± 2.07	0.05 ± 0.01	-16.4 ± 0.85	PCL concentration: 0.4 %	
				206.3 ± 1.30	0.07 ± 0.01	-15.8 ± 0.66	PCL concentration: 0.6 %	
PCL NP	Nanoprecipitation method	Viscosity1.07g/dl	PVA	268	0.03	-9.10		(Singh *et al.*, 2013)
PCL NP	Nanoprecipitation method	Mw 14000 g·mol^{-1}	Tween 80	88.1	0.21	-		(Colmenares-Roldan *et al.*, 2018)
		Mw 45000 g·mol^{-1}		97.5	0.19	-		
		Mw 80000 g·mol^{-1}		135.2	0.18	-		
PCL nanosphere	Double emulsion solvent evaporation technique	Mw 14000 g·mol^{-1}	PVA	812 ± 64	0.34 ± 0.03	-		(Singh *et al.*, 2013)
PCL microsphere	Emulsion/solvent evaporation method	Mw 70000 - 90000 g·mol^{-1}	na	33.97 µm	-	-		(Mendes *et al*, 2011)
PCL microspheres	Evaporation method	Mw 14000 g·mol^{-1}	na	24.09 µm	-	-	Organic phase was added by syringe	(Dhanka, Shetty e Srivastava, 2017)
Paclitaxel loaded PCL NPs	Emulsion-solvent evaporation technique	Mw 14000 g·mol^{-1}	PVA	215.6	-	-7.52		(Sathyamoorthy *et al.*, 2017)
Gatifloxacin loaded PCL NPs	Nanoprecipitation method	Mw 45000 g·mol^{-1}	PVA	184.6 ± 1.27	0.19	-30.1 ± 2.78		(Maaz *et al.*, 2015)
Carboplatin loaded PCL NPs	Double emulsion solvent evaporation technique	Mw 65000 g·mol^{-1}	PVA	311.6 ± 4.7	0.21 ± 0.03	16.3 ± 3.7		(Alex *et al.*, 2016)

Table 2: Methods of producing blend nanoparticles containing PCL and their characterization

Nanoparticles	Production method	Polymer	Surfactant/ emulsifier	Size (nm)	PDI	Zeta potential (mV)	Observations	References
PCL/Chitosan NPs	Nanoprecipitation method	PCL: Mw 14000 g·mol^{-1} Chitosan: 75 - 85% DD	Polysorbate 80/ Tween 80	318 ± 35	0.24 ± 0.02	36.2 ± 1.8		(Vásquez Marcano *et al.*, 2018)
PCL/Chitosan NPs	Nanoprecipitation technique	PCL Mw 14000 g·mol^{-1} Chitosan 95% DD, 8 cP viscosity	Tween 80	539.1 ± 113.7	0.25 ± 0.04	21.7 ± 0.5		(Jesus *et al.*, 2018)
PCL/Chitosan NPs	Double emulsion method	PCL: Mw 14000 g·mol^{-1} Chitosan: ~81% DD	PVA	512.8 ± 13.8	0.41 ± 0.04	30.9 ± 1.3		(Prado *et al.*, 2017)
mePEG-PCL NPs	Nanoprecipitation	na	na	154	0.17	-		(Danafar e Schumacher, 2016)
Di-block copolymer (mePEG-PCL)	Single emulsion and solvent evaporation method	mePEG: *M*w 2 g·mol^{-1} PEG: *M*w 6 g·mol^{-1}	PVA	190.3 ± 1.7	0.17 ± 0.04	−0.04 ± 0.04	The nomenclature of these copolymers was referred to the feed ratio.	(Li *et al.*, 2009)
				285.8 ± 4.2	0.05 ± 0.08	−11.47 ± 0.64		
Tri-block copolymer (PCL-PEG-PCL)				333.7 ± 4.2	0.2 ± 0.04	−12.88 ± 1.65		
				444.3 ± 7.0	0.21 ± 0.01	−7.85 ± 1.40		

Abbreviations: DD - deacetylation; mePEG -Methoxypoly(ethylene glycol); Mw - Molecular weight; PEG - Polyethylene glycol and PVA - polyvinyl alcohol

1.3 β-Glucan

Natural polysaccharides are used in a variety of applications due to their unique properties. One interesting class of polysaccharides comprises 1,3-β-glucans, which are glucopyranose polysaccharides with (1,3) glycosidic linkages and varying degree of (1,6) branches.

1,3-β-glucans can form single or triple helical structures, which can be used to prepare resilient gels by applying heat and humidity (Lehtovaara, Verma e Gu, 2012). The properties of these gels are governed by the structure of the polysaccharide, which is determined by the degree of branching and the molecular weight. Their properties can also be modified by covalently attaching functional units to the polysaccharide backbone (Lehtovaara, Verma e Gu, 2012).

1,3-β-glucans are derived from various natural sources, such as microbial (Sutherland, 2001), some cereals grains (oat and barley) and are abundantly distributed in the cell walls of fungi and yeast which differs each other by the linkages between glucose units.

Curdlan is a linear neutral polymer composed only by 1,3-β-glucosidic linkages and it is produced by *Agrobacterium* formerly known as *Alcaligenes faecalis* (McIntosh, Stone e Stanisich, 2005). This glucan has been a good model for the study of 1,3-β-glucan helical structures as it lacks the interference of periodic branching (Lehtovaara, Verma e Gu, 2012).

It is associated to curdlan a variety of applications and one that it is highlighted is its unusual gelling property. This is because depending on the temperature, curdlan can form two types of gels, if the temperature is high (above 80 °C) it can form a high-set irreversible gel, while in lower temperatures it forms a low-set reversible gel (Zhan, Lin e Zhang, 2012).

The β-glucan is water insoluble because of the extensive intra and intermolecular hydrogen bonds, however it is quickly solubilized in dimethyl sulfoxide (DMSO), formic acid and in alkaline solutions as in NaOH (Cai e Zhang, 2017) when a triple helix structure, is unstructured to single strands (Hwang *et al.*, 2018).

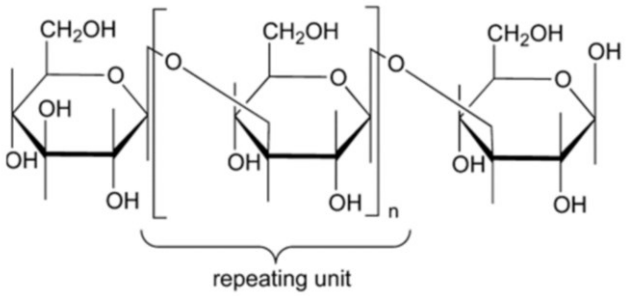

Figure 1: Chemical structure of curdlan, representing its 1,3-β-glucosidic linkages (Adapted from (Zhang e Edgar, 2014).

Curdlan is therefore widely used in food industry, been approved as a food additive by the FDA (Zhan, Lin e Zhang, 2012). One example was reported by Wang and co-workers using curdlan to improve the firmness and the texture of noodles (Wang *et al.*, 2010). More recently, it was also discovered biomedical applications namely in the field of immunology as an anti-carcinogenic (Zhou *et al.*, 2017) and in wound healing (Kim *et al.*, 2012). The interaction of 1,3-β-glucans with immune cells generates a potent pro-inflammatory effect consisting of stimulation in the production of cytokines, increased phagocyte and lymphocyte proliferation, oxidative burst, and phagocytosis against opsonized tissues (Lehtovaara, Verma e Gu, 2012).

Furthermore, curdlan is also known for being a biological response modifier, which means it is able to enhance or restore the immune system (McIntosh, Stone e Stanisich, 2005). This ability of curdlan is due to the fact that this polymer behaves as pathogen-associated molecular patterns (PAMP), which means that when it enters in the human body it is recognised by receptors of the innate immune system. The receptors for β-Glucans recognition are mainly the toll-like receptor 2 (TLR-2), complement receptor 3 (CR3) and dectin-1 (Akramien *et al.*, 2007).

Toll-like receptors (TLRs) are a group of structurally related molecules that are expressed on the cell surface and serve as pattern recognition receptors (PRRs) to detect the presence of microbial infection (Song, 2012). Toll-like receptors can trigger broad inflammatory responses that elicit rapid innate immunity and promote activation of the adaptive immune reaction (Zhang, Kim e Huang, 2018) whereas CR3 is a PRRs recognizes a large number of other ligands, among them β-glucan. Dectin-1 is a C-type lectin-like carbohydrate recognition domain, located on the macrophage surface and has special involvement in the detection and phagocytosis of fungal pathogens. It is also a transmembrane protein with many particular functions, e.g., binding of a fungal PAMP, uptake and killing of invading cells, induction of the production of cytokines and chemokines (Novak e Vetvicka, 2008).

After the binding of the ligand to this receptor, a series of reactions occurs to try to eliminate the foreign material. It can induce phagocytosis with the consequent production of cytokines as IL-2, IL-6, IL-10, IL- 12 and TNF-α, it can also release arachidonic acid that is known as capable of initiating inflammation and it can triggers the formation of reactive oxygen species (Sun e Zhao, 2007).

In short, all these receptors came together in what is thought to be the right mechanism for the incorporation of curdlan, which is the polymer captured by macrophages through dectin-1 and toll-like receptor 2 and then the large molecule is fragmented in small β-Glucans that

are released and taken up by the circulating dendritic cells through CR3. In this way, we can have the stimulation of both innate and adaptive immune response (Chan, Chan e Sze, 2009). Apart from this, the glucan has been encouraged in the application as a drug delivery system, where it can be used as gels, nanoparticles, microparticles or complexes (Lehtovaara, Verma e Gu, 2012). The combined pharmacological and structure-forming capabilities may be utilized simultaneously in a single system, such as gel encapsulation of indomethacin, prednisolone, and salbutamol sulphate (Lehtovaara, Verma e Gu, 2012). In Curdlan gel suppositories has been the hallmark example of Curdlan application in this area. The obtaining of tablets from dry mixtures of Curdlan/theophylline obtained by spray drying was also reported. The authors of this study demonstrated good pharmacokinetic (Kanke, Katayama e Nakamura, 1995) results performed with the theophylline tablets. Moreover, nanoparticle drug delivery approaches have been successfully used with the synthesis of solid lipid nanoparticles consisting of curdlan coated cacao butter particles. The stabilized nanoparticles were loaded with verapamil, which was quickly released within 12 h due to its high solubility in the lipid core (Kim, Na e Choi, 2005).

In addition of using curdlan as it is, nowadays there is an interest in modifying it to make it more functional like the project described by Zhou and co-workers, where they used carboxymethyl curdlan as an hydrophilic carrier to doxorubicin, an anti-carcinogenic drug (Zhou *et al.*, 2017).

1.3.1 Production methods for glucan nanoparticles

Different methods have been reported in the literature for the preparation of glucan nanoparticles. The nanoprecipitation method is more common and was observed previously with the PCL particles. In Table 3, is possible to observe that some author used this methodology to produce glucan NPs.

The glucan in a triple helix structure that can be unstructured to single strands by heat using different solvents. This methodology was used by (Hwang *et al.*, 2018) where they sliced the glucan into low molecular weight using various concentrations of Trifluoroacetic acid (TFA). The same procedure was adopted by (Jia *et al.*, 2015) where the glucan was denatured into single chains to produce the NPs and then loaded it with selenium.

The glucan nanoparticles have been used for drug delivery by (Subedi, Kang e Choi, 2009) (Nasrollahi *et al.*, 2015) loading it with doxorubicin, an anticancer drug. Both studies evaluated the influence on the polymer and drug concentration and were observed that the increase in polymer concentration significantly increases the particle size, even using different production

methods. Another author (Upadhyay *et al.*, 2017), loaded Rifabutin, an antibiotic used to treat tuberculosis, into glucan microparticles and the alkaline-acid method was used, which consists of alkaline extraction followed by acid precipitation.

Zhang and co-workers used a different methodology, the ionic gelation method that consists of the interaction between the positively charged amine group and negatively charged groups in the aqueous environment to form the nanoparticles. In the study, the bovine serum albumin (BSA) protein was loaded to the microparticles (Zhang *et al.*, 2014).

The dialysis process is also used to prepare glucan nanoparticles; this methodology consists of a simple surfactant removal route by sedimentation-redispersion while retaining the original colloidal state. In this study was observed nanoparticle sizes ranging from 132 to 487 nm (Wu *et al.*, 2013).

Table 3: Different nanoparticle characterization found in the literature for glucan regarding production method

Nanoparticles	Production method	Source of the Polymer	Size (nm)	PDI	Zeta potential (mV)	Observations	References
Glucan NPs	Nanoprecipitation Method	*Pythium aphanidermat*	60	0.32	-35.2		(Anusuya e Sathiyabama, 2014)
1,3 β-Glucan NPs	Dialysis process	*Saccharomyces cerevisiae*	132 - 487	0.09 - 0.34	-		(Wu *et al.*, 2013)
Rifabutin loaded Glucan microparticles	Alkaline and acidic extraction method	*Saccharomyces cerevisiae*	2.9 - 6.1 µm	-	-20.7		(Upadhyay *et al.*, 2017)
TFA-treated Glucan NPs	Nanoprecipitation method	*Saccharomyces cerevisiae*	900 ± 200 300 ± 50	-	-	Different concentrations: (TFA 1:1) (TFA 1:4)	(Hwang *et al.*, 2018)
Solid lipid nanoparticles (SLN) loaded with doxorubicin and curdlan	Solvent emulsification-diffusion method	*Alcaligenes faecalis*	230 280 350	-	-	Increasing curdlan concentration significantly increases the particle size	(Subedi, Kang e Choi, 2009)
BSA-glucan microparticles	Ionic gelation method	*Saccharomyces cerevisiae*	2 - 4 µm	-	-		(Zhang *et al.*, 2014)
Glucan - PLGA NPs	Emulsion evaporation	*Alcaligenes faecalis*	281 ± 7	0.19 ± 0.03	-28.6 ± 2		(Tukulula *et al.*, 2018)
Dox using 1,3 β- glucan: Glu/Dox-1	Nanoprecipitation method	*Alcaligenes faecalis*	342 ± 52	0.2 ± 0.03	-	Dox with ratios of 5%, 10%, 20% and 25%	(Nasrollahi *et al.*, 2015)
Glu/Dox-2			370 ± 27	0.2 ± 0.03			
Glu/Dox-3			391 ± 23	0.3 ± 0.02			
Selenium nanoparticles with glucan with triple helical conformation known as Lentinan (t-LNT)	Nanoprecipitation method	*Lentinus edodes*	52	-	-2	t-LNT	(Jia *et al.*, 2015)
			44		-2	Se/s-LNT	
			33		-6	Se/t-LNT	
Superparamagnetic iron oxide nanoparticles coated glucan	Alkaline co-precipitation	β-glucan	51.8 ± 26.3	-	-11.42 ± 3.8		(Vu-Quang *et al.*, 2012)

Abbreviations: BSA - Bovine serum albumin; Dox- Doxorubicin; TFA - Trifluoroacetic acid; Se/s - single chain and Se/t – triple chain.

1.4 Nanoparticle toxicity

Despite remarkable advances in pharmaceutical and medical fields, the toxicity and human health risks from exposure to nanomaterials are attracting considerable and increasing concern worldwide (Agarwal *et al*., 2013). Due to the complexity of nanomaterials, current studies have shown different point of views on their use and safety. It has become clear that the toxicity of nanoparticles is largely determined by their physical and chemical characteristics, such as their size, shape, specific surface area, surface charge, catalytic activity, and the presence or absence of a shell and active groups on the surface (Sukhanova *et al*., 2018).

Therefore, a detailed assessment of nanoparticles through toxicological studies is crucial to assure their biological safety. However, there are still few reliable reports on toxicological research of polymeric nanoparticles (Mazzarino *et al*., 2015).

One of the main concerns in the nanoparticle production and toxicological tests is the presence of endotoxins. The common endotoxin known is the lipopolysaccharide (LPS), component of the cell wall of Gram-negative bacteria. In the human body, endotoxin triggers the activation of the body's defence system, which, in turn, elevates the body temperature and elicits the "pyrogenic" response (Goulg, 1995).

LPS is naturally present everywhere in our surroundings and can therefore be introduced to the system through the water used as the solvent, chemicals, raw materials, or equipment used in the preparation of the nanoparticles (Sandle, 2015).

Several studies were done to optimize production of nanoparticles to minimize LPS contamination. Efficient removal of LPS is difficult to achieve due to its extreme heterogeneity, both in terms of composition and structure and also due to size differences (Sandle, 2013). In addition, LPS is thermostable and insensitive to pH changes. Applying high temperatures, such as 250 °C for 45 min, or high concentrations of acids and bases would be an efficient method to remove LPS, but such treatment may also affect the properties of nanoparticles. Therefore, the safer approach is to keep the entire production process contaminant-free (Sandle, 2015). Being this the major cause for false-positive reports about the inflammatory properties of nanoparticles, which can cause the misinterpretation in the immunotoxicological results (Boraschi *et al*., 2017).

This is important because nanoparticles (and pharmaceutical products alike) are commonly contaminated with endotoxins. Through induction of inflammatory signalling mediators (e.g. cytokines, chemokines, prostaglandins) endotoxins can lead to fever, fibril reactions and organ

damage, and this has often been a dose-limiting factor (Dobrovolskaia, Germolec e Weaver, 2009).

1.4.1 Effects of nanoparticles in the immune system

The immune system exerts its function through innate immunity and adaptive immunity. Innate immunity is the first line of defense against microbial invasion, which interacts with the foreign materials and cleans the pathogen or pathogen-infected cells, which is nonspecific to pathogen (Jiao *et al.*, 2014). The function of innate immunity is to realize by the phagocytic cells (macrophages, dendritic cells, neutrophils, and mast cells), the phagocytosis of the pathogen and the release of cytokines, both to clear pathogen. If the pathogen cannot be effectively cleared by innate immunity, the adaptive immunity, as the second line of defense in human body, will be activated. During these processes, some phagocytic cells act as antigen-presenting cells (APCs) and present specific antigens to specialized cells which are responsible for adaptive immunity, such as T cells and B cells (Hussain, Vanoirbeek e Hoet, 2012).

Each type of lymphocyte displays a different response: B cells support the humoral immune response, producing the antibodies that are going to bind to the pathogen, blocking its harmful action, while T cells are part of the cell mediated immune response, where they directly or indirectly through the communication with other cells like macrophages destroy the pathogen (Crotty, 2015). With that, the immunological memory is created and the immune system respond more rapidly and effectively to pathogens that have been encountered previously (Janeway *et al*., 2001).

With this in account, it is easy to understand that when nanoparticles are applied *in vivo* they can behave in two ways. On one side, they can act as being part of the human body, which means they are recognized as self and are not able to cause an immune response or on the other side, nanoparticles are recognized as foreign materials, causing an immune response that could be of immunosuppression or immunostimulation (Jiao *et al.*, 2014).

It is important to know more about the interaction of NPs with the immune system and the possible induction of inflammation for understanding their potential health risks and to know how the immune system recognises and eliminates NPs. From the literature is possible to observe that particles, not only can be able to modulate the immune responses, but also escaping immune surveillance thereby exerting more effectively their therapeutic potential (Shvedova, Kagan e Fadeel, 2010). Moreover, in the current safe-by-design approach of the nanomedicines, the environmental risks have also to be assessed (Boraschi, Moein Moghimi e Duschl, 2016).

1.5 Immunotoxicity of PCL and PCL/Glucan nanoparticles

Although there are several studies that evaluate the *in vitro* toxicity of PCL and glucan as a polymer there are only a few reports that show the effects of PCL and glucan particles on the immune system and the results found in the literature are, in some cases contradictory. A review of the literature concerning existing immunotoxicity studies is summarized in Table 4 and 5. These studies used PCL and glucan to produce nanoparticles and the information about polymer molecular weight (Mw), nanomaterial characterization, the performed assay and the results observed were collected.

By analysis of Table 4, it is possible to conclude that using RAW 264.7 and A549 cells line, the cell viability is influenced in a concentration-dependent manner. In the study performed by (Singh e Ramarao, 2013), is possible to observed a decrease in the cell viability in concentrations above 300 µg/mL, whereas in the studies conducted by (Jesus *et al*., 2013) the concentrations that shows the same effect is upon 18.8 µg/mL.

On the other side, in the tests performed by (Abamor *et al.*, 2018) using *Nigella sativa* oil (NSO) loaded into PCL NPs, no cytoxicity was observed, even in higher concentrations (1000 µg/ml). In the study when the oil free was tested it was observed a decrease in the cell viability, so in this case apparently, the addition of drug into the nanoparticle prevents the oil toxicity.

Another study conducted by Jesus and colleagues, it was investigated the cell viability using PCL blend to chitosan on spleen cells and concentrations above 37.5 µg/mL resulted in significant toxicity with 50% decrease in cell viability (Jesus *et al.*, 2018). In this study, the nanoparticles were produced under LPS free conditions and testes to verify LPS absence with an endotoxin detection assay.

The investigation for possible effects of NPs on inflammation was reported by (Singh e Ramarao, 2013) and (Abamor *et al.*, 2018) where it was used two different macrophage cell line and the induction of nitric oxide (NO) and oxygen reactive species (ROS) production was observed for the PCL nanoparticles but in different concentrations.

For induction of cytokines, two types of cells were studied, the RAW 264.7 and spleen cells, and the results show that PCL NPs stimulates the production of IL-6 and TNF-α, a pro-inflammatory cytokine involved in the innate immune response (Singh e Ramarao, 2013) and (Singh *et al.*, 2006). In both studies, it was not mentioned if the nanoparticles were prepared in LPS-free, which can indicate a false positive result.

In Table 5 is summarized studies that were performed using glucan from different sources.

It was evaluated the cell viability in different cell lines and several results were obtained. For instance, a study conducted by (Yu *et al.*, 2015) labeled the BSA to glucan microparticle,

(Upadhyay *et al.*, 2017) used Rifabutin and (Vu-Quang *et al.*, 2012) used superparamagnetic iron oxide encapsulated into glucan NPs. All the studies utilized a similar macrophage cell line and no reduction of cell viability was observed.

On the other hand, some studies demonstrated that using a different cell lines for cancer therapy, the nanoparticles became more cytotoxic. A study conducted by Nasrollahi and co-workers, shows that the NPs has a superior antitumor activity on murine 4T1cells compared to MCF71 a breast cancer cell line (Nasrollahi *et al.*, 2015). Another study compared two human cancer cell lines and noted different viability when used curcumin loaded to glucan NPs (Le *et al.*, 2016).

Contradictory results were observed using selenium added to glucan NPs that had different origins. While in (Jia *et al.*, 2015) the results did not show an interference in cell viability using human cervix carcinoma cells (Hela) for (Li *et al.*, 2019) it was observed a decrease in viability in a concentration-dependent manner, even though the nanoparticle present similar characteristics. In both studies was tested the reactive oxygen species (ROS), and an increase of its production was observed.

These contradictory results demonstrated that a better nanoparticle characterization as the size, zeta potential and other properties can also influence their immunotoxicity and unfortunately this information is not always present in the reports published (Dobrovolskaia e McNeil, 2007).

Another aspect that is important to relate is the information about the nanoparticle endotoxin contamination that supposedly has the potential to induce inflammation even at low concentrations (Dobrovolskaia, 2016). In the reports here analysed, only one of them refers the use of methods to detect and avoid the endotoxin contamination. In fact, the endotoxin contamination is the reason of the failure of 30 % of nanotechnology formulations in the early stages of pre-clinical development (Dobrovolskaia, 2016).

Considering all these variables and the application of these polymers as drug delivery, it is important to understand how the nanoparticle has an influence on efficacy and safety evaluation. Therefore, it was chosen to be the case of the study of this work to develop methods in order to test the immunotoxicological effect of nanomaterials.

Table 4: Comparison of results in studies of immunotoxicity *in vitro* using PCL nanoparticles

Nanoparticles	Nanomaterial characterization	Endpoint	Method	Model	Concentrations	LPS-free	Results	References
PCL NP	165.3 nm ± 35.1; 0.16 151.2 nm ± 8.3; 0.098	Cell viability	MTT assay	A549 cells	0.29 µg/mL to 300 µg/mL .	-	Concentrations superior to 18.8 µg/mL resulting in significant toxicity	(Jesus *et al.*, 2013)
PCL NPs	363 nm; 0.039; −8.2 mV	Cell viability	MTT assay	RAW 264.7 cells and A549 cell line	0 to 1000 µg /ml	-	Concentration-dependent (above 300 µg/ml) reduction in cell viability	(Singh e Ramarao, 2013)
		ROS	(DCF-DA)	RAW 264.7 cells	0 to 1000 µg/ml	-	Concentrations above 300 µg/ml showed 1.5- to 2-fold stimulation of ROS production	
		TNF-α and IL-6	Elisa	RAW 264.7 cells	300 µg/ml	-	Stimulate the release of IL-6 and 1.5- to 2-fold increase in TNF-α	
PCL NPs	267 nm ± 3	IL-6	Elisa	Spleen cells	20 µg/mL	-	PCL induced elevated IL-6 production, significantly higher	(Singh *et al.*, 2006)
PCL/Chitosan NPs	201.7 nm 0.29 ± 0.04; -1.4 ± 4.6 mV	Cell viability	MTT assay	Spleen cells	0.15 µg/mL to 150 µg/mL	Yes	Concentrations above 37.5 µg/mL, resulting in significant toxicity with 50% decrease in cell viability	(Jesus *et al.*, 2018)
PCL Microsphere MTX-PCL MPs	PCL MPs: 24.09 µm ± 0.55 MTX-PCL: 23.88 µm ± 1.15	Hemolysis	na	Human blood	0.5; 1; 2.5 and 5 mg/mL	-	No significant hemolysis (<5%)	(Dhanka, Shetty e Srivastava, 2017)
PCL-NSO NPs	202 ± 24 0.08; −4.92 ± 0.88 390 nm; 0.2 ; -8.29 mV	Cell viability	MTT assay	J774 macrophage cells	50 to 1000 µg/ml	-	No cytotoxic effect was observed	(Abamor *et al.*, 2018)
	202 ± 24 0.08; −4.92 ± 0.88	NO	Griess reaction	J774 macrophage cells		-	Concentrations above 500 µg/mL leads to 1.6 -fold enhancement released in nitric oxide amounts	

Abbreviations: DCF-DA - 2′, 7′ - Dichlorofluorescin diacetate; ELISA - Enzyme-linked immunosorbent assay; MTX - methotrexate, RAW 264.7 - Murine macrophage cell line; NSO - *Nigella sativa* oil; TNF-α -Tumor necrosis alpha factor and IL-6 –Interleukin.

Table 5: Comparison of results in studies of immunotoxicity *in vitro* using glucan nanoparticles

Nanoparticles	Nanomaterial characterization	Endpoint	Method	Model	Concentrations	LPS-free	Results	References
β-Glucan microparticles	2–5 µm	ROS	Chemiluminescence assay	PBMC from pigs	100, 200 and 400 µg/mL	-	1.5 fold stimulation in ROS production by neutrophils	(Baert *et al.*, 2016)
BSA-Glucan microparticles	2–4 µm	Cell viability	MTT assay	RAW 264.7 cells	3 to 400 µg/mL	-	No decrease in cell viability	(Yu *et al.*, 2015)
Doxorubicin- Glucan NPs	391 nm ± 23; 0.3	Cell viability	MTT assay	MCF7 cells Murine 4T1 cells	Dox - 0.3 µM	-	The NPs has a superior antitumor activity on 4T1 compared to MCF71 (viability < 70%)	(Nasrollahi *et al.*, 2015)
	163 nm ± 14; 0.1							
Rifabutin-Glucan microparticles	2.9 to 6.1 µm	Cell viability	MTT assay	J774A.1 cells	0 -100 µg/mL	-	Did not show decrease in cell viability	(Upadhyay *et al.*, 2017)
Curcumin-Glucan NPs	60 -70 nm	Cell viability	Sulforhodamine colorimetric method	Human cancer cell lines: Hep-G2 and LU-1	na	-	Hep-G2: IC50: 6.82 µg/mL LU-1: IC50:15.53 µg/ml)	(Lee *et al.*, 2016)
Lipossomes-Glucan NPs	30.2 nm ±10.5; 0.66	Hemolysis		Human blood	0 to 40 µg/mL	-	Hemolysis range of 8-10% with increasing concentrations of 0-40 µg/mL	(Zakir Hossain e Khiyami, 2015)
	180.1nm ± 11.3; 0.9 ± 0.08							
SPIONs-Glucan NPs	51.8 nm ± 2.63 11.42± 3.8 mV	Cell viability	MTT assay	Isolated peritoneal macrophages	5, 25, 50, and 100 µg/mL	-	No decrease in cell viability	(Vu-Quang *et al.*, 2012)
Selenium-Glucan NPs	52 nm; -2mV	Cell viability	MTT assay	HeLa cells	100 µg/mL	-	Did not show the inhibition of Hela cells *in vitro*	(Jia *et al.*, 2015)
	44 nm; -2 m	ROS	DCF-DA		200 µg/mL	-	The smaller is the size of SeNPs, the higher is the ROS production	
	33 nm; -6mV							
Selenium-Glucan NPs	53.7 nm ± 4.0	Cell viability	MTT assay	Hela cells	2.5, 5, 10, 20 and 40 µg/mL	-	Decrease in viability in concentration-dependent manner	(Li *et al.*, 2019)
		ROS	DCF-DA		10, 20 and 40 µg/mL	-	Increased in a dose-dependent manner	

Abbreviations: BSA - Bovine serum albumin; HeLa - human cervix carcinoma cells and SPIONs - superparamagnetic iron oxide nanoparticle.

1.6 Aim of the thesis

Comprehend the importance of the characterization of nanoparticles on the interpretation of the nano-safety assessment results is fundamental to develop a safe-by-design methodology of new nanomaterials. For this reason, the main objective of this work was to prepare and characterize PCL and PCL/Glucan nanoparticles and study the influence of the inclusion of a second polymer, glucan, into PCL NPs on the immunotoxicity properties of the nanoparticles. With this purpose, this thesis include several tasks with results:

- To develop a method to prepare a nanosized PCL/Glucan and PCL nanoparticles;
- To characterize (physical and chemical properties) the nanoparticles and evaluate their capacity to adsorb proteins to facilitate the protein internalization in cells;
- To evaluate *in vitro* immunotoxicological tests using murine macrophage cell line (RAW 264.7), human peripheral blood mononuclear and whole blood, in order to evaluate the influence of NPs composition on immunomodulation effects.

Chapter II

Development of a method to produce the PCL/Glucan and PCL NPs and characterization

Chapter II - Development of a method to produce the PCL/Glucan and PCL NPs and characterization

2.1 Materials and methods

2.1.1 Materials

Curdlan, (1, 3)-β-glucan (P-Curdl) was purchased from Megazyme (Bray, Ireland). PCL (average Mw 60 000 $g \cdot mol^{-1}$), Tween®80, NaOH, Bovine serum albumin (BSA, 96 % fraction V), Myoglobin from equine skeletal muscle (95 % to 100 %), Lysozyme (≥ 80 %), 5-(4,6 dichlorotriazinyl) aminofluorescein (DTAF) and Sodium tetraborate, were purchased from Sigma Aldrich Corp. (MO,USA). Pierce™ Bicinchoninic acid (BCA) protein assay was purchased from Thermo Fisher Scientific Inc. (Waltham, MA, USA). Limulus amebocyte lysate (LAL) assay (Pyrochrome ® kit, Cape Cod, Inc. (Falmouth, MA, USA).

2.1.2 Methods

2.1.2.1 PCL/Glucan NP production – method optimization

The technique to produce PCL/Glucan NPs was adapted and optimized from the nanoprecipitation method for PCL (Jesus *et.al*, 2018). For the aqueous phase, glucan in concentration of 0.025 % was dissolved in NaOH (2 %) containing 5 % of the surfactant Tween 80®, for 3 h under magnetic stirring. The organic phase consisted in PCL 0.2 %, dissolved in acetone at 60 °C to enhance solubilisation of the polymer. For the NPs production, the PCL solution (after cooling) was added dropwise to the glucan solution, under higher speed homogenization (Ystral X120, Ballrechten-Dottingen, DE), and let in agitation for 1 min after the complete mixture of both solutions. After this process, which theoretically induced PCL precipitation, several strategies were tested with the aim of coating the NPs preformed, with the glucan that remained in solution. Diverse volumes of the acetic acid solution (10 %) were added to decrease the pH and induce glucan precipitation around the already formed PCL NPs. In all tested condition, after production, the suspension of NPs was placed under magnetic stirring for 1 h to achieve particle maturation.

2.1.2.2 PCL NP production – method optimization

The method to produce PCL NPs was similar to the method described above to produce PCL/Glucan NPs, in order to have to comparable NP formulation. Therefore, the same procedure described in 2.1.2.1 was adopted for the production of PCL NPs. In this case, all solutions used had the same concentrations, with the exception for the aqueous phase solution that did not contain glucan.

2.1.2.3 Nanoparticle concentration

The NP suspensions were concentrated and washed with milli-Q or pyrogen-free water, by centrifugation, using 2 mL tubes at 16 000 g or 20 000 g for 1 h. This procedure was repeated twice.

2.1.2.4 Nanoparticle characterization

2.1.2.4.1 Transmittance

Transmittance of freshly prepared NPs (before centrifugation) was measured at 500 nm, relatively to a blank solution, using an UV-Visible 1603 Shimadzu spectrophotometer (Kyoto, Japan).

2.1.2.4.2 Size, Polydispersity index (PDI) and Zeta Potential (ZP)

The Zetasizer Nano ZS (Malvern Instruments, Ltd., Worcestershire, UK) was used to measure the particle size and PDI by Dynamic light scattering (DLS) and zeta potential through electrophoretic light scattering (ELS).

2.1.2.4.3 Transmission electron microscopy (TEM)

TEM was performed using a JEOL JEM 1400, 120 kV (JEOL, Peabody, MA, USA). For sample preparation, concentrated PCL and PCL/Glucan NPs were diluted in ultrapure water and then a drop was dried out on a mesh grid, before observation.

2.1.2.4.4 Stability tests

2.1.2.4.4.1 Long-term

The PCL and PCL/Glucan NPs suspended in apyrogenic water were maintained at room temperature (RT). The study was conducted for 20 days, and size, PDI and zeta potential was measured using Zetasizer Nano ZS (Malvern Instruments, Ltd. Worcestershire, UK). For each measurement, NPs were further diluted in apyrogenic water before measurement (100 µL + 900 of µL water).

2.1.2.4.4.2 Culture media

In order to recreate the possible events during *in vitro* studies with cells, the NPs stability in the different culture media was assessed. Non-cytotoxic concentrations of NPs in Roswell Park Memorial Institute cell culture medium (RPMI) and in Dulbecco's Modified Eagle Medium (DMEM) were chosen (based on the assays described in Chapter III) to evaluate size, PDI and zeta potential. Measurements were done just after the addition of the nanoparticle suspensions in the different culture media and 24 h after incubation at 37 °C through Zetasizer Nano ZS (Malvern Instruments, Ltd., Worcestershire, UK). The concentrations are shown in Table 6.

Table 6 - Concentrations used in the test of NPs stability in different culture media

	PCL NP (µg/mL)	**PCL/Glucan NP (µg/mL)**
DMEM	35.16	35.16
RPMI	282	562.5

2.1.2.4.5 Production of endotoxin-free NPs and evaluation of endotoxin contamination

The NPs were produced at endotoxin-free conditions, where all the material used were let in NaOH solution (0.5 M) for at least 22 h and posteriorly washed in apyrogenic water. We also tested the NPs in milliQ water to observe the difference between them.

Limulus amebocyte lysate (LAL) assay was performed according to kit manufacturer's instructions for detection of LPS presence on diverse samples. Briefly, to determinate the

concentration of the LPS a standard curve was created using diluted concentrations of control standard endotoxin (CSE) (2 EU/mL) 1; 0.5; 0.25; 0.125; 0.063; 0.031; 0,016 and 0.008.
The PCL/Glucan and PCL NPs (100 µg/mL) was added to a 96 well plate with an equal volume of Glucashield® buffer mixed to Pyrochrome® solution (ratio 1:1), mixed from 5 to 30 s and incubated at 37 ºC for 28 min. After incubation, the reaction was stopped by adding 25 µL of acetic acid (50 %). Finally, the colorimetric detection was evaluated through absorbance measure at 405 nm. The quantification of LPS was extrapolated from the standard curve, constructed by plotting optical density readings against standard endotoxin concentrations.

2.1.2.4.6 Attenuated total reflectance-Fourier transform infrared spectroscopy (ATR-FTIR) Analysis

ATR-FTIR was used to quantify the amount of glucan present in the nanoparticles. The lyophilized samples were run in a Spectrum Two FTIR spectrometer from PerkinElmer (Waltham, MA, USA) equipped with a single reflection ATR accessory. The FTIR spectra were collected by 50 scans with 4 cm^{-1} resolution in the 4000 cm^{-1} to 650 cm^{-1} region.

2.1.2.4.7 Protein adsorption (BCA protein assay)

Different concentrations of Bovine serum albumin (BSA), Myoglobin, lysozyme (0, 100, 300 and 500 µg/mL) were incubated with 500 µg/mL of PCL NPs or with 500 µg/mL of PCL/Glucan NPs, for 1 h under rotational agitation. After this time, the sample in 2 mL tubes were centrifuged for 30 min at 21 000 g and the supernatant collected for non-bound protein quantification. Pierce™ Bicinchoninic acid (BCA) protein assay was performed in microplates placed in incubation at 37 °C for 30 min. The absorbance was measured on a plate reader at 570 nm. The percentage of loading efficacy (% LE) and the percentage of loading capacity (% LC) of the NPs was calculated using the following equations (Eq. 1 and Eq. 2, respectively):

$$\text{LE (\%)} = \frac{(\text{total amount of protein (µg/mL)} - \text{non bound protein (µg/mL)})}{\text{total amount of protein (µg/mL)}} \times 100 \quad \text{(Eq.1)}$$

$$\text{LC (\%)} = \frac{(\text{total amount of protein (µg/mL)} - \text{non bound protein (µg/mL)})}{\text{weight of the nanoparticles (µg/mL)}} \times 100 \quad \text{(Eq. 2)}$$

2.2 Results and discussion

2.2.1 PCL/Glucan NPs with 180 nm were efficiently produced using the nanoprecipitation technique

The main objective of this work was to produce polymeric NPs with a size close to 100 nm, comprising two different polymers: PCL and 1,3-β-glucan. Since we could not find in the literature any reliable method describing the mixture of both polymers, a new methodology had to be developed that could lead to the production of the nanoparticles with the characteristics described. PCL is a polyester soluble in organic solvents (e.g. acetone), and widely described to form nanoparticles upon precipitation in aqueous solvents (Jesus *et al.*, 2018). Regarding glucan, one study by (Cai e Zhang, 2017) also described the production of glucan NPs by nanoprecipitation, in this case by dissolving the polymer in sodium hydroxide (NaOH) and then precipitate it using acetic acid, since the glucan is insoluble in acidic environments.

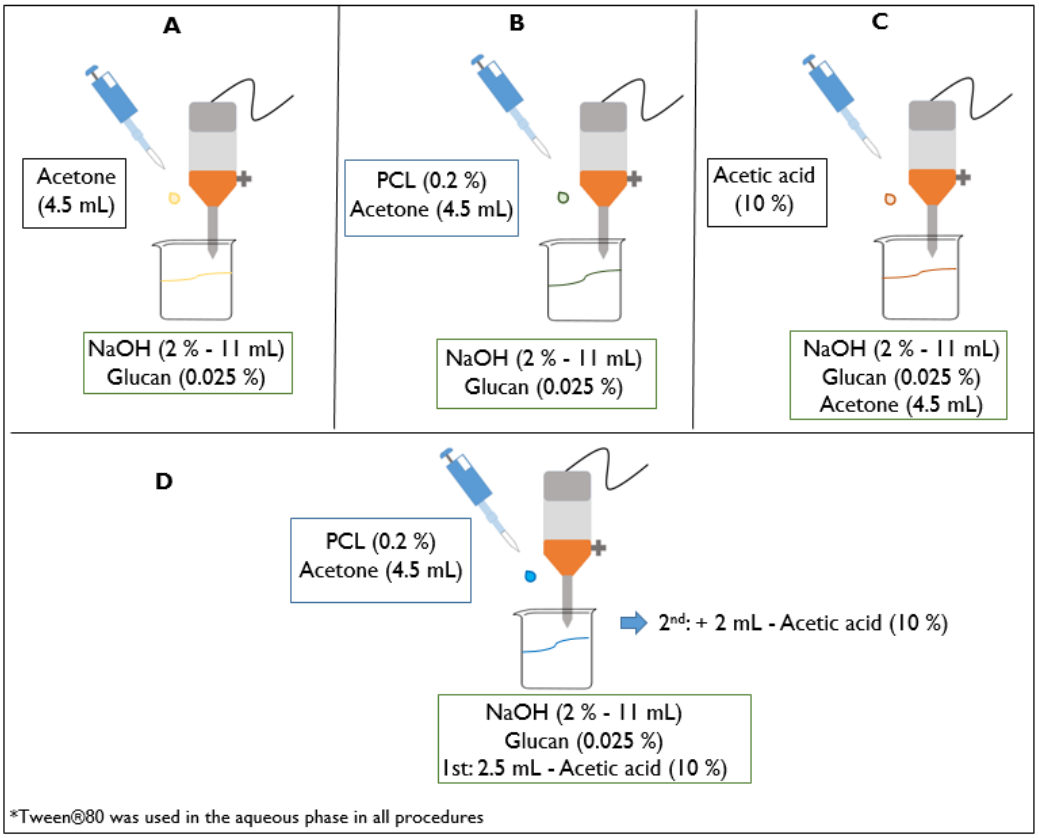

Figure 2: Schematic representation for the development of production method for PCL/Glucan NPs.

Therefore, our primary hypothesis was to dissolve PCL in acetone, and add dropwise this solution to a solution of glucan dissolved in NaOH/Tween®80. At this step, our objective was to precipitate only PCL, but first we needed to confirm if the glucan would also start to precipitate with the addition of acetone. To do that, as shown in Fig. 2A, a solution with glucan dissolved in NaOH/ Tween®80 was placed under a high speed homogenizer and acetone was added dropwise. After 1 h of magnetic stirring maturation, there was no formation of nanoparticles (also confirmed by the inability to measure any particle size in Zetasizer Nano ZS). In conclusion, we found that the glucan does not precipitate with the addition of acetone in the solution.

Alongside, as shown in the Fig. 2B, we wanted to test if we could precipitate the PCL in the solution of glucan in NaOH/ Tween®80. In this case, what we observed was the formation of agglomerates even though Tween®80 was present in the suspension. Since in our group we had experience with PCL NP production using nanoprecipitation (Jesus *et al.*, 2018), we knew that if PCL solution was precipitated into an acetic acid/ Tween®80 solution, PCL NPs would form in a stable suspension and would not form aggregates as we verified with the NaOH/ Tween®80 solution. Thus, the next step was adding several amounts of acetic acid (10 %) to the NaOH/Tween®80 solution to see if we could stabilize the NPs. However, first we had to test how much acetic acid we could use without inducing the precipitation of glucan as well. To test this, as shown in Fig. 2C and Table 7, several volumes of acetic acid (10 %) were added to the glucan solution containing acetone (mimicking the final conditions from Fig. 2A) to see at which point glucan would start to precipitate.

Table 7: Overall summary of the conditions tested to produce PCL/Glucan in NaOH (2 %) with the addition of different acetic acid volumes (10 %), n=1.

Acetone added to Glucan + NaOH/Tween®80				
Acetic acid	**pH**	**Size (nm)**	**PDI**	**ZP (mV)**
0 mL	13.7	---		
2 mL	13.11	---		
3 mL	12.87	---		
4 mL	7.68	68.1	0.354	- 7.2
4.5 mL	5.9	177	0.255	- 4.8
5 mL	5.4	213	0.283	- 1.2

As we can see from Table 7, only with the addition of 4 mL of acetic acid, turning the pH solution from 13.7 to 7.68, we could observe NPs formation in a smaller size (68.1 nm). As our intention was to obtain NPs slightly bigger, we decided to select the 4.5 mL of acetic acid for further tests, since it generated NPs around 177 nm.

Finally, we hypothesized that in order to precipitate PCL in glucan solution (NaOH/ Tween®80) without causing the agglomerates and without causing glucan precipitation, we would need to have less than 4 mL of acetic acid (10 %) in the aqueous phase at the moment we add the PCL dissolved in acetone. Therefore, as shown in Fig. 2D, the addition of PCL to glucan solution was performed in the presence of 2.5 mL of acetic acid, and after PCL NPs were formed, more 2 mL of acetic acid were added. This way, we could make sure that the formation of the PCL NPs occurred firstly and only with the addition of more acetic acid, changing the pH solution to 5.9 (final volume of acetic acid - 4.5 mL), the glucan would precipitate around the already formed PCL NPs. Results from the size obtained with this procedure are shown in Table 8.

Table 8: Overall summary of the conditions tested to produce PCL/Glucan NPs with the addition of different acetic acid volumes (10 %), mean ± SD, n=2.

PCL + Acetone added dropwise to Glucan + NaOH/Tween®80/Acetic acid			
Acetic acid	**Size (nm)**	**PDI**	**T (%)**
2.5 mL	288 ± 2.7	0.125 ± 0.02	55.5 ± 3.3
4.5 mL	195 ± 1.8	0.322 ± 0.01	51.2 ± 6.3
After (1h)	182 ± 3.2	0.311 ± 0.02	37.1 ± 3.1

From Table 8, we can observe that adding 2.5 mL of acetic acid (10 %) in the glucan solution prior to PCL solution addition, the produced NPs had a mean size around 288 nm. Afterward, with the addition of more 2 mL of acetic acid the NPs size diminished to 195 nm, however the PDI increased indicating a more heterogeneous NP population in terms of size. From the transmittance results, we can conclude that the PCL/Glucan NP continue its formation during the maturation time and therefore, this time is crucial to have better yields. Indeed, after 1 h maturation, the transmittance decreases from 51 % to 37 %, while size and PDI were kept stable, meaning that more NPs were being formed. With these results, we concluded the optimization of the method to produce PCL/Glucan NPs as displayed in Fig. 2D.

After NP production, in order to concentrate the nanoparticles and remove all the solvents used in the NP preparation, diverse conditions were tested through centrifugation. The NP suspension was aliquoted in 2 mL tubes and as is possible to observe in Table 9, firstly, it was tested a speed of 16 000 g for 1 h. After that, the supernatant was collected and measured for size and transmittance. The transmittance of 63.7 % indicated the presence of NPs with sizes measured around 112.73 nm. Nevertheless, the NPs pellet was suspended in water and the centrifugation was then repeated. A transmittance of 66.9 % was obtained in the 2nd supernatant, with particle sizes around 49.4 nm, as show in the Table 9. Therefore, to achieve a clear supernatant and avoid losing NPs in this procedure, the speed was increased to 20 000 g. With this increase, although there were still NPs present in the supernatants, the transmittance was increased, especially after the 2nd centrifugation (93.9 %), which was a good indicator that few NPs were being discarded during the washing steps.

Table 9: Overall characterization of supernatants obtained from PCL/Glucan NPs centrifugation. Size (nm), PDI and transmittance (T %) of the supernatants were measured (n=1).

Speed/ Time	16000 g/ 1h			20000 g/ 1h		
	Size	PDI	T	Size	PDI	T
1° Centrifugation	112.73	0.259	63.7	113.51	0.281	70.1
2° Centrifugation	49.4	0.201	66.9	111.8	0.287	93.9

When analysing NP size, it is also important to analyse the PDI and to complement the characterization with the size distribution. In Fig. 3 there is a summary of the PCL/Glucan NPs characteristics, after 1 h of maturation and after two centrifugations (20000 g, 1 h). We can see from the graphs that before and after centrifugation there is only one well defined peak for the PCL/Glucan NP size population. It shows that that there is no production of agglomerates in the formulation, even after the sample concentration. In addition, results show slightly decreased in size and PDI, which we can attribute to the change in the suspension media (to water) after centrifugation.

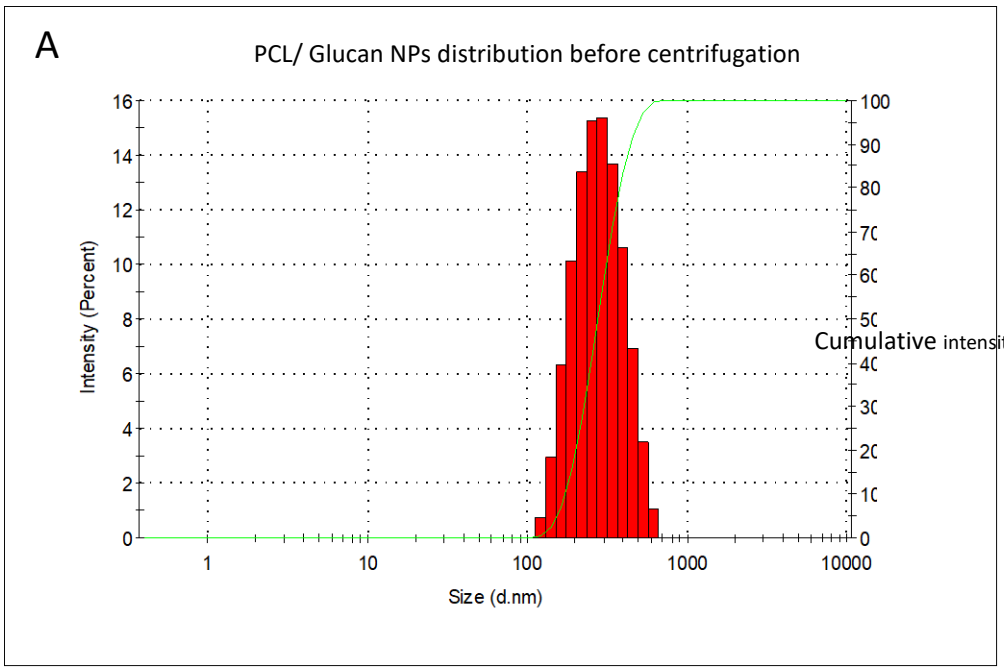

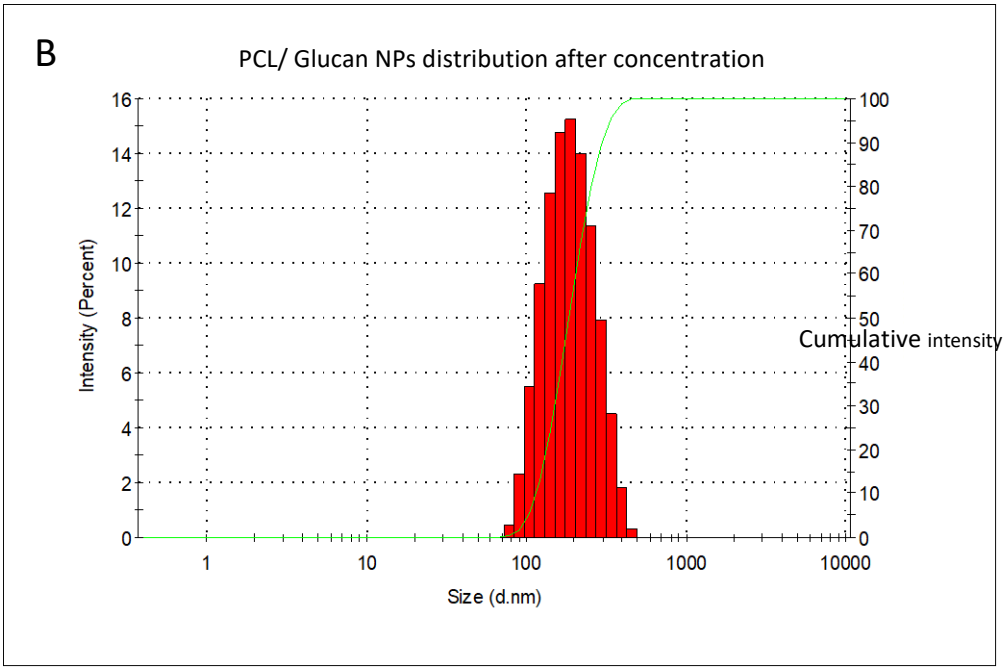

Size (nm)	PDI
181.3	0.189

Figure 3: Characterization of the size of PCL/Glucan NPs (A) before centrifugation and (B) after sample concentration.

2.2.2 PCL NPs were produced according to the optimized PCL/Glucan NPs nanoprecipitation technique

With the purpose to use the PCL NPs as a control, the nanoparticles were produced according to the optimized method to produce PCL/Glucan NPs. Therefore, 2.5 mL of acetic acid (10 %) were added to 11 mL of NaOH (2 %)/ Tween®80 (5 %) to constitute the aqueous phase. To this solution were added dropwise 4.5 mL of PCL solution (0.2 % dissolved in acetone). Similarly to PCL/Glucan NPs, after PCL NP production, two different centrifugation velocities were tested in order to determine the best experimental conditions to concentrate the NPs and remove all the solvents used in the NP preparation. The results from the supernatants analysis are described in Table 10.

Table 10: Overall characterization of supernatants of PCL NPs obtained after centrifugation. Size (nm), PDI and transmittance (T %) of the supernatants were measured (n=1).

Speed/ Time	16000 g/ 1h			20000 g/ 1h		
	Size	PDI	T	Size	PDI	T
1° Centrifugation	107.6	0.259	78.7	128.07	0.326	68.8
2° Centrifugation	67.8	0.266	87.8	89.15	0.321	90.2

In the case of PCL NPs, the differences using 16 000 g and 20 000 g were not so evident as in the case of PCL/Glucan NPs (Table 9), with only smaller improvements regarding transmittance increase with the higher speed centrifugation. Nevertheless, the selected condition to further concentrate PCL NPs was the 20000 g (1 h) to maintain the conditions used for PCL/Glucan NPs.

To conclude, Fig. 4 summarizes the PCL NPs characteristics regarding size, PDI and size distribution, after 1hr of maturation and after two centrifugations (20 000 g, 1 h).

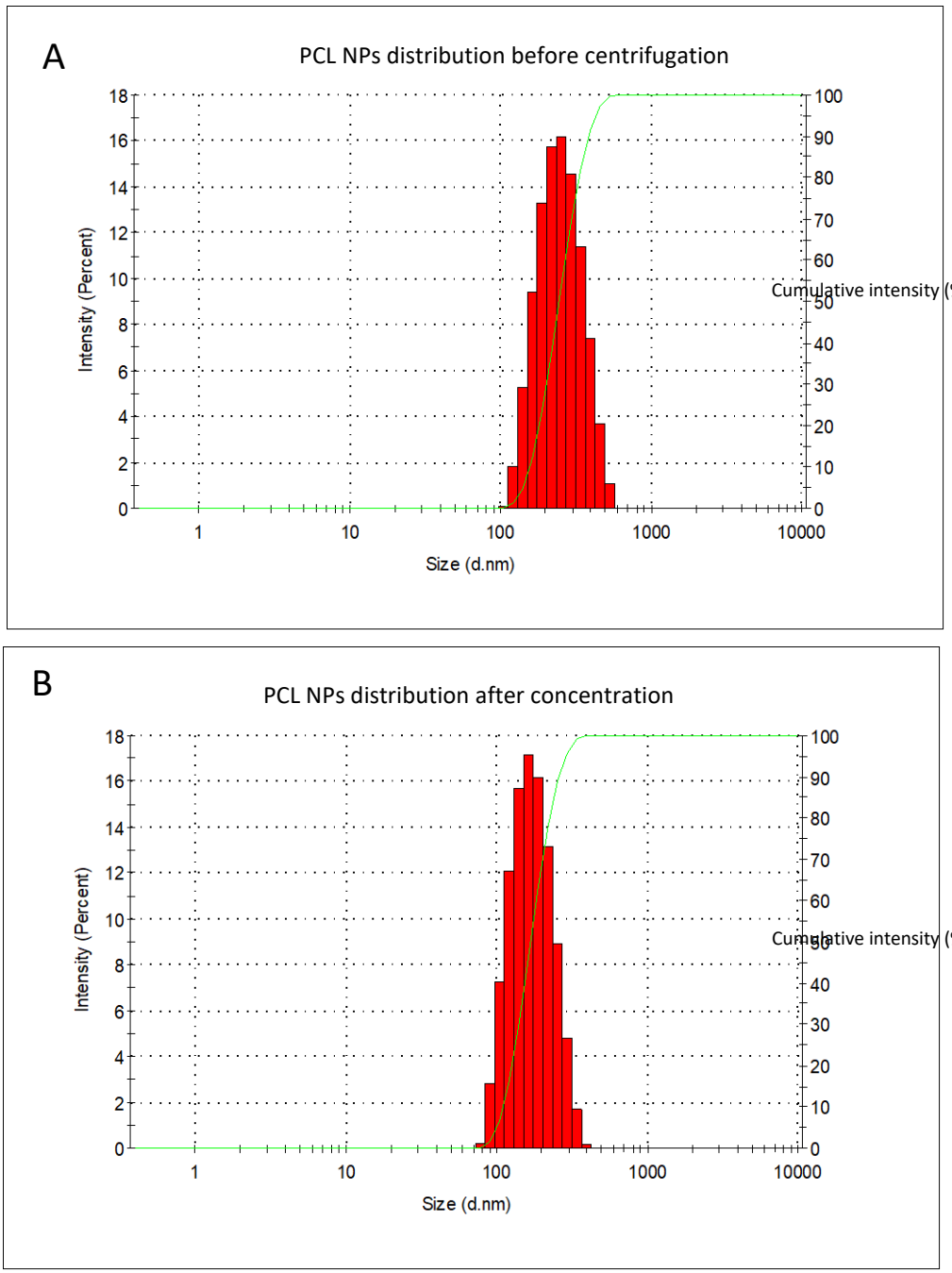

Size (nm)	PDI
175.23	0.107

Figure 4: Characterization of the size of PCL NPs before centrifugation (A) and after concentration with respective size (B).

In general, there were no important differences between NPs before and after concentration. In both we can observe only one peak confirming the absence of agglomerates. It was also noted, as for PCL/Glucan NPs, that a slightly decreased in size and PDI after NPs concentration. Again, this might be explained by the change in the NP dispersion media, as the initial solvents are replaced by water after centrifugation.

2.2.3 Both NPs present a similar zeta potential profile

In order to study surface properties over a pH influence for both nanoparticles, we tested the zeta potential in a pH range from 2 to 14. For that, 100 µL of the formulations were added to different tubes contain several pH solutions.

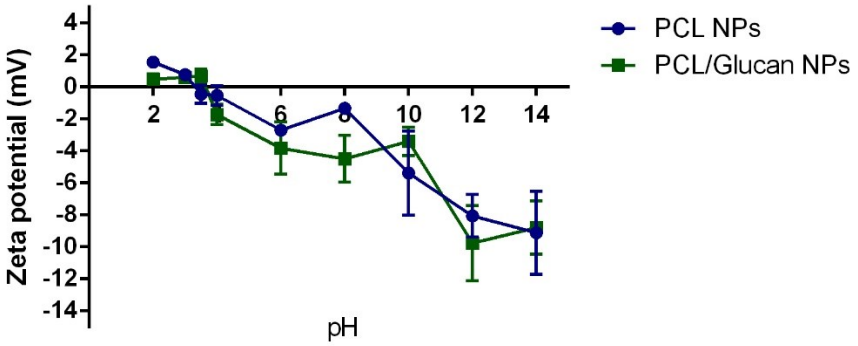

Figure 5: PCL/Glucan and PCL NPs zeta potential according to pH, (Mean ± SEM, n=3).

PCL/Glucan and PCL NPs, when suspended in different pH, showed similar values for zeta potential. They presented slightly positive zeta potential values (almost zero) between pH 2 and 4 and negative values for pH values greater than 4 and up to 14. These results are important because gives the information at which pH value the particles are potentially unstable. In fact, one of the most important factors involved in the agglomeration process are the electrostatic interactions among particles. Therefore, the surface charge of nanoparticles reflects their long-term stability (Berg *et al.*, 2009).

2.2.4 PCL/Glucan and PCL NPs have a round-shaped morphology according to Transmission electron microscopy (TEM)

To evaluate the morphology of the PCL/Glucan and PCL NPs, TEM analysis were performed. As seen in the Fig. 6 A to D the PCL/Glucan NPs presented a round shape and an intense black colour with size around 180 nm. Fig. 6C also illustrates particles with sizes ranging from 145 nm to 195 nm, confirming the DLS size measurements as well as the PDI suggesting a small polydispersity of populations.

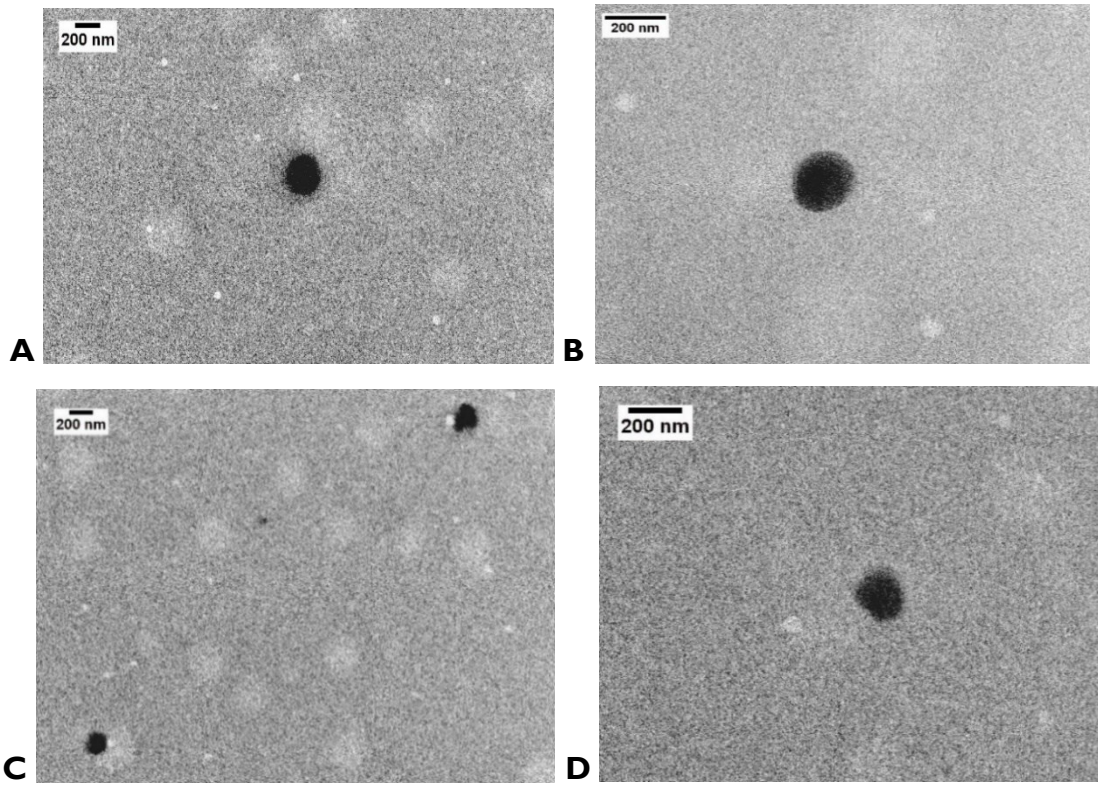

Figure 6: TEM images of PCL/Glucan NPs after being concentrated and washed.

As seen in the Fig. 7A to Fig. 7D, PCL NPs presented a round shape with size around 190 nm. However, in the Fig. 7C it is visible particles with more irregular shape than PCL/Glucan NPs.

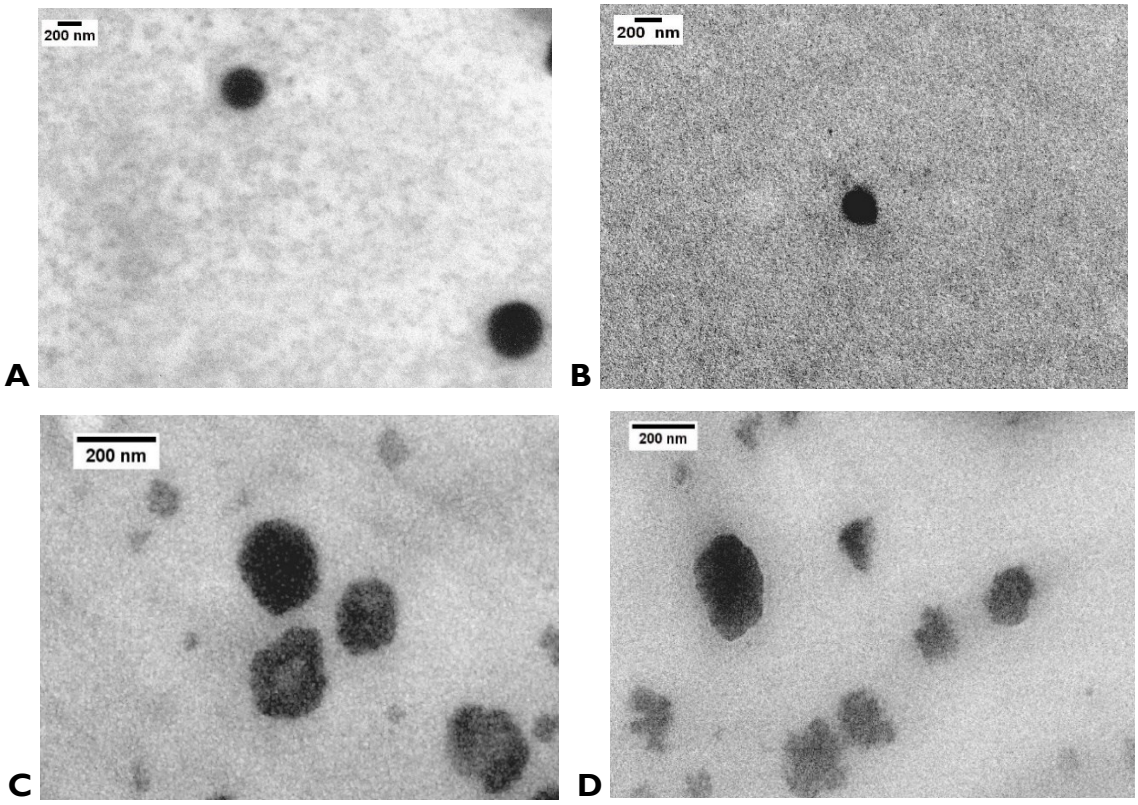

Figure 7: TEM images of PCL NPs after being concentrated and washed.

2.2.5 PCL/Glucan and PCL NP suspension is stable up to 3 weeks at room temperature

To evaluate the PCL/Glucan and PCL NPs stability at long-term in laboratory, it was conducted a study for 3 weeks where individual batches of each NP type were placed at room temperature (20 °C). The stability is important during the cellular studies in order to have the same batch characteristics for long term since the tests are not performed at the same time. According to Fig. 8A and 8B it is possible to conclude that during the time tested both nanoparticles were stable regarding size and PDI. The size remained the same and no aggregation was observed.

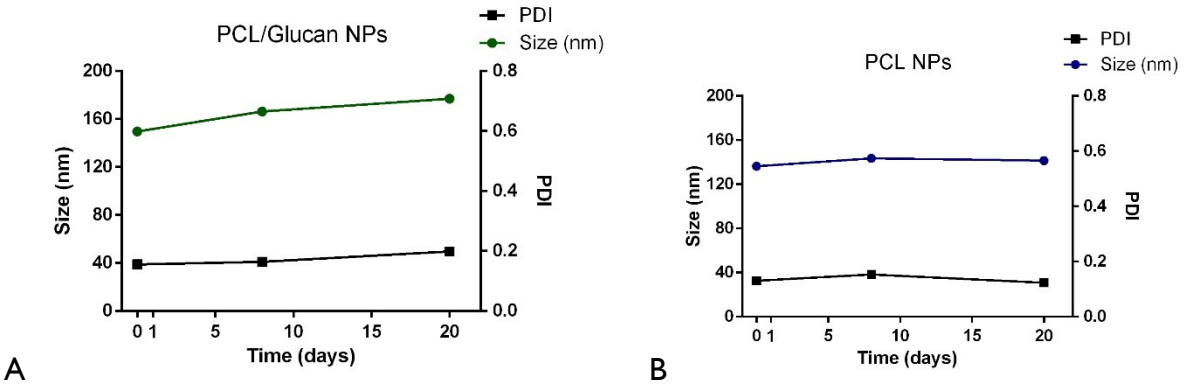

Figure 8: Stability test for long term at RT: A) PCL/Glucan NPs and B) PCL NPs, presenting in each graph the mean size and PDI. Results are the mean of 3 measurements, n=1.

Zeta potential, which is indicative of the particle surface charge, is an important and widely used characteristic of nanometer-sized objects in liquids, such as pharmaceuticals, inks, foams, liposomes, and exosomes. The zeta potential represents the value of the electrostatic potential at the plane of shear (Clogston e Patri, 2011).

Table 11: Measurement of zeta potential (mV) of the PCL/Glucan and PCL NPs in long term at room temperature. Results are the mean ± SD, n=2.

Time (days)	PCL/Glucan NPs (ZP mV ± SD)	PCL NPs (ZP mV ± SD)
0	-1.59 ± 0.52	- 2.54 ± 0.23
8	- 1.75 ± 0.4	- 2.23 ± 0.16
20	- 0.49 ± 0.25	- 1.88 ± 0.16

Table 11 shows the zeta potential over time. For both NPs, the charge tends to decrease, however, these small variations are not considered relevant for the stability of the nanoparticles.

2.2.6 Both NPs experience a decrease in size when suspended in DMEM but not in RPMI cell culture media

To recreate what happens when the NPs are incubated with cells, the different NPs were placed in culture media, DMEM and RPMI at 37 °C for 24 h, in order to evaluate the size, PDI and zeta potential.

As it is possible to observe in Fig. 9A, in DMEM, the PCL/Glucan NPs experience a size reduction right after being dispersed in cell culture media. Conversely, PDI increases indicating a higher heterogeneity in particle size distribution in DMEM. On the other hand, when PCL/Glucan NPs were dispersed in RPMI (Fig. 9B) the size and PDI remain stable for the whole experiment.

For PCL NPs, in DMEM (Fig. 9C) there is a particle size reduction to almost half of the initial size while in the RPMI (Fig. 9D) the size has only a slight decrease. This size reduction is accompanied by PDI increase, which corresponds to a larger size distribution in the particle sample demonstrating the polydispersity of populations (Cai e Zhang, 2017). For the NP dispersed in RPMI the PDI remains the same.

The NPs need to remain stable in the extra and intracellular environments long enough to be able to release their drug into the cell or target tissue and to provide sufficient protection for the drug on its journey to the target (Masarudin *et al.*, 2015). According to the stability results herein presented, we can conclude that both NPs, in relation to size and PDI, show a good stability over time and therefore could be considered good nanocarriers.

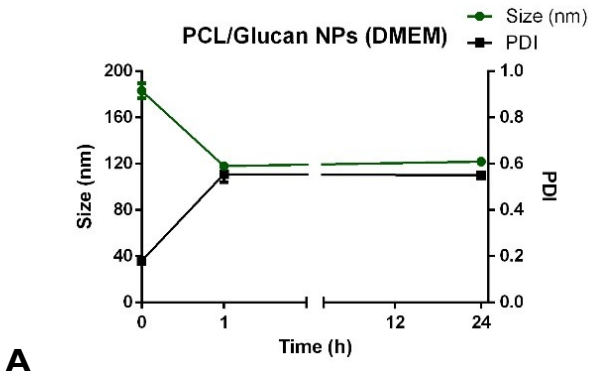

A

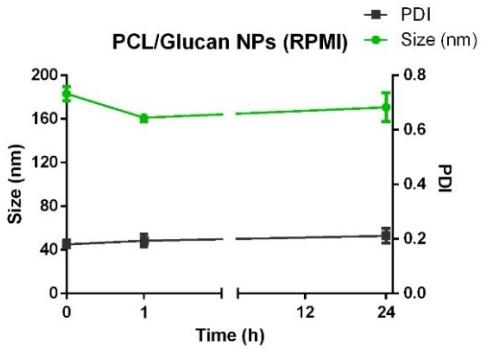

B

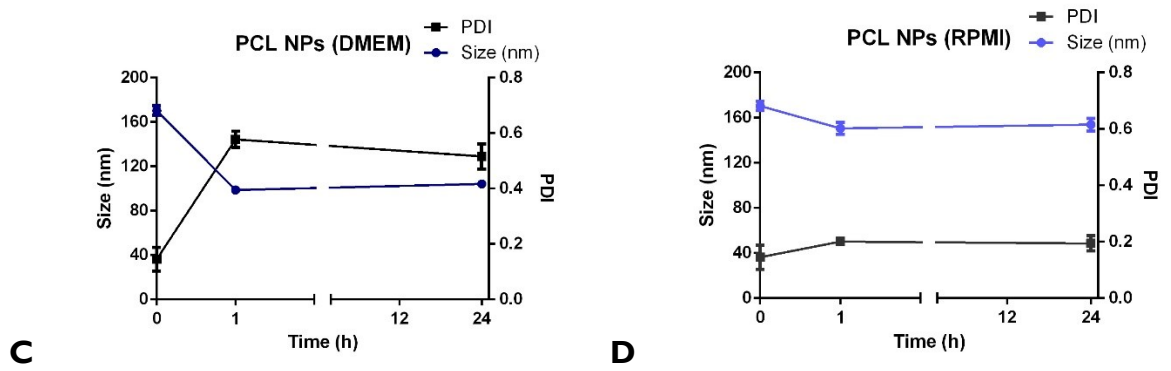

Figure 9: Stability test (A) in DMEM, (B) in RPMI of PCL/Glucan and PCL NPs(C) in DMEM, (D) in RPMI. Results are the mean ± SEM, n=3.

The ZP was measured at the beginning of the experiment and in the end with the objective of knowing if this parameter was affected over time. Some authors agreed that it can be challenging to measure ZP in the cell culture medium. Enriched with plenty of ions, the cell culture mediums have very high conductivity and interfere with ZP measurements. Such high conductivity can generate enough heat under constant voltage, which may degrade the sample (Satzer *et al.*, 2016).

As indicated by Table 12, for both PCL/Glucan NPs and PCL NPs no major alterations to the neutral zeta potential of the NPs was found. The PCL NPs in DMEM acquired a slightly more negative ZP changing from -0.11 mV to -3.72 mV however, this difference does not indicate a concerning change in nanoparticle stability.

Even adding the fact that in the literature, when the zeta potential is close to neutrality means that particles have a bigger disposition to form aggregates since they are considered stable when values are lower than -25 mV and higher than 25 mV (Tantra, Schulze e Quincey, 2010). Although none of our nanoparticles did present values in that range, it was not observed the presence of aggregates.

Table 12: Measurement of zeta potential in mV of the PCL and PCL/Glucan NPs 1 h and 24 h after incubation in the cell culture media of DMEM and in RPMI. Results are the mean ± SD, n=3.

n=3	PCL/Glucan NPs (ZP mV ± SD)		PCL NPs (ZP mV ± SD)	
Time (h)	**DMEM**	**RPMI**	**DMEM**	**RPMI**
0	- 0.11 ± 0.34	- 0.11 ± 0.34	- 0.05 ± 0.03	- 0.05 ± 0.03
1	- 1.66 ± 2.62	- 1.55 ± 2.67	- 0.91 ± 1.33	- 0.51 ± 0.26
24	-3.72 ± 0.25	- 1.28 ± 2.14	- 0.64 ± 2.77	- 1.66 ± 1.94

2.2.7 PCL NP was successfully produced in LPS-free although the PCL/Glucan interfere in the assay

Limulus amebocyte lysate (LAL) test is recommended for the quantification of endotoxins in a wide variety of samples in research laboratories and industries. It consists of the activation of a proteolytic cascade that result in the reaction with LAL (aqueous extract of blood cells from the horseshoe crab *Limulus Polyphemus*) when in the presence of endotoxins. This reaction induces the cleavage of colorless artificial peptide substrate present in Pyrochrome® LAL. Here we tested the presence of LPS in the NPs after production in miliQ water and apyrogenic water under endotoxin-free conditions in a sterile environment and decontamination with NaOH solution (0.5 M) for at least 22 h. The LPS quantification is according to the standard curve that is presented in Fig. 10A.

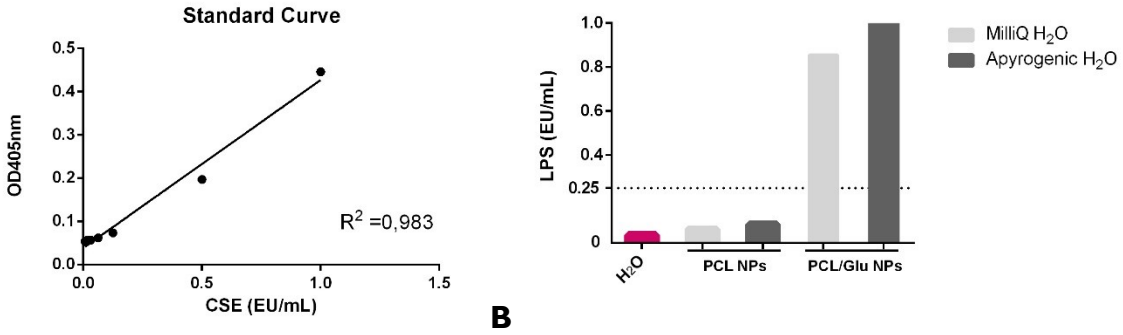

Figure 10: LAL assay A) Standard curve B) Indication of LPS presence in the produced NPs.

The expected level of endotoxin in the laboratories material is normally up to 0.25 EU/mL, any concentration above that is considered endotoxin contamination in the NPs samples. Thus, from Fig. 10B is possible to observe that in PCL NPs there was no indication of significantly LPS quantity in the different formulations using milliQ and apyrogenic water. The

same was not observed for PCL/Glucan NPs where the quantity was above the tolerance limit. It can be explained by the fact that curdlan is produced by non-pathogenic bacteria, *Alcaligenes faecalis* and that can contribute to glucan-derived interference in the assay because of factor G activation that leads to the production of the coagulant proteins, which has the same results as when there are LPS present in the solution.

As an alternative for that, was used Glucashield®, a buffer utilized to reconstitute LAL and render the reagent insensitive to glucan interference. In our case, the use of this buffer did not contribute to eliminating the interference of the assay.

After these results, the NPs produced for the immunotoxicological assays (NO, ROS and cytokines production and hemolysis assay) proposed in this study and that had the LPS as a positive control, were produced under endotoxin-free conditions concentrated in apyrogenic water.

2.2.8 ATR-FTIR confirm the presence of glucan in the PCL NPs

ATR-FTIR is a fast technique that allows the qualitative analysis of organic compounds based in the characteristic modes of vibration which cause the appearance of bands in the infrared spectrum at specific frequencies (Souza, De e Poppi, 2012).
ATR-FTIR was used to compare the chemical structures present in PCL and PCL/Glucan NPs. The bands at 3405 and 2942 cm^{-1} were assigned to OH and CH_2 bond, respectively. The next bands at 1715 and 1732 cm^{-1} arose from bending mode of CO and 1120 and 1075 cm^{-1} are associated with carbonyl stretching.

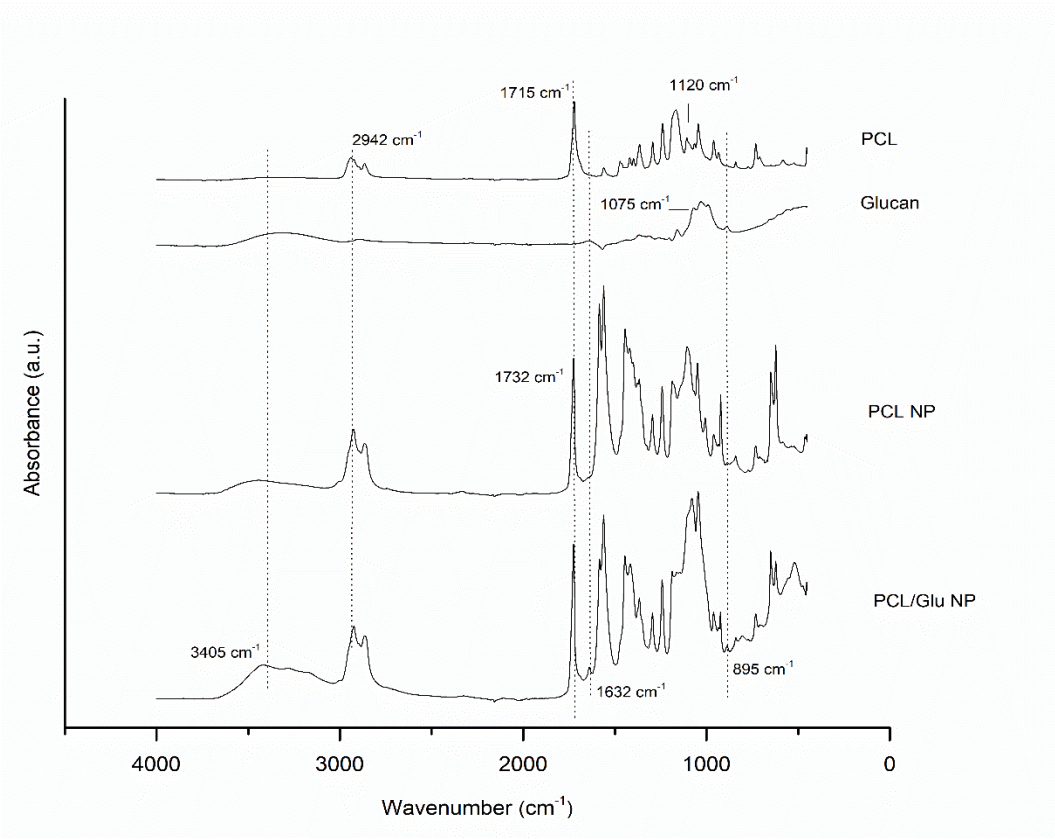

Figure 11: ATR-FTIR spectra of PCL, Glucan, PCL NPs and PCL/Glucan NPs.

The band at 3405 cm^{-1} is attributed to OH and appear in the spectrum of PCL and PCL/Glucan NPs, this can be associated with residual quantity water in the samples or traces of surfactant. PCL polymer, show asymmetric band in the region of 2942 cm^{-1} indicates the CH_2 which can be observed in PCL and PCL/Glucan NPs. The intensive overlapped band at 1730 cm^{-1} correspond to carbonyl stretching. For glucan, the characteristic absorption at 895 cm^{-1} is indicative of glycosidic linkages.

A typical band attributed to glucan at 1632 cm^{-1} and 895 cm^{-1} can be observed only in the PCL/Glucan NPs, these results demonstrate the presence of glucan in the blend NPs, however hypothetically in a lower concentration.

2.2.9 Both NPs present higher protein loading efficacy and capacity for Myoglobin

The encapsulation of proteins into polymeric nanoparticles is a promising methodology to provide protection against hostile environmental conditions for proteins (e.g., pH, T, proteolysis) (Wu *et al.*, 2014). Thus, there has been considerable interest in developing effective delivery devices for proteins in order to provide their controllable release as well as maintain their structural integrity (Danafar e Schumacher, 2016). In some cases, like on vaccine

development, it is preferably to adsorb antigens on the surface of the previously prepared particles and avoid the contact of the antigens with organic solvents, used during particle preparation.

With the intention to study the ability of both PCL and PCL/Glucan NPs to adsorb different proteins on their surface, three model proteins (Myoglobin, BSA and Lysozyme) with different isoelectric points (IP), molecular weights (MW) and structures were used in this study. A fixed concentration of NPs (500 µg/mL) was incubated with different concentrations of proteins (100, 300 and 500 µg/mL) for 1 h. The results are shown in Fig. 12, allowing a comparison between the two NP formulations.

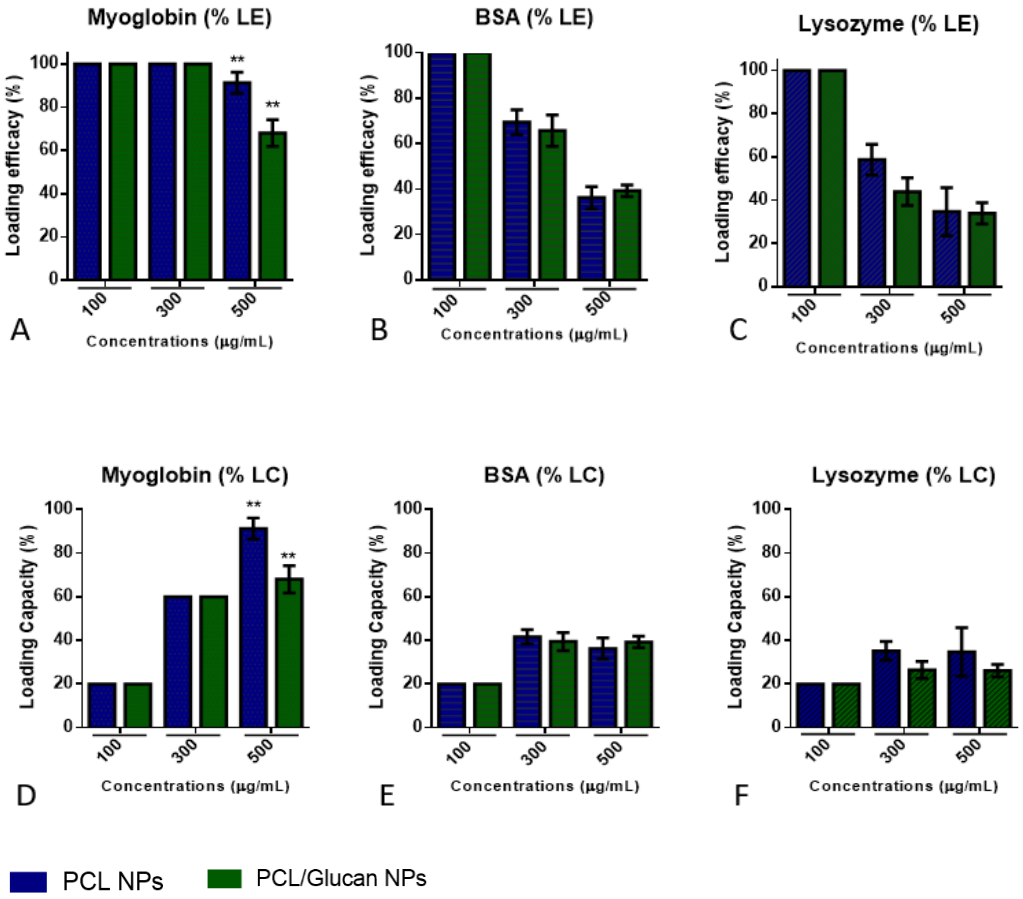

Figure 12: Proteins loading efficacy (LE) and loading capacity (LC) results for PCL NPs and PCL/Glucan NPs obtained with: A), D) Myoglobin; B), E) BSA; and C), F) Lysozyme. Results are the mean ± SEM, n=3, **p<0.05.

Protein loading efficacy or protein adsorption efficacy is the percentage that is successfully adsorbed onto NPs, while the loading capacity is the amount of protein per unit weight of the

NP, indicating the percentage of NP mass that is due to the encapsulated protein (Yu *et al.*, 2016)

From the three proteins tested, better results were achieved with myoglobin, and those results were statistically different for PCL NPs when compared to PCL/Glucan NPs. Indeed, both NPs showed 100 % loading efficacy for concentrations up to 300 μg/mL of myoglobin and when the protein concentration increased to 500 μg/mL, the loading efficacy decreased more significantly for PCL/Glucan NPs. For this protein, PCL NPs showed to be better nanocarriers, with a loading capacity around 90 %.

On the other hand, for both PCL NPs and PCL/Glucan NPs, the loading capacity of BSA and lysozyme never reached the 50 %.

Chapter III
Immunotoxicology studies

Chapter III – Immunotoxicology studies

3.1 Material and methods

3.1.1 Material

Curdlan (P-Curdl) was purchased from Megazyme (Bray, Ireland). PCL (Mw 60 000 $g.mol^{-1}$), Tween® 80, NaOH, MTT (3-[4, 5-dimethylthiazol- 2-yl]-2, 5-diphenyl tetrazolium bromide), murine cell line RAW 264.7, Dimethyl sulfoxide (DMSO), lipopolysaccharide (LPS) and BSA-Fluorescein isothiocyanate (FITC) were purchased from Sigma Aldrich Corp. (MO, USA). IL-6 and TNF-α standard for ELISA kits were acquired from PeproTech (Rocky Hill, NJ, USA). Trypsin-EDTA, fetal bovine serum (FBS), trypsin, plasma membrane and nuclear Labelling Kit (Hoechst 33342 and Alexa Fluor® 594) were acquired from Life Technologies Corporation (Paisley, UK). Lymphoprep™ was acquired from Axis-Shield (Dundee, Scotland).

3.1.2 Methods

3.1.2.1 Nanoparticle preparation

3.1.2.1.1 PCL/Glucan nanoparticles

The technique to produce PCL/Glucan NPs was based on a nanoprecipitation method. An organic phase containing 0.2 % PCL dissolved in 4.5 mL of acetone was added dropwise to an aqueous solution of glucan (0.025 %) dissolved in NaOH (2 % - 11 mL), acetic acid (10 % - 4.5 mL) and Tween®80 (5 %), under high speed homogenization and then left for maturation under magnetic stirring for 1 h. Subsequently, the solution was centrifuged twice with apyrogenic or miliQ water (1 h at 20000 g) and the nanoparticles were concentrated in 2 mL. The methodology is represented in figure 13.

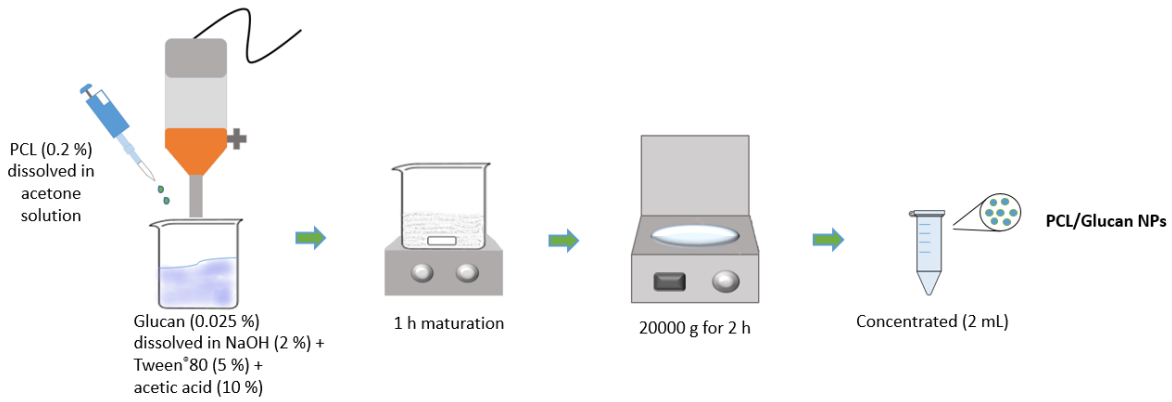

Figure 13: Schematic representation of the developed method for PCL/Glucan NPs production.

3.1.2.1.2 PCL nanoparticles

The technique to produce PCL nanoparticles was based on a nanoprecipitation method. An organic phase containing PCL 0.2 % dissolved in 4.5 mL of acetone was added dropwise to an aqueous solution of NaOH (2 % - 11 mL), acetic acid (10 % - 4.5 mL) and Tween®80 (5 %), under high speed homogenization and then left for maturation under magnetic stirring for 1 h. Subsequently, the solution was centrifuged twice (1 h at 2000 g) and the nanoparticles were concentrated in 2 mL. The methodology is represented in figure 14.

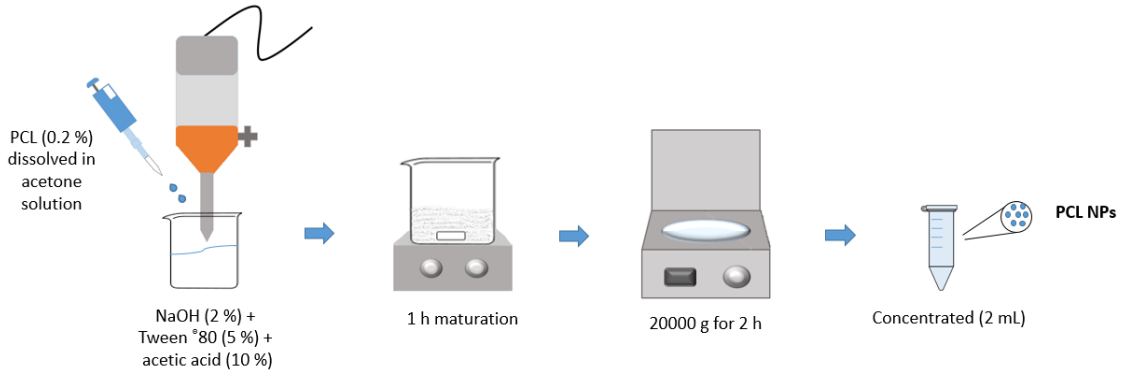

Figure 14: Schematic representation of the developed method for PCL NPs production.

3.1.2.1.3 LPS-Free nanoparticle production

The nanoparticles were produced in a sterile environment in order to produce endotoxin-free nanoparticles. All the material used in the process were let in NaOH solution (0.5 M) for at least 22 h for decontamination and posteriorly washed with apyrogenic water.

3.1.2.2 Immunotoxicology evaluation

3.1.2.2.1 *In vitro* assays with a murine macrophage cell line (RAW 264.7)

3.1.2.2.1.1 Cell culture

The murine macrophage cell line (RAW 264.7) was cultured in DMEM (Dulbecco's Modified Eagle's Medium) supplemented with 10 % inactivated FBS (Fetal Bovine Serum), 3.7 g/L sodium bicarbonate, 10 mM Hepes and 1 % penicillin/streptomycin. These semi adherent cells

were maintained in 75 cm^2 flasks with 20 mL of growth medium in a humidified atmosphere at 37 °C with 5 % CO_2. Subcultures were performed by detaching the cells mechanically after being grown at a confluence of approximately 70 % to 80 % and by diluting 1:2 to 1:6 every 2 to 3 days.

3.1.2.2.1.2 Nanoparticle influence on the cellular viability of RAW 264.7

The RAW 264.7 mouse macrophage cell line were planted into 96-well plate at a density of 2 x 10^5 cells per well in 100 µL culture medium DMEM in a humid atmosphere at 37 °C, 5 % CO_2 for 24 h. The medium was removed and 150 µL of new a medium and 50 µL of a serial nanoparticle dilution in water, previously prepared at concentration ranging between 1.1 µg/mL to 1125 µg/mL was added. After 24 h it was added 20 µL MTT (5 mg/mL in phosphate buffered saline (PBS, pH: 7.4) in each well following incubation for 1.5 h at 37 °C. Thereafter, the supernatant was aspirated and 150 µL of DMSO was added to solubilize the formazan product and the solution was mixed thoroughly for 2 min. The absorbance was measured at 540 nm with reference wavelength set at 630 nm using a microplate reader. The cell viability (%) was calculated in relation to the positive control (cells in the culture medium without nanoparticles), using the following equation:

$$\text{Cell viability (\%)} = \frac{Abs\ sample\ (540\ nm) - Abs\ sample\ (630\ nm)}{Abs\ control\ (540\ nm) - Abs\ control\ (630\ nm)} \times 100 \quad \text{(Eq. 3)}$$

The results were confirmed by flow cytometry with the propidium iodide (PI). Briefly, different concentrations of nanoparticles used for MTT assay were tested: 1.1, 17.6, 141, 1125 µg/mL. A 96 well plate with cells at density of 2 x 10^5 cell/mL were incubated at 37 °C, 5 % CO_2 for 24 h. After this time, the cells were incubated with the different formulations of nanoparticles for 24 h. For the flow cytometry analysis (BD FACSCalibur Flow Cytometer (BD Biosciences, San Jose, CA, USA), the cells were washed with PBS, mechanically detached from the well plates and analysed following PI addition to the cell suspension (1 µL (50 µg/mL) added to each 250 µl of cell suspension). The results were expressed as the % of PI positive cells.

3.1.2.2.1.3 Nitric Oxide (NO) assay

The RAW 264.7 were seeded in a 48-well plate at a cell density of 4.5 x 10^5 cell/mL in DMEM and incubated for 24 h at 37 °C in a humidified atmosphere containing 5 % CO_2. The medium

was removed and 375 µL of phenol red-free DMEM and a volume of 125 µL of the nanoparticle suspensions were added to evaluate if the formulations could induce the NO production. In order to evaluate if the nanoparticles could induce the inhibition of NO production, the cells were stimulated with lipopolysaccharide (LPS) diluted in phenol red-free DMEM, for that, it was added 250 µL of phenol red-free DMEM, 125 µL of nanoparticles suspensions and 125 µL of LPS (1 µg/mL) in each well; the LPS was also used as a positive control. The NPs concentrations tested were 70 µg/mL, 35 µg/mL, 7 µg/mL and 3.5 µg/mL. After 24 h of incubation, 100 µL of the supernatants were collect and mixed with equal volume of Griess reagent (1 % (w/v) sulphanilamide in 2.5 % (v/v) phosphoric acid and 0.1 % (w/v) naphthyl ethylenediamine dihydrochloride in 2.5 % (v/v) phosphoric acid) in a 96-well plate at room temperature for 10 min. Finally, the colorimetric detection was evaluate through absorbance measure at 550 nm, using a microplate reader. To determinate the NO quantity a standard curve was created using diluted concentrations (0.625; 1; 1.25; 2.5; 5; 10; 20; 30; 50; 60; 70 and 80) µM) of sodium nitrite solution ($NaNO_2$ - 1 mg/mL) in phenol red-free DMEM. After collecting the supernatants, the MTT assay was executed so as to evaluate the cell viability of the concentrations tested. Therefore, the remnant supernatant was removed and 200 µL of DMEM and 20 µL of MTT solution (5 mg/mL in PBS, pH: 7.4) was added in each well and let incubate for 1.5 h at 37 ° C. Subsequently the supernatant was aspired and 200 µL of DMSO was used to dissolve the formazan crystals formed. The absorbance was measured at 540 nm with reference wavelength set at 630 nm using a microplate reader.

3.1.2.2.1.4 Reactive oxygen species (ROS) assay

The RAW 264.7 cell line were seeded into 96-well black plate at a cell density of 5.0 x 10^5 cells/mL in DMEM in a humid atmosphere at 37 °C, 5 % CO_2 for 24 h. Diluted nanoparticles were added to the wells, with concentrations 70 µg/mL, 35 µg/mL and 7 µg/mL and left incubating for 24 h.

After this time, the culture medium was removed by aspiration and 100 µL of serum-free medium with probe (DCFDA) was added except in the negative control (only cells) and leave for 2 h. LPS was previously prepared by diluting in DMSO for 50 µM final concentration and then it was diluted in DMEM in a final concentration of 1 µg/mL and used as a positive control. The fluorescence was measure through excitation of 485 nm and emission of 528 nm. In order to evaluate the cell viability under these conditions, after the reading, 20 µL of MTT were added to each well and the assay was completed as described in sub-chapter 3.1.3.1.3.

3.1.2.2.2 *In vitro* assays in Human Peripheral Blood Mononuclear Cell Line (PBMC)

3.1.2.2.2.1 Isolation of PBMCs from human peripheral blood by density gradient

The whole blood was diluted in saline solution (0.9 % NaCl) in a proportion of 1:5 and 2.5 mL of Lymphoprep™ was used to isolate the mononuclear cells. Then, it was centrifuged for 20 min at 1190 g, 20 °C to form the ring of mononuclear cell between the plasm and the separation liquid. The PBMC were carefully aspirated and added to a 15 mL tube while PBS (pH 7.4 at 37 °C) was added to bring the final volume up to 12 mL and again centrifuged for 10 min at 487 g, 20 °C. The supernatant was discarded and the pellets were homogenized. The operation was repeated until the supernatant was clear. Then the cells were resuspended in 3 mL of RPMI. The cell viability was determined in presence of Trypan blue, an azo dye, by adding 180 µL of PBS and 20 µL of the cellular suspension with 50 µL of Trypan blue and subsequently the cells were counted in the Neubauer chamber.

3.1.2.2.2.2 Nanoparticle influence on the cellular viability of PBMC

The PBMCs were seeded in a 96-well plate at a cell density of 5×10^6 monocytes/mL in RPMI and left incubating in a humidified atmosphere at 37 °C, 5 % CO_2 for 24 h. Serial dilutions of the PCL and PCL/Glucan NP were prepared in different concentrations from 4.4 µg/mL to 1125 µg/mL and added to the cells. After 24 h, the MTT assay was executed, in order to evaluate the cell viability, thus 20 µL of MTT solution (5 mg/mL in PBS. pH 7.4) was added to each well during 4 h at 37 °C. After this time, the plate was centrifuged for 25 min at 800 g and the supernatants were carefully removed. Afterward, 100 µL of DMSO was added to dissolve the formed crystals. The absorbance was measured at 540 nm with 630 nm as wavelength reference using a microplate reader. The relative cell viability (%) was calculated in relation to the control (only cells in culture media) by the equation 3.

The results were confirmed by flow cytometry PI assay using 4 concentrations of nanoparticles previously tested with the MTT assay (4.4 µg/mL, 35 µg/mL, 562.5 µg/mL and 1125 µg/mL). A 96 well plate with cells at density 5×10^6 monocytes/mL were incubated at 37 °C a 5 % CO_2 for 24 h. After this time, the cells were incubated with the different formulations of nanoparticles for 24 h. For the flow cytometry analysis, the plates were centrifuged for 25 min at 800 g. Supernatants were aspirated and the cells were collected with PBS, and subsequently analysed following PI addition to the cell suspension (1 µL (50 µg/mL) to each 250 µL of cell

suspension) and analysed in a BD FACSCalibur Flow Cytometer (BD Biosciences, San Jose, CA, USA). The results were expressed as the % of PI positive cells.

3.1.2.2.2.3 Uptake studies

3.1.2.2.2.3.1 Flow cytometry for cellular uptake by BSA-FITC loaded nanoparticles

The cellular uptake of BSA-FITC loaded NPs was studied by flow cytometry using PBMCs. The cells were seeded in the 48-well plate (5 x 10^6 monocytes/mL). In the next day, 100 µg/mL of BSA-FITC were incubated with 500 µg/mL of PCL or PCL/Glucan NPs for 1 h and then, 40 µL of the BSA loaded NPs were added to each well. Similarly, 20 µL of BSA-FITC (50 µg/mL) were tested and the results used for comparison. After a 4 h incubation period, the plate was centrifuged at 800 g for 25 min and the supernatant removed. The cells were washed with 300 µL of PBS and transferred to an appropriate cytometry tube and then analyzed by flow cytometry. After the first analysis, it was added to the same sample 2 µL of trypan blue at 25 % (final concentration 0.2 %) the cells were analysed again. Results were expressed as the mean fluorescence increase of samples related to the control (cells).

3.1.2.2.2.3.2 Flow cytometry for cellular uptake by Rhodamine loaded nanoparticles

The nanoparticles were prepared as described in the item 3.2.1 and 3.2.2 with addition of rhodamine (1 mg/mL) dissolved in acetic acid (10 % - 2 mL) and added to the aqueous solution of NaOH (2 % - 11 mL).

The cellular uptake of rhodamine loaded NPs was studied by flow cytometry using PBMCs seeded in the 48-well plates (5 x 10^6 monocytes/mL). In the next day, the rhodamine loaded PCL/Glucan (34.5 µg/mL) and PCL NPs (69 µg/mL) were incubated for 4 h, well as the free rhodamine (0.85 µg/mL) to use as a control. After that, the plate was centrifuged at 800 g for 25 min and the supernatant removed. The cells were washed with 300 µL of PBS and analyzed by flow cytometry. Results were expressed as the mean fluorescence increase of samples related to the control (cells).

3.1.2.2.2.3.3 Confocal laser scanning microscopy (CSLM) for uptake study using BSA-FITC loaded nanoparticles

For CSLM studies, PBMCs were seeded on poly-D-lysine covered glass coverslips in 24 well plates at density of 5 x 10^6 monocytes/well and cultured at 37 °C in 5 % CO_2. After 24 h incubation, the medium was replaced and cells were incubated with PCL/Glucan-BSA-FITC and PCL-BSA-FITC NPs (69 µg/mL) for 4 h. Following the uptake period, the supernatants were removed; cells were washed three times with PBS pH 7.4 and fixed with 4 % paraformaldehyde for 20 min at 37 °C. Again, cells were washed three times with PBS before the staining.

Nucleus were stained with a cell permeable nucleic acid (Hoeschst 33342), and their plasma membranes stained with cell impermeable Alexa Fluor wheat germ agglutinin. After labelling, the cells were washed twice with PBS and coverslips mounted on microscope slides and examined under an inverted laser scanning confocal microscope (Zeiss LSM 710, Carl Zeiss, Oberkochen, DE) equipped with imaging software (Zen Black 2012 software, Carl Zeiss).

3.1.2.2.2.3.4 CSLM for uptake study using rhodamine loaded nanoparticles

The same procedure described in 3.1.3.2.3.3 was used to analyse the rhodamine loaded nanoparticles under the CSLM. Briefly, the Rhodamine-PCL/Glucan NPs (34.5 µg/mL) and Rhodamine-PCL NPs (69 µg/mL) were incubated in a 24 well plate previously prepared for 4 h. Following the uptake period, wells containing NPs were removed, cells washed three times with PBS pH 7.4 and fixed with 4 % paraformaldehyde for 20 min at 37 °C. Again, cells were washed three times with PBS before the staining.

The rhodamine dye was used to stain the NPs and Hoeschst 33342 was used to stain the nucleus. After labelling, cells were washed twice with PBS and coverslips mounted on microscope slides and examined under an inverted laser scanning confocal microscope (Zeiss LSM 710, Carl Zeiss, Oberkochen, DE) equipped with imaging software (Zen Black 2012 software, Carl Zeiss).

3.1.2.2.2.4 Cytokine quantification

The PBMCs cells was seeded in a 96-well plate at a cell density of 2 x 10^6 cell/mL and incubated with formulations of PCL and PCL/Glucan NPs (50 µg/mL) and controls (LPS (2 ng/ml) as a positive control and cells with culture medium as a negative control) for 24 h in a humidified atmosphere at 37 °C, 5 % CO_2. After this time, the plates were centrifuged (25 min at 800 g) and the supernatants were removed and stored at -80 °C to further analysis.

To measure the cytokines it was used ELISA (Enzyme-Linked Immunosorbent *Assay)* technique according to kit manufacturer's instructions (Prepotech). Briefly, high binding 96 well-plates were coated with 100 µL of antibody's TNF- α and IL-6 which were left at room temperature overnight. Plates were washed 4 times with wash buffer (PBS, Tween 20) and added block buffer (1 % BSA in PBS) in each well and left for 1 h at room temperature. After washing, several dilutions of standard cytokines and 100 µL of the supernatants samples previously obtained, were added and incubated for 2 h. Each sample represented a pool of one condition done in triplicate in one day. Afterwards, the plates were washed again for 4 times and 100 µL of detection antibody was added and let incubated for another 2 h. Then, the plates were washed and it was added 100 µL of Avidin-HRP (Horseradish peroxidase) conjugated for 30 min. After the final washing, 100 µL of substrate solution ABTS (2,2'-azino-bis(3-ethylbenzothiazoline-6-sulphonic) was put in each well and let incubating at room temperature for colour development. The absorbance values were then measured at 405 nm with 630 nm as wavelength using a microplate reader. Concentrations of the cytokines were calculated from absorbance values, using the calibration curves.

3.1.2.2.2.4.1 Cell viability for cytokine quantification

Cell viability was evaluated using a modified Alamar Blue assay. Briefly, after the supernatant collection (3.1.3.2.4), the cells were incubated with 100 µL of 10 % (v/v) Alamar blue dye in RPMI medium, prepared from a 0.1 mg/mL stock solution of Alamar Blue. After 72 h of incubation at 37 °C in 5 % CO_2, the absorbance was measured at 570 nm and 600 nm using a microplate reader.

3.1.2.2.3 Whole blood

3.1.2.2.3.1 Hemolysis assay

The human whole blood was collected from a volunteer healthy donor and stabilized with Lithium heparin as an anticoagulant. The fresh whole blood was diluted in PBS (pH 7.4) to adjust the total hemoglobin in 10 mg/mL. Different concentrations of nanoparticles (100 µL) to achieve a final concentration ranging from 15 µg/mL to 300 µg/mL were added to 700 µL of PBS and 100 µL of the diluted blood in eppendorfs and incubated for 3 h at 37 °C and to determine the possible interferences of the nanoparticles with the assay, samples were incubated at the same concentrations with just PBS. After 3 h, the eppendorfs were centrifuged

at 800 g for 15 min where the intact red blood cells are as a pellet and the amount of hemoglobin is released into the solution to be spectrophotometrically measured. After the centrifugation, 100 µL of the supernatants were transferred to a 96-wellplate and 100 µL of cyanmethemoglobin (CMH) reagent were added. The absorbance was read at 540 nm using a microplate reader. To test the performance of hemolysis assay, PBS was used as a negative control (NC) and Triton-X-100 as a positive control (PC). The samples absorbance was measured at a wavelength of 570 nm (two measurements from each test tube). The percentage of hemolysis was calculated by the following equation.

$$\text{Hemolysis } (\%) = \frac{(\text{Abs sample} - \text{Abs negative control})}{(\text{Abs positive control} - \text{Abs negative control})} \times 100 \qquad \text{(Eq.4)}$$

3.1.2.3 Statistical analysis

Data were analysed using GraphPad Prism 6 (GraphPad Software, Inc., La Jolla, CA, USA), in which significant differences were obtained from t-test correct from multiple comparisons using Holm-Sidàk method ($p<0.05$), one-way ANOVA corrected for Dunnett method and Bonferroni ($p<0.05$). The respective statistical tests are described along the results. Statistical data was expressed as means ± standard error (SEM) of the mean.

3.2 Results and discussion

3.2.1 No statistical differences were observed between PCL and PCL/Glucan for cell viability in RAW 264.7

Toxicity studies *in vitro* might relate to the nanoparticle toxic profile that may be observed *in vivo*. To evaluate cell viability the MTT assay was used, which is a rapid and precise assay that measures the metabolic activity of living cells. The murine macrophage cell line, RAW 264.7, is often used to initially screen natural products for bioactivity and to predict their potential effect on cells. The cell line response is considered to reflect the potential human response and is used to evaluate the effective bioactivity of the product (Merly e Smith, 2017) and our purpose is this study was to know how our nanoparticles could interact with the cells of the immune system.

Through this method, the cell viability resultant from the incubation with different concentrations of PCL and PCL/Glucan NPs was studied and the results are shown in the Fig. 15. Furthermore, cytotoxicity results obtained with MTT assay were confirmed by flow cytometry PI assay.

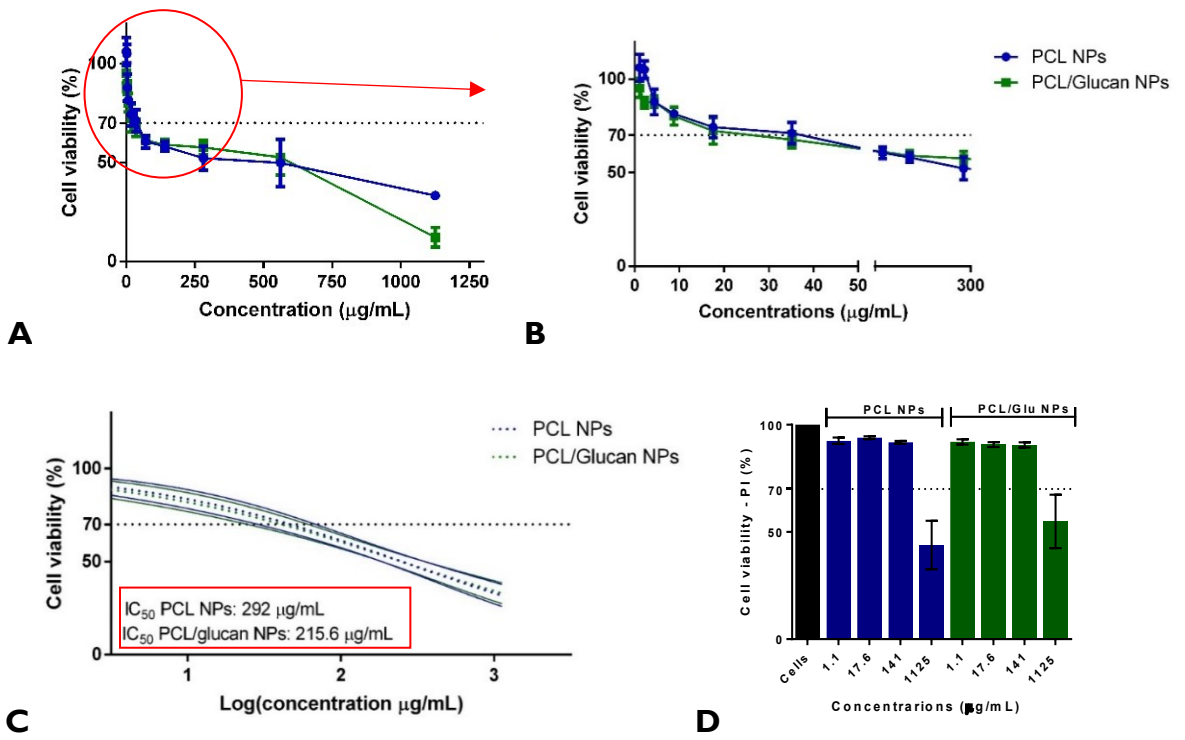

Figure 15: Cytotoxicity of PCL/Glucan and PCL NPs. A) Representation of all concentrations tested by the MTT assay after 24 h of incubation with NPs B) Detail (with the lower concentrations of the NPs) of the previous graph. C) The same MTT results presented in the

log of the concentration to calculate the IC50. D) Cytotoxicity evaluated with PI (flow cytometry). Data was analyzed using t- test corrected for multiple comparisons using the Holm-Šídák method $p<0.05$). (Mean ± SEM; n=4).

The NPs concentration used in the all immunotoxicology studies were calculated considering that all quantity of PCL that was dissolved in acetone formed NPs and for the PCL/Glucan NPs the same was assumed but in this case with the glucan presence in the NPs.

The half-maximal inhibitory concentration (IC50) indicates how much of a specific pharmacologic agent is required to inhibit a given biological activity by half (Aykul e Martinez-Hackert, 2016). According to Fig. 15C, the results shows that both nanoparticles have a similar cytotoxicity profile and do not show statistical difference between them (IC50: PCL 292 µg/mL and PCL/Glucan NPs 215.6 µg/mL). In fact, the concentrations tested that showed cell viability above 70 % were below 35.16 µg/mL. That value, compared to other nanoparticles studied in our laboratory (i.e chitosan), shows that the particles begin to be more cytotoxicity at lower concentrations.

Our results are quite different from those shown by Abamor and co-workers, which used PCL NPs with a size between 200 nm and 390 nm and that particles were loaded with NSO (*Nigella sativa* oil). In this study the cell viability was tested in concentrations ranging from 50 µg/ml to 1000 µg/ml and the authors observed a cell viability of 80 % for all concentrations tested. On the other hand, it was shown that NSO itself were more cytotoxic (IC50: 125 µg/mL) and the addition of the NSO into PCL NPs prevented its toxicity on macrophages (Abamor *et al.*, 2018).

Another study correlates the decrease in cell viability with the NP size. It was used PCL NPs (360 nm) and observed toxicity in concentrations above 300 µg/mL, in the same study they reported that bigger NPs had better viability (Singh e Ramarao, 2013). In our study, it occurred a change in the NPs characteristics when in DMEM medium (Fig. 9C), since the NPs decreased in size (98.7 nm) when compared with initial size (170.4 nm) and this may have influenced in the results for cell viability.

In the literature, a variety of studies demonstrated the biocompatibility of β-glucans. In one of them, Ji Lee and co-workers used laminarin, which is a type of 1,3-β-glucan and proved its effect on cell viability in RAW 264.7, having detected cell proliferation in concentrations

(between 100 µg/mL to 500 µg/mL. That stimulation was also in a concentration dependent manner (Lee *et al.*, 2012). The same results were noticed by Yu and colleagues, BSA-loaded glucan microparticles (2 µm to 4 µm), did not decrease cell viability in concentrations up to 400 µg/mL (Yu *et al.*, 2015).

In the present work, glucan NPs were not tested since this study had previously been done in our laboratory. In this previous study, the effect of the size of the glucan NPs on their immunotoxicological properties was studied (data not published). For instance, NPs around 300 nm did not cause cytotoxicity although, the same results were not observed when the NPs were smaller (around 100 nm), which indicates the importance of the NPs size in macrophages activation (data not published). All these results suggest that the different production methods, NPs sizes and the encapsulation into NPs of a specific drug could influence the result of the viability of immune cell lines.

Despite we cannot exclude the effect of glucan for PCL/Glucan NPs toxicity, since the IC50 is similar to the IC50 of PCL NPs, we can hypothesize, that the effect is rather related to the PCL core or it is related to the NPs size, which is similar for both nanoparticles.

3.2.2 PCL/Glucan NPs induces the inhibition of NO production at the higher NP concentration

Nitric oxide (NO) mediates many physiological functions and, consequently, it is commonly investigated under many different pathological conditions related to inflammation. NO is a key regulatory molecule with extensive metabolic, vascular, and cellular effects (Tessari *et al.*, 2010). While low levels of NO are beneficial for several physiological and cellular functions, high levels of NO may cause detrimental effects in the cells (Pacher, Beckman e Liaudet, 2007). The NO assay is based on the Griess reaction that fundamentally detect nitrite (NO^{-2}) that, under acidic conditions reacts with sulphanilamide and produce an azo compound that is quantified by measuring spectrophotometric absorption (Giustarini *et al.*, 2008).

In order to evaluate if the NPs have an effect on inflammation induction, we performed NO assay by incubating the nanoparticles with LPS-induced RAW 264.7. The NPs were prepared in apyrogenic water, LPS-free and sterile conditions with the purpose of eliminating possible contaminations that could interfere with the assay. In addition, the nanoparticle concentrations chosen did not present any toxicity. The results are shown in Fig. 16.

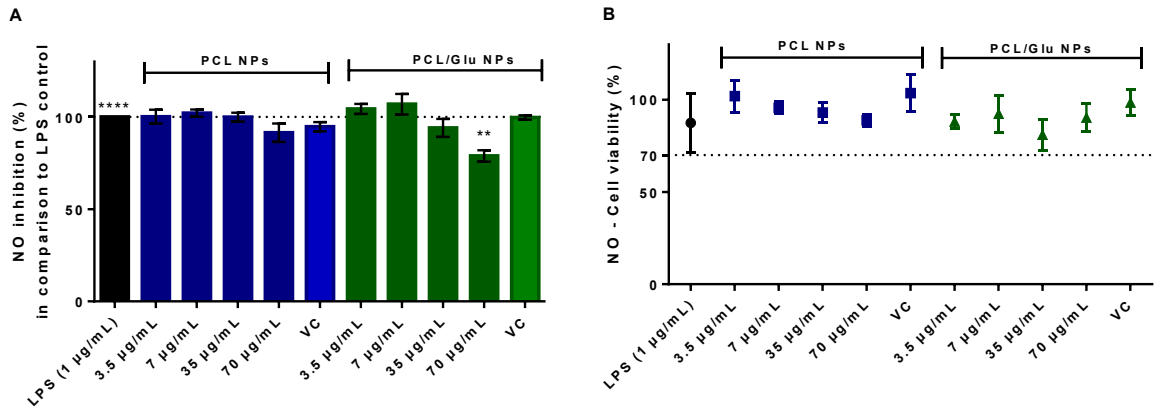

Figure 16: A) NO inhibition by LPS stimulated RAW 264.7 cell line after 24 h in culture with PCL and PCL/Glucan NPs, (Mean ± SEM; n=4). B) Effect on the cell viability after the incubation for 24 hrs with PCL and PCL/Glucan NPs (Mean ± SEM; n=3) and VC: vehicle control. Data analysed by one-way ANOVA comparing to LPS corrected for Dunnett method (** $p<0.01$ and **** $p<0.0001$).

According to the Fig. 16A, the PCL NPs did not inhibited NO production in any of the concentrations tested in comparison to LPS, the positive control.
On the other hand, for PCL/Glucan NPs the inhibition of NO production was observed in concentration of 70 µg/mL. The amount of the induced NO was decrease noticeable by the presence of glucan in the PCL/Glucan NPs, showing the inhibitive effect already reported in a few studies.

For instance, Choi and colleagues reported that the β-glucan (extracted from a yeast-like fungus) inhibited the production of NO in macrophages. They claimed that inhibition was due to the vitalization of macrophages by LPS through the HO-1 induction and the STAT1 pathways inhibition (Choi et al., 2016). The same results had Xu and co-workers were they studied Glucan from *Lentinus edodes* and it showed strong inhibition of LPS-induced pro-inflammatory mediators (Xu *et al.*, 2012). Therefore, our results are in agreement with the literature.

Importantly, for PCL and PCL/Glucan NPs, the vehicle control (VC- supernatants collected from the last washing step of the NPs) were also tested at the same dilution as the most concentrated NP formulation. Results show that the VC had no effect on the NO inhibition, meaning that the effect verified with PCL/Glucan NPs is indeed due to the NPs.

In order to check whether the decrease of the NO formation was due to NP toxicity at the higher concentration, after removing the supernatants for NO assay, the MTT assay was carried out. According to the Fig. 15B, there was no decrease in the cell viability.

3.2.3 PCL and PCL/Glucan NPs did not induce the NO production in RAW 264.7

Depending on the concentration tested, the effect may be stimulatory or may be inhibitory. With the aim of evaluating whether the PCL and PCL/Glucan NPs would be able to induce the production of NO by themselves, another test was done in the absence of LPS in the culture media. The induction of NO production by RAW 264.7 cell line was measured using the Griess reaction method after the incubation with the nanoparticles. The NPs were prepared in apyrogenic water, LPS-free and sterile conditions. The results are displayed in Fig. 17.

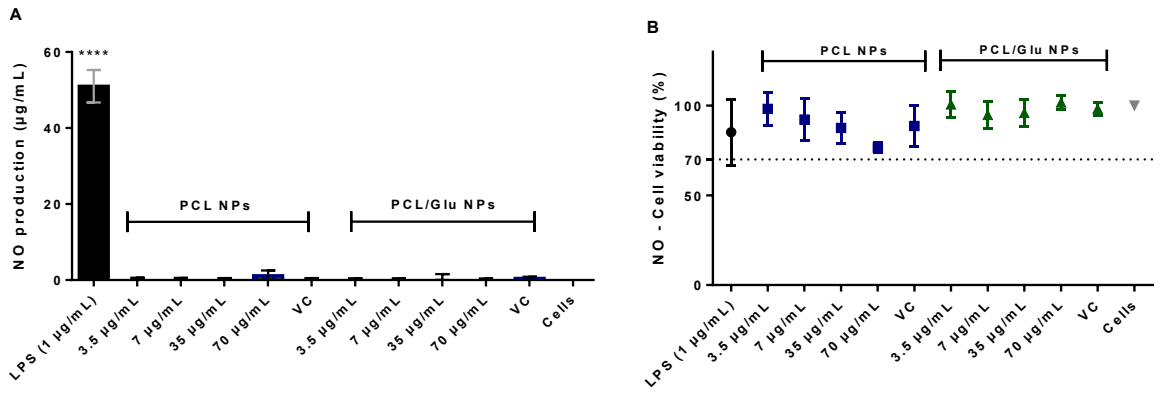

Figure 17: A) NO production by RAW 264.7 cell line after 24 h in culture with presence of PCL NPs and PCL/Glucan NPs, (Mean ± SEM; n =4). B) Effect on the cell viability after 24 h of incubation with PCL and PCL/Glucan NPs (Mean ± SEM; n=3), VC: vehicle control. Data analysed by one-way ANOVA comparing to LPS corrected for Dunnett method (****p< 0.0001).

None of the concentrations tested for PCL and PCL/Glucan NPs induced NO production in comparison with the LPS as a positive control (Fig.17A).

Despite that, a different result was found in literature, where a range of the PCL NP (202 nm) concentrations (50 µg/ml to 1000 µg/ml) were incubated with mouse J774 macrophage cell line. It was observed that the PCL NPs increased the NO production for all concentrations

tested (Abamor *et al.*, 2018). To note that the authors did not reported in the manuscript the result of the LAL assay, which would allow to confirm the absence of contaminants, like LPS in the NPs sample.

The same was observed in a study with glucan, it was observed that polysaccharides like glucan stimulate the NO production in a concentration-dependent manner in peritoneum macrophages (Akramiene *et al.*, 2007). Another studied conducted by Lee and co-workers used Laminarin (a glucan found in brown algae) that activated macrophages to release NO via a mechanism involving, at least in part, calcium signalling (Lee *et al.*, 2012).
However, in our case, the presence of glucan in the PCL/Glucan was not enough to induce the NO production.

In each experiment, after collecting the supernatant to quantify the NO, the MTT assay was performed to evaluate the metabolic activity of the cells during the NO assay. It was important to conclude that the nanoparticles were in non-cytotoxic concentrations and LPS-free, the cell viability were above 70 % in all concentrations tested (Fig. 17B).

3.2.4 None of the nanoparticles induce the ROS production

Reactive oxygen species (ROS) in immune cells are best known for their role in directly killing pathogens through the oxidative burst-mediated by NADPH oxidases in phagosomes (Sena e Chandel, 2012). Dying cells produce high levels of ROS, which are released into extracellular area when the cellular membrane is degraded during cell death. Attachment of dying cells to macrophages requires intercellular communication in which ROS may play a role. In this regard, ROS plays a critical regulatory role in determining the initiation and outcome of cellular phagocytosis (Tan *et al.*, 2016).

To study the possible effects of our NPs on ROS production we performed an assay based on DCF fluorescein assay. For that, NPs were produced in LPS-free condition.
Analyzing the Fig.18A, it can be inferred that the NPs did no induce the ROS production in the concentrations tested in comparison to the positive control (LPS).

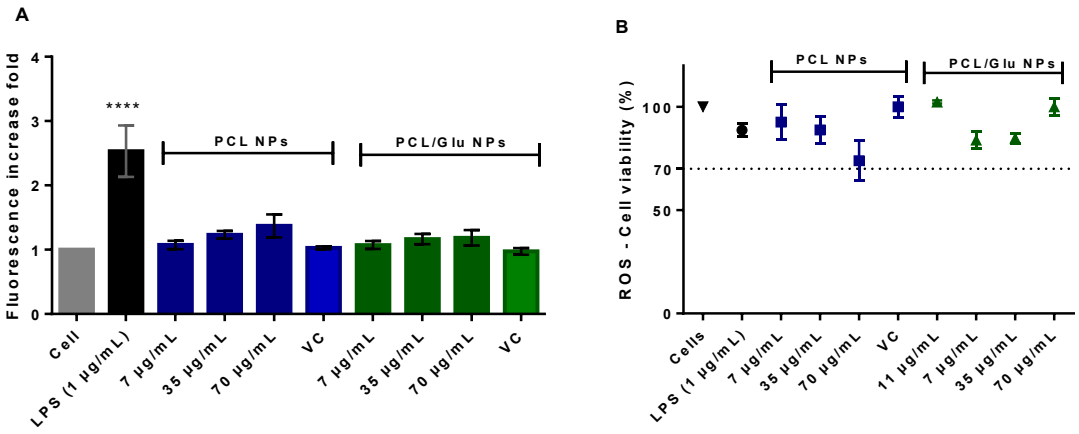

Figure 18: A) ROS production RAW 264.7 cell line after 24 h in culture with PCL NPs and PCL/Glucan NPs (Mean ± SEM; n=6). Data analysed by one-way ANOVA comparing to cell control and corrected for Dunnett method (****p< 0.0001). B) Effect on the cell viability after 24 h of incubation with PCL and PCL/Glucan NPs (Mean ± SEM; n=3) during the ROS assays. Data analysed by one-way ANOVA comparing to LPS corrected for Dunnett method, VC: vehicle control.

These results are in agreement with the literature. One study by Sing e Ramarao demonstrates that PCL NPs (363 nm) did not induced ROS production, in RAW 264.7cell line, for concentrations higher than 100 µg/mL whereas with higher concentration (300 µg/ml) showed 1.5- to 2-fold stimulation of ROS production (Singh e Ramarao, 2013). In fact, in our study, to maintain cell viability under the assay conditions we did not test values higher than 100 µg/mL. Nevertheless, with 70 µg/mL a tendency to increase the fluorescence is noticeable.

For glucan, one study correlates the nanoparticle size to the ROS production. Selenium NPs combined with Lentinan (Se/s-LNT, 33nm to 52 nm) were tested in the human cervix carcinoma (HeLa) cells in concentrations ranged from 12 µg/mL to 52 µg/mL. It was observed that in a smaller size, the ROS production is higher (Jia *et al.*, 2015). Another study made by (Baert *et al.*, 2016) tested β-glucan microparticles (GPs: 2 µm to5 µm), in PMBC of pigs and in all concentrations tested (100 µg/ml to 400 µg/ml) was observed the induction of ROS production.

In our study, the PCL/Glucan NPs did not induce the ROS production in any concentration tested (Fig. 18A). Therefore, the tendency for the appearance of the stimulation observed with the highest concentration of PCL disappears, when glucan is associated with PCL NPs.

In each experiment, after measuring the fluorescence, the MTT assay was accomplished to confirm that the chosen concentrations did not cause any decrease in cell viability (Fig. 18B). So if the cells were affected by the nanoparticles used, that could influence in the quantity of ROS produced and lead us to a discordant conclusion.

3.2.5 Higher concentration of PCL/Glucan NPs are less cytotoxic than PCL NPs for cell viability in human PBMCs

PBMCs are an important tool to assess the nanoparticle effects in immune system. They contain several types of cells such as lymphocytes, monocytes or macrophages. For this reason, the relatively easy availability of human PBMCs is very important for researchers to study the toxicity of new drugs or nanomedicine (Pourahmad e Salimi, 2015).
In the present study, the PBMCs were incubated with PCL and PCL/Glucan NPs for 24 h and the cell viability was evaluated by MTT and with PI. The results are shown in the Fig. 19.

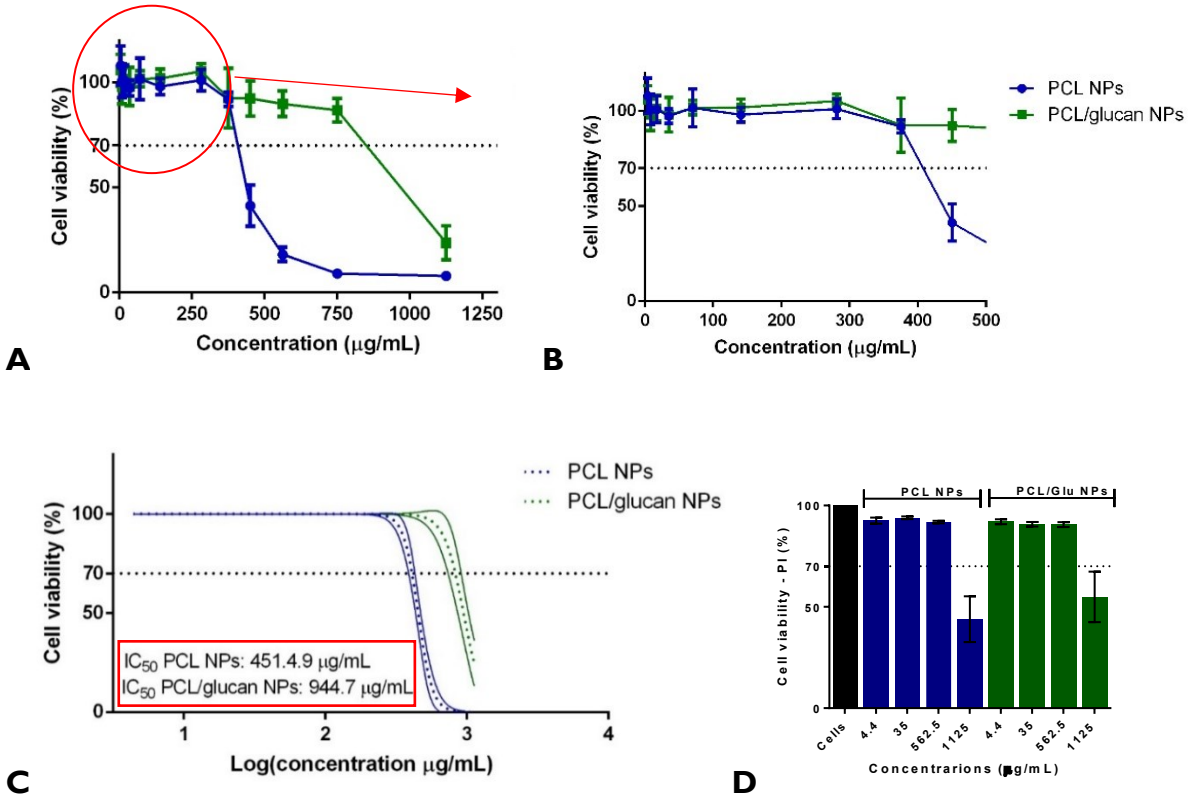

Figure 19: Cytotoxicity of PCL/Glucan and PCL NPs in human PBMCs assessed by MTT assay after 24 h of incubation with PCL and PCL/Glucan NPs. A) Representation of all concentrations tested. B) Detail (with the lower concentrations of the NPs) of the previous graph. C) The same MTT results presented in the log of the concentration to calculate the

IC50. D) Cytotoxicity evaluated with PI (flow cytometry). Data was analyzed using t-test corrected for multiple comparisons using the Holm-Šídák method ($p<0.05$). (Mean ± SEM; n=8). D) PI assay.

According to Fig. 19, the results demonstrated that for concentrations above 375 μg/mL PCL NPs showed to induce an accentuated decrease in cell viability in more than 50 %, while for PCL/Glucan NPs the cell viability starts to decrease only in concentrations above 750 μg/mL, the double of concentration observed for PCL NPs.
For this reason, the IC50 calculated for both NPs are distinct: 944.7 μg/mL and 451.9 μg/mL for PCL/Glucan and PCL NPs, respectively.

A study performed by Hwang and colleagues studied the cell viability in PBMCs (2.5 μg/mL to 50 μg/mL) using silica conjugated with Glucan NP (50 nm). The results showed that when the NP concentration was 12.5 μg/mL the cell viability decreased rapidly in a concentration-dependent manner and this was explained by authors through the size of the nanoparticles (Hwang *et al.*, 2018). In another report, the cell viability was tested in goat peripheral blood leukocytes after incubation with β-glucan and the results showed that the it did not affect leukocyte viability at the 200 μg/ml glucan concentration (Medina-Córdova *et al.*, 2018).

Previous work from our group, evaluated cell viability in the primary cell culture of spleen cells for PCL and PCL/Chitosan NPs (Jesus *et al.*, 2018). It could be observed a reduction of citotoxicity when the PCL NPs were blend with chitosan. For instance, in concentrations above 75 μg/mL was detected an increase of 50 % in cell viability compared to bare PCL NPs. These demonstrate an enhancement of biocompatibility of PCL/chitosan NP. This result is in agreement with the results obtained now, where bare PCL NPs are more toxic than PCL/Glucan NPs. In summary, we can conclude that the incorporation of glucan into PCL NPs increases the biocompatibility of the nanoparticle system when evaluated with human PBMCs.

3.2.6 The presence of glucan in the NPs increases its ability as a delivery system for proteins

The particulate delivery systems such as nanoparticles should allow concentrating and protecting biomolecules against degradation during administration. Moreover, particles

potentially increase the cell internalization of the bioactive molecules, which is important for its function.

Flow cytometry analysis of PBMCs were performed in order to understand if the PCL and PCL/Glucan NPs facilitate the protein cell internalization. For that, PBMCs were incubated with free FITC-BSA and with FITC-BSA adsorbed on both NPs.

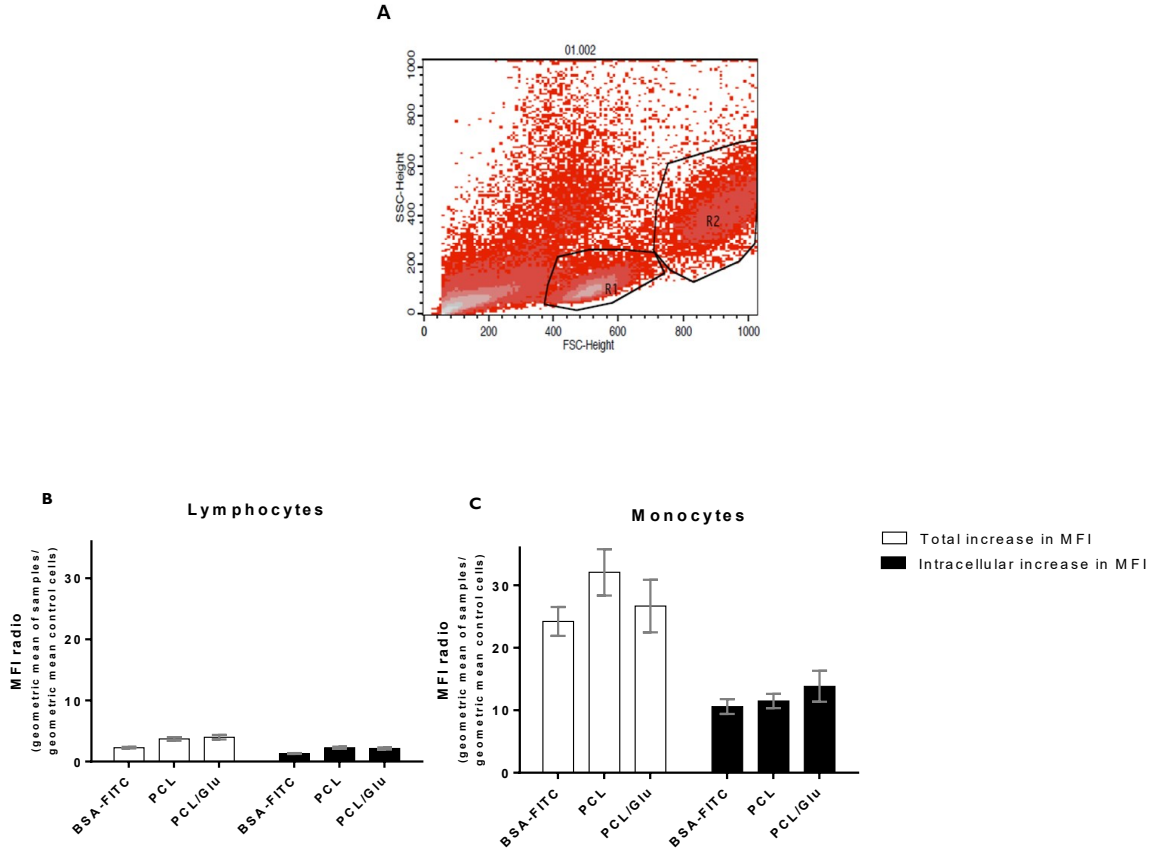

Figure 20: Cellular uptake of BSA (free or adsorbed on PCL or PCL/Glucan NPs surface) performed with PBMCs A) Flow cytometry setting regions used to identify PBMCs subpopulation: lymphocytes and monocytes were identified on a FSC vs SSC dot plot using free draw regions. B) Flow cytometry analysis of monocytes (R2 region) after 4 h incubation with formulations. C) Flow cytometry analysis of monocytes (R2 region) after 4 h incubation with formulations. Results obtained in the presence (black) or absence (white) of trypan blue. The results expressed as mean fluorescence intensity (MFI) ratio (left Y axis) between the geometric mean of the sample and the geometric mean of the background. Data are expressed as mean ± SEM, n=3. Data was analyzed using one-way ANOVA for multiple comparisons using Bonferroni ($p<0.05$).

According to Fig. 20, the total increase in MFI (white columns) corresponds to the BSA-FITC fluorescence that is either on the cell surface and in cell cytoplasm while the intracellular increase in MFI (black columns) corresponds only to the BSA-FITC fluorescence measured from the cell cytoplasm. It is possible to observe that for lymphocytes, the BSA-FITC uptake (total and intracellular) is similar for when is delivered by both nanoparticles and slightly lower when the BSA-FITC is used. On the other hand, for monocytes, although PCL NPs delivered more BSA-FITC to the cells, when analysing the intracellular delivery, the PCL/Glucan NPs led to a slightly better cell internalization, with the fluorescence fold 13.82 ± 2.47 in comparison with the control (BSA-FITC) 10.58 ± 1.19. This difference may be due to the presence of glucan into PCL NPs once the glucan is known for its recognition by macrophages, through the receptor dectin-1.

To illustrate these results, confocal laser scanning microscopy (CSLM) visualization of PBMCs uptake of the BSA-FITC adsorbed on the nanoparticle surface was performed. The confocal microscopy images of PBMCs cells following 4 h incubation with FITC-BSA (3.7 µg/mL) labeled to PCL and PCL/Glucan NPs (69 µg/mL) are shown in figure 21 and 22.

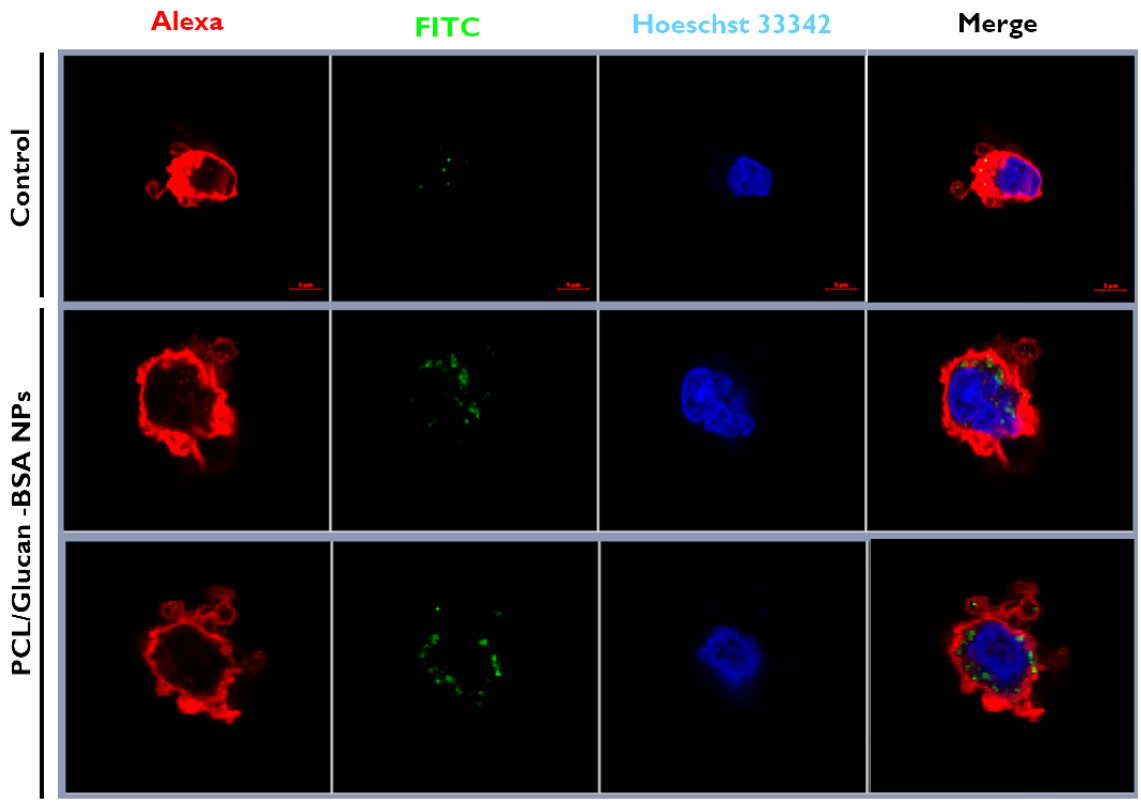

Figure 21: The cellular uptake of BSA-FITC delivered by PCL/Glucan NPs and the control was evaluate by BSA-FITC free protein. Confocal microscopy images show single and merged images of the cell membrane (red), the BSA-FITC (green) and the nucleus (blue).

The nanoparticle ability to deliver a model antigen was evaluated. According to Fig. 21 the NPs show to be a good nanosized polymeric delivery system, since is possible to observe higher concentration of the fluorophore BSA-FITC (green) when it was deliver by the PCL/Glucan NPs when compared to the BSA-FITC added freely to the cells.

Therefore, the higher cell internalization rate of BSA-FITC delivered by PCL/Glucan NPs that was documented by flow cytometry was confirmed by CSLM. That result was expected as particulate β-glucans bind to Dectin-1 receptor, broadly expressed on populations of myeloid cells (monocytes/macrophages and neutrophils) (Taylor *et al.*, 2002) which is extensively reported by several researchers and this fact may facilitate the internalization of the protein since protein is associated with NP.

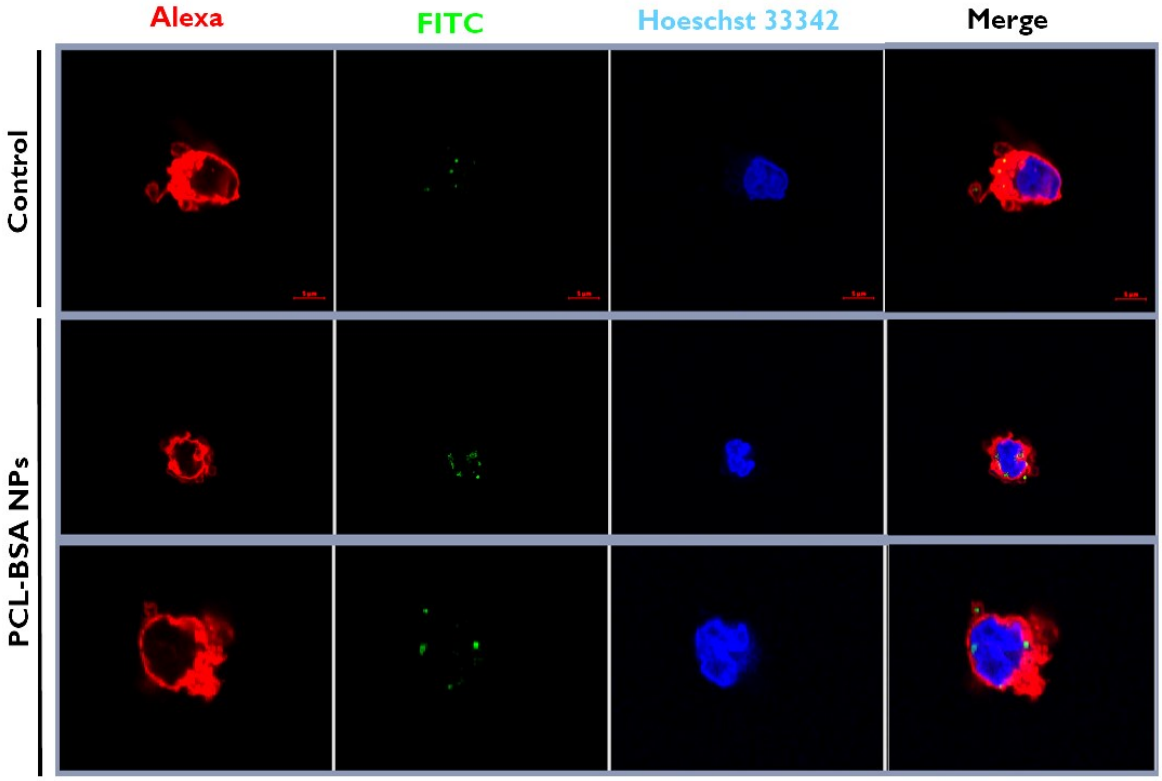

Figure 22: The cellular uptake of BSA-FITC delivered by PCL NPs and the control was evaluate by BSA-FITC free protein. Confocal microscopy images show single and merged images of the cell membrane (red), the BSA-FITC (green) and the nucleus (blue).

Similarly to PCL/Glucan NPs, PCL NPs also improved the delivery of BSA-FITC to PBMCs as it can be seen in Fig. 22.

3.2.7 PCL/Glucan NPs are more efficiently internalized by PBMCs than PCL NPs

After knowing that both PCL and PCL/Glucan NPs were good delivery systems for protein, we intended to investigate the ability of PCL/Glucan and PCL NPs to be internalized by PBMCs. In the previous studies with BSA-FITC we only assessed the protein uptake, rather than the NPs uptake. To study the NPs uptake, we encapsulated a fluorescent dye rhodamine, and later visualized NP uptake by CLSM.

Firstly, we produce the loaded nanoparticles with rhodamine. Rhodamine was dissolved in the aqueous phase during NP preparation. During the production process, we observed that our nanoparticles were not able to completely encapsulate all the rhodamine, and the supernatant between the washes turned pink. Therefore, it was not possible to quantify the rhodamine concentration present in each of the NPs which makes the comparisons between the two delivery systems not feasible.

As for all the assays described before, the cellular viability under the assay conditions was assessed by using MTT. In this case, it was observed for PCL/Glucan NPs in the higher concentration (69 µg/mL) a great decrease in cell viability. Thus, only the lower concentration (34.5 µg/mL) was choose for the uptake studies.

Images of the cells (Fig. 23A) confirm that PCL/Glucan NPs were internalized by monocytes and the NPs are localized in the cytoplasm (showed in white), proving the effective uptake by those cells. Flow cytometry analysis (Fig. 23B) revealed that the PCL/Glucan NPs has a slightly better internalization in monocytes than in lymphocytes.

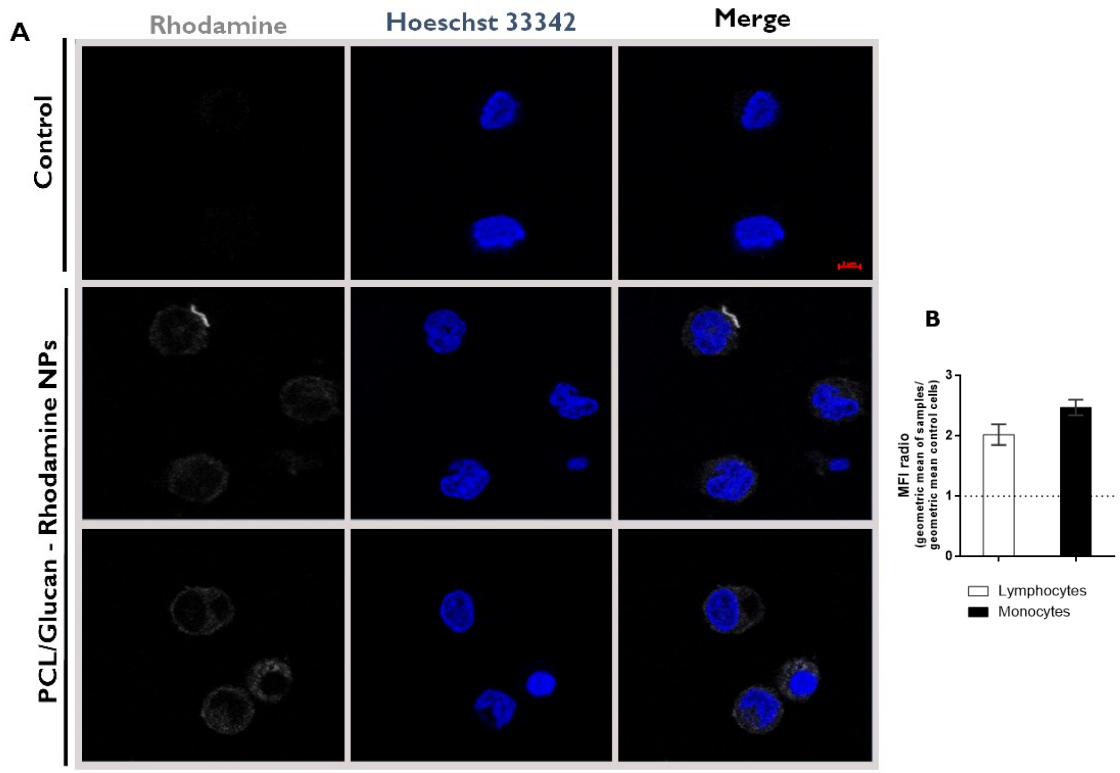

Figure 23: (A) Confocal microscopy images show single and merged images of the rhodamine loaded to PCL/Glucan NPs (white) and nucleus (blue) as well as cell control. (B) Flow cytometry analysis of NPs uptake by monocytes (R2 region) after 4 h incubation with PBMCs. NPs uptake was evaluated and the results expressed as mean fluorescence intensity (MFI) ratio (left Y axis) between the geometric mean of the sample and the geometric mean of the background. Data are expressed as mean ± SEM, n=3.

As shown in Fig. 24A, CLSM observations indicated that rhodamine loaded PCL NPs were internalized by the cells and also there is no difference between the uptake for lymphocytes and monocytes according to Fig. 24B.

Further studies regarding rhodamine quantification are required to optimize the NPs uptake studies and allow a comparison between the two delivery systems. So far, since we do not know how much rhodamine was loaded in each NP, we cannot be sure that the higher MFI increase for PCL/Glucan NPs corresponds to more NPs uptake, or to a higher rhodamine loading.

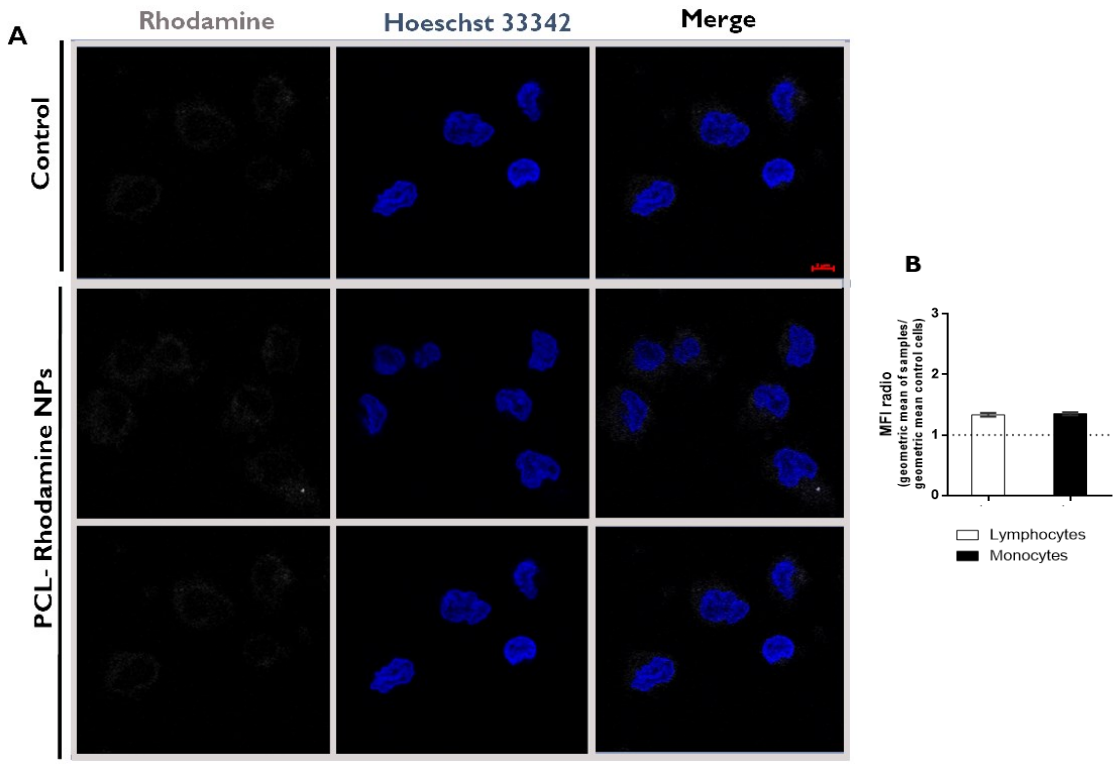

Figure 24: (A) Confocal microscopy images show single and merged images of the Rhodamine loaded to PCL NPs (white) and nucleus (blue) as wells as the cell control. (B) Flow cytometry analysis of NPs uptake by monocytes (R2 region) after 4 h incubation with PBMCs. NPs uptake was evaluated and the results expressed as mean fluorescence intensity (MFI) ratio (left Y axis) between the geometric mean of the sample and the geometric mean of the background. Data are expressed as mean ± SEM, n=3.

3.2.8 PCL NPs induce more IL-6 production than PCL/Glucan NPs however, both show similar induction of TNF-α.

Inflammatory pathways impact the pathogenesis of a number of chronic diseases and involve common inflammatory mediators and regulatory pathways. Inflammatory stimuli activate intracellular signalling pathways that then activate the production of inflammatory mediators (Ray, Huang e Tsuji, 2012). Cytokines are important biomarkers related to immune responses and are produced by many cells of the immune system (neutrophils, monocytes, macrophages, B-cells, and T-cells). The proinflammatory cytokines tumor necrosis factor (TNF-α) and interleukin (IL-6) are known to be two of the most important signalling molecules involved in conducting the response to foreign materials, and their upregulation is considered to be an accurate measure of inflammation (Wojdasiewicz, Poniatowski e Szukiewicz, 2014).

After cellular recognition, our NPs can be seen as invaders and induce the production of inflammatory mediators. Because of that, the purpose of our experiment was to evaluate the ability of PCL/Glucan and PCL NPs to induce cytokines production by lymphocytes isolated in PBMCs. For that, the cells were stimulated with different concentrations of LPS-free NPs during 24 h and the supernatants of the cultures were analyzed by ELISA to quantify the TNF-α. The concentration utilized was of 50 μg/mL and the cell viability was confirmed by Alamar blue assay.

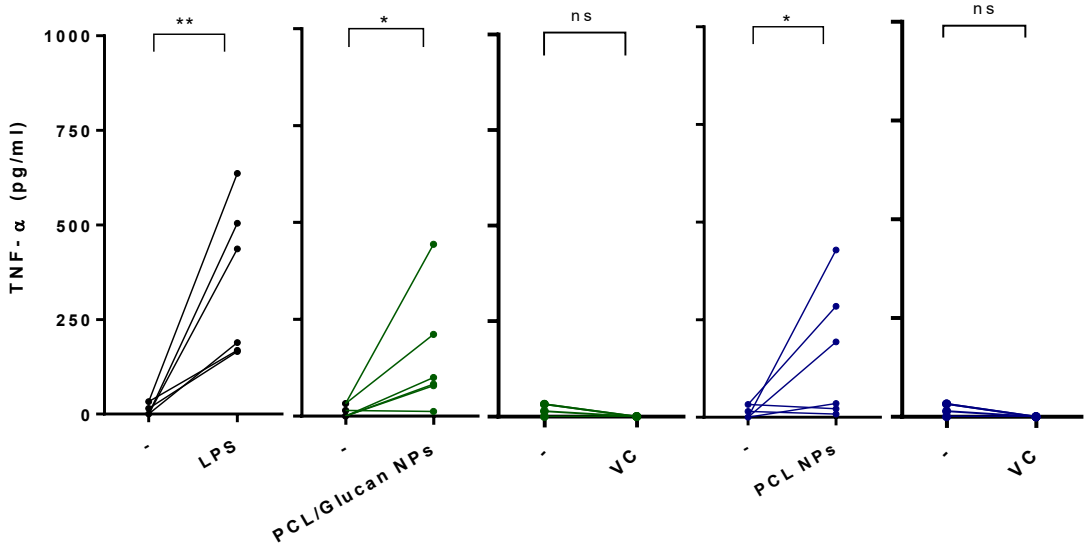

Figure 25: Effect of PCL and PCL/Glucan NPs on TNF-α production by PBMCs. This cytokine was measured using commercially available ELISA kits. LPS 2 ng/mL was used as a positive control and as expected induced elevated concentrations of this cytokine. Supernatants were harvested after 24 h of incubation with the formulations. Results represent the mean, n=6. Data were analyzed using t test comparing each result to the negative control. (*p<0.1; **p<0.01).

From Fig. 25, it is possible to observe that both nanoparticles induces the TNF-α production and seems not to have much difference between them. However, some quantitative differences in cytokine responses were observed for different donors.

In relation to glucan, there are a few studies using the polymer, for instance, Stopinšek and co-workers, did a comparison between different kinds of β-glucans, and for curdlan showed a concentration-dependent stimulation in the TNF-α, using human PBMCs (Stopinšek *et al.*, 2011). Another study using yeast β-glucan isolated from *Lactobacillus fermentum,* tested the

cytokine induction in PBMCs and shows an induced significant rise in TNF-α levels (Vitilic *et al.*, 2018).

And the same occurs when using yeast glucan as a particle, the Huang and co-workers revealed the yeast β-glucan particles (2 μm to 4 μm) reported a strong stimulation of TNF-α using wild-type murine bone marrow-derived myeloid dendritic cells (BMDCs), in a dose dependent manner (Huang *et al.*, 2009).

In regard to PCL, a study conducted by (Singh e Ramarao, 2013) tested the induction of cytokines by PCL NPs in RAW 264.7 cells and the results show a higher stimulation in the release of TNF-α (Singh e Ramarao, 2013). In polymers, a study was made to quantify the expression levels of proinflammatory cytokines in PCL surface using real-time polymerase chain reaction (RT-PCR). The results revealed that levels TNF- α were upregulated on bare PCL (Khandwekar *et al.*, 2011).

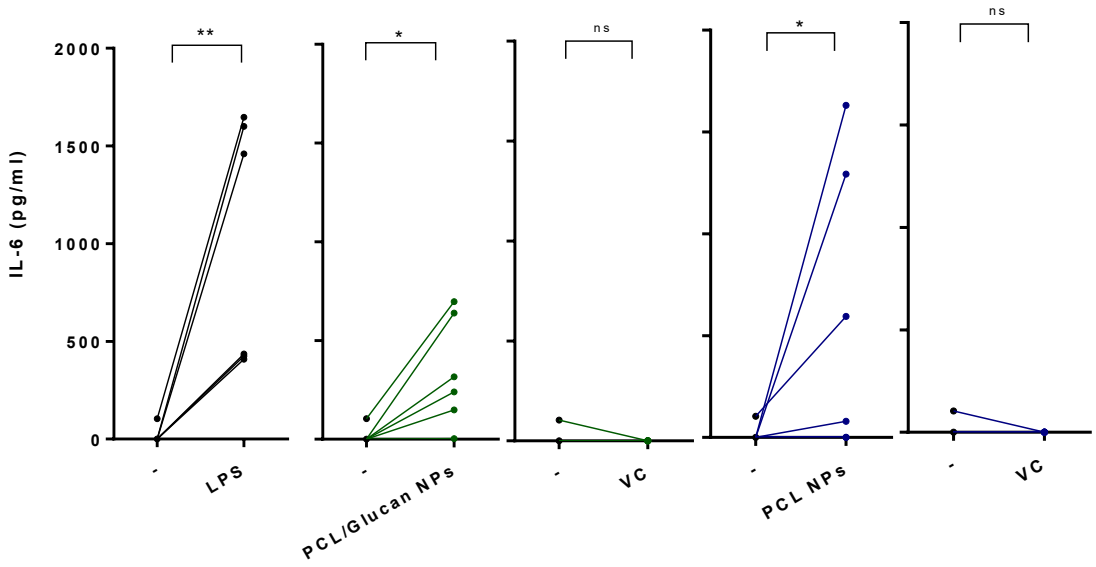

Figure 26: Effect of PCL and PCL/Glucan NPs on IL-6 production by PBMCs. This cytokine was measured using commercially available ELISA kits. LPS 2 ng/mL was used as a positive control and as expected induced elevated concentrations of this cytokine. Supernatants were harvested after 24 h of incubation with the formulations. Results represent the mean, n=6. Data were analyzed using t test comparing each result to the negative control (*p<0.1; **p<0.01).

IL-6 is a pro-inflammatory and anti-wound healing chemokine commonly analyzed when studying the inflammatory response induced by different biomaterials (Rees *et al.*, 2015). According to Fig. 26, PCL/Glucan NPs, induced a more reproducible but lower cytokine production in comparison to PCL NPs. In this last case, there was great divergence between the donors, from which 3 were markedly positive and 3 were negative.

A study reported by Huang and co-workers evaluated a cytokine production in human monocyte-derived dendritic cells by yeast β-glucan particles obtained from Saccharomyces *cerevisiae* and downregulation in IL-6 secretion was noted (Huang *et al.*, 2009). Conversely, in a study conducted by Noss and co-workers was observed that the curdlan, in human whole blood cultures, has a moderate cytokine production between 13 different kinds of β-glucan tested (Noss *et al.*, 2013).
Singh and colleagues tested the induction of cytokines by PCL NPs in RAW 264.7 cells and the results showed stimulation in the release of IL-6 (Singh e Ramarao, 2013). Other study performed by (Singh *et al.*, 2006) evaluated the induction of IL-6 by PCL blend to PLGA NPs (263 ± 3) in spleen cells, and the results showed a significantly higher cytokines induction in the concentration of 20 μg/mL. However, the opposite is observed when only the polymer is used in a study executed by Javanmard and co-workers it was developed a mimic blood vessel structurally made by the polymer PCL and studies in peripheral blood monocytes show a significantly decrease in IL-6 production compared to control (Haghjooy Javanmard *et al.*, 2016). Importantly, for both particle, the vehicle control did not induce cytokines production meaning the effect was specific from the nanoparticles.

At last, some considerations should be done regarding LPS-free conditions used for NP production. Indeed, several strategies were adopted to prevent endotoxin contamination, namely pyrogen-free water and NaOH treatment of all the laboratory material. However, since the results suggested that PCL NPs and PCL/glucan NPs induced IL-6 and TNF-α, endotoxin quantification of the LPS in the formulations could help understand if the strategies to prevent endotoxin contamination were successful and if these cytokines were induced by the endotoxin-free NPs.

3.2.9 PCL/Glucan NPs present a hemolytic activity higher than PCL NPs

Erythrocytes (red blood cells) are the major constituents of the blood contributing to nearly 45% of the blood volume which contains hemoglobin, a red colour heme protein that carries

oxygen to all the tissues of the body for energy generation (Evanl e Anand, 2011). Hemolysis is the rupture of red blood cells that can lead to anemia, jaundice and others pathological conditions.

In view of that, hemolysis is an immunotoxicological assay that was performed to evaluate the biocompatibility of the NPs with blood components. To evaluate the hemolytic activity of PCL and PCL/Glucan NPs in human blood, several concentrations were tested. Furthermore, we wanted to evaluate the NPs hemocompatibility in distinct conditions, thus in Fig. 27A are the results for NPs produced in LPS-free conditions and apyrogenic water and Fig. 27B the NPs produced in no endotoxin-free conditions and concentrated in milliQ water.

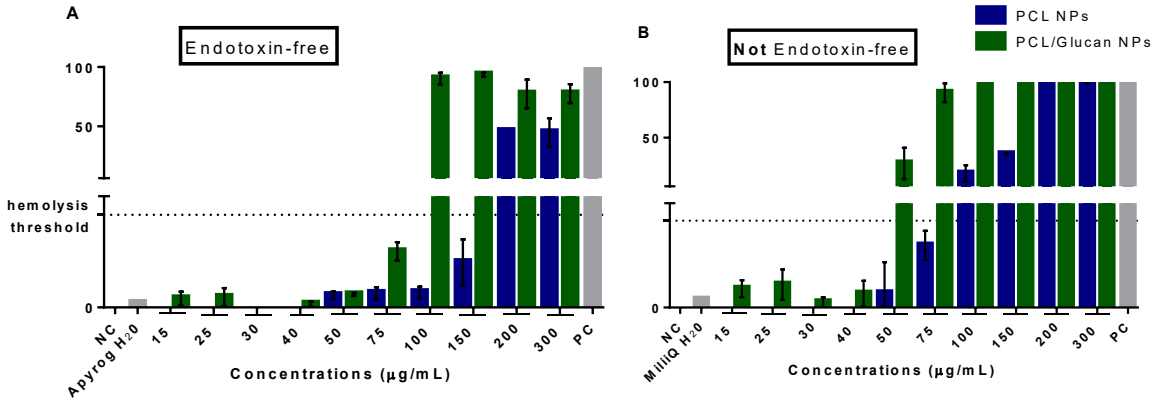

Figure 27: Results of hemolysis assay. A) Hemolytic effect of different concentrations for PCL/Glucan and PCL NPs concentrated in apyrogenic water and under LPS-Free conditions, in human whole blood (mean ± SEM, n=8). B) PCL/Glucan and PCL NPs produced in a no endotoxin-free environment and concentrated in milliQ water. Results were expressed in comparison with cells treated with Triton X-100 (positive control (PC) 100 % hemolysis) and cells treated only with PBS (negative control (NC) - 0% hemolysis).

According to Fig. 27 it is possible to observe differences between the tested conditions. The NPs produced in no endotoxin-free conditions (Fig. 27B) showed to have more hemolytic activity than when the NPs were produced in a sterile environment and using apyrogenic water (Fig. 27A).

In order to explain these differences, we evaluated the possible influence of LPS in the hemolysis assays, so we incubated several concentrations of PCL/Glucan and PCL NPs in the presence of two LPS concentrations (1 µg/mL and 0.4 ng/mL - these concentrations are enough to indicate contamination of the samples and interfere in the assay such as cytokines

production). Our results (data not shown) demonstrated that the presence of LPS in the sample did not increase the NPs hemolytic activity.

We could not explain the divergent results obtained with the two conditions tested, our intention was to see differences in the hemolysis when in LPS presence, however even in the controls utilized, different waters and the two different LPS concentration, the hemolysis was not induced.

Despite the differences between the tested conditions, the behavior of PCL/Glucan and PCL NPs maintain, where the PCL NPs demonstrated better hemocompatibility and in view of the safety conditions that we assume is important in the evaluation of a safe NPs, we decided to compare and discuss our results with NPs produced in LPS-free conditions.

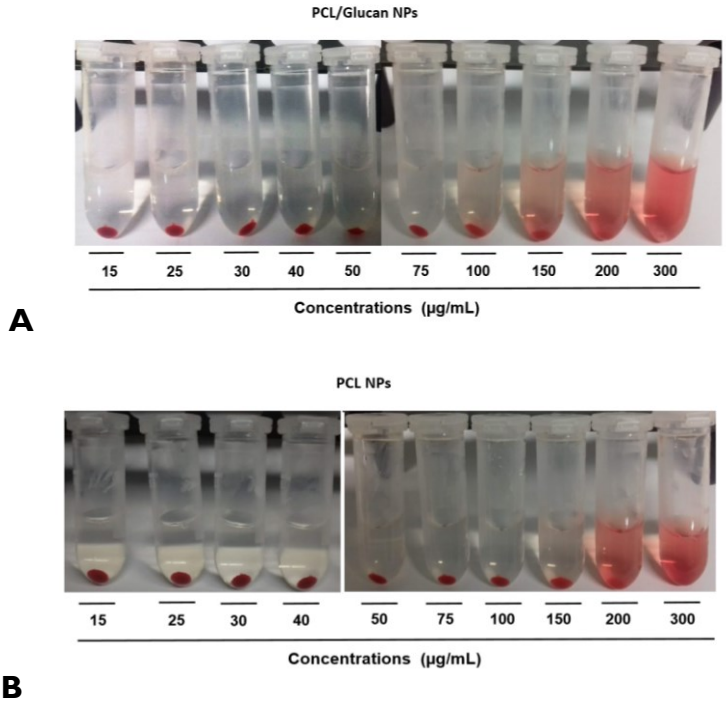

Figure 28: Visual evidence of the eppendorfs containing diluted total blood after being incubated with different concentration of PCL/Glucan NPs and C) PCL NPs in an endotoxin-free condition and concentrated in apyrogenic water.

The results in Fig. 27A showed that none of the NPs solvent (apyrogenic water and NC - PBS) caused hemolysis in human blood as the percentage of hemolysis was less than 5 % accordingly to ASTM E2524- 08 (standard test method for analysis hemolytic properties of nanoparticles)(Choi *et al.*, 2011). Controls with the NPs but without blood were prepared to evaluate the possible NPs interferences with the assay and no interferences were detected.

The PCL/Glucan NPs demonstrated hemolytic activity in concentrations above 100 µg/mL. In general, there are not many studies about hemocompability of glucan NPs in whole blood. Zakir Hossain and colleagues studied liposomes encapsulated with glucan (30.2 nm) and showed a hemolysis range of 8 % to10 % with increasing concentrations of 0 µg/mL to 40 µg/mL (Zakir Hossain e Khiyami, 2015). As a polymer, a study used curdlan to coat the PLGA NPs and the polymer improved the NPs biocompatibility of the in whole sheep blood erythrocytes (Lehtovaara, Verma e Gu, 2012).

The PCL is one of the most extensively employed polyesters in biomedical and tissue engineering applications due to its characteristics; there are several studies where the polymer is used as nanofiber, scaffold, nanostructured surfaces that prove the hemocompatibility of the polymer (Horakova *et al.*, 2018) (Haghjooy Javanmard *et al.*, 2016) (Jiang *et al.*, 2011). As a nanoparticle, methotrexate loaded to PCL microspheres (23.88 ± 1.15) was studied by Dhanka and co-workers and no hemolysis was reported, the same is observed when it used the conjugated polymers (PCL-Chitosan) did not show any hemolytic activity (Vásquez Marcano *et al.*, 2018) (Dhanka, Shetty e Srivastava, 2017).

In our results, the PCL NPs show hemocompatibility up to 150 µg/mL, this may happen due to the NPs size. A study shows that large surface area ensures effective adsorption of NPs on the cell surface and the particles smaller than 100 nm are effectively adsorbed on the erythrocyte surface without causing damage in the cell whereas 600 nm particles deformed the membrane and entered the cells, resulting in hemolysis (Zhao *et al.*, 2011).

These results can be supported by the visualisation of the tubes containing the diluted total blood incubated with the different formulations show in Fig. 28A-B.

Chapter IV -
Concluding remarks and future perspectives

Chapter IV – Concluding remarks and future perspectives

The interest in nanotechnology has emerged exponentially during the past years and with it several possible applications such as development of novel drug delivery system using polymers. Nanoparticles can provide enormous advantages regarding stability, specificity, drug delivery capacity, ability for control the release of the drug and the possibility to use in different routes of administration.

Despite several studies in the literature describing methods of preparation, drug encapsulation and efficiency of nanomedicines only a few reports are found in concern the immunotoxicity impact of the nanoparticles in the immune system cells.

The work present here showed the production of a new polymeric delivery system using two polymers glucan and PCL. Those polymers were chosen due to their characteristics, PCL is a widely used as polymer and is approved by FDA while glucan has an important immunomodulatory properties, being capable of modifying the biological response, which means it is able to enhance or restore the immune system.

Our main goal was to evaluate if the glucan presence in the PCL NPs would modify its performance as protein delivery system and the imunotoxicological properties of the PCL NPs. The studies demonstrated that in relation to the NPs ability as a delivery system for proteins the PCL/Glucan showed to increase the cellular uptake of the proteins when compared to the free protein and PCL NPs. In relation to the NPs internalization by the primary cells PBMCs, the PCL/Glucan NPs proved to be efficiently internalized by monocytes. Therefore, deeper knowledge in understanding the interactions involved in NPs uptake is needed when using it as a drug delivery system and the possibility to control the delivery and release of drug to a specific site at the precise time. Relative to the immunotoxicity assays the glucan presence in the PCL NPs showed better cell viability when tested in PBMCs although no differences were observed when a different cell line as a RAW 264.7 was tested. For both NPs was observed the same cytotoxicity profile. To develop a safer nanoparticle is necessary to pay special attention to the size once in the literature showed that smaller NPs tends to be more cytotoxic.

Another difference was observed in the hemolysis assays, PCL NPs showed to be more hemocompatible than PCL/Glucan NPs. The presence of glucan in the PCL NPs did not improve the hemocompatibility of the NP, on the contrary, the PCL/Glucan NPs demonstrated more hemolytic effects.

For the immunomodulation assays, both NPs showed a good result with no production of NO and ROS, however, the PCL/Glucan NPs presented capacity of inhibitory effect in NO production. Regarding cytokines production, PCL induced more IL-6 production than PCL/Glucan. However both showed similar induction of TNF-α. For that assay is important to assure the absence of endotoxin in the NPs in order to avoid false positive.

At last, some considerations should be done regarding LPS-free conditions used for NP production. Indeed, several strategies were adopted to prevent endotoxin contamination, namely pyrogen-free water and NaOH treatment of all the laboratory material as was confirmed by LAL assay for PCL NPs. The PCL/Glucan NPs showed glucan interference on the LAL assay that was not resolved with the use of a known buffer Glucashield®. To overcome this challenge, some alternatives are important to have in mind in the future when study immunotoxicological assays that are very sensitive for LPS, such as cytokine production. One of them is to use polymyxin B as an inhibitor of LPS and in this way make sure that the effect is rather related to the NPs, increasing the robustness to the assay.

According to manufacturer's instructions, the interference of the NPs on LAL assay, can be detected by adding to the samples a known amount of control standard endotoxin (CSE) and subtract the endotoxin measured in the sample with the normal samples (without addition of CSE), if the value is within the range of the confidence interval is not consider the NP interference.

Furthermore, other immunotoxicological assays should be done to increase the information necessary for the *in vivo* application. However, the guidelines do not list them, systematically, leaving the subject a bit ambiguous. In addition, determined guidelines specifically applied to the safety of nanomaterials are needed and the biological effect on the immune system is important to consider for the development of a safe-by-design for new nanomedicines.

Chapter V

References

Chapter V - References

ABAMOR, Emrah Sefik *et al.* - *Nigella sativa* oil entrapped polycaprolactone nanoparticles for leishmaniasis treatment. **IET Nanobiotechnology**. . ISSN 1751-8741. (2018). doi: 10.1049/iet-nbt.2018.5115.

AKRAMIENE, Dalia *et al.* - Effects of beta-glucans on the immune system. **Medicina**. . ISSN 1648-9144. (2007). doi: 10.1016/S0928-8244(02)00345-0.

ALEX, Angel Treasa *et al.* - Development and evaluation of carboplatin-loaded PCL nanoparticles for intranasal delivery. **Drug Delivery**. . ISSN 15210464. (2016). doi: 10.3109/10717544.2014.948643.

ALEXIS, Frank *et al.* - Factors affecting the clearance and biodistribution of polymeric nanoparticles. Em **Molecular Pharmaceutics.**

ANUSUYA, Sathiyanarayanan; SATHIYABAMA, Muthukrishnan - Preparation of β-d-glucan nanoparticles and its antifungal activity. **International Journal of Biological Macromolecules**. . ISSN 18790003. (2014). doi: 10.1016/j.ijbiomac.2014.07.011.

AVILA, *et al.* - Microcapsules PCL with essential oil citronella. **Adv. Tissue Eng. Regen Med. Open Access**. (2017); 2(2):159–162. doi: 10.15406/atroa.2017.02.00024.

AYKUL, Senem; MARTINEZ-HACKERT, Erik - Determination of half-maximal inhibitory concentration using biosensor-based protein interaction analysis. **Analytical Biochemistry**. . ISSN 10960309. (2016). doi: 10.1016/j.ab.2016.06.025.

AZIMI, Bahareh *et al.* - Poly (∈-caprolactone) Fiber: An Overview. **Journal of Engineered Fibers and Fabrics**. . ISSN 1558-9250. (2018). doi: 10.1177/155892501400900309.

BAERT, Kim *et al.* - Duality of β-glucan microparticles: Antigen carrier and immunostimulants. **International Journal of Nanomedicine**. . ISSN 11782013. (2016). doi: 10.2147/IJN.S101881.

BADRI, Waisudin *et al.* - Effect of process and formulation parameters on polycaprolactone nanoparticles prepared by solvent displacement. **Colloids and Surfaces A: Physicochemical and Engineering Aspects**. . ISSN 18734359. (2017). doi:

10.1016/j.colsurfa.2016.12.029.

BERG, J. Michael *et al.* - The relationship between pH and zeta potential of ~ 30 nm metal oxide nanoparticle suspensions relevant to in vitro toxicological evaluations. **Nanotoxicology**. . ISSN 17435390. (2009). doi: 10.3109/17435390903276941.

BHOWMIK, Arijit; KHAN, Rajni; GHOSH, Mrinal Kanti - Blood Brain Barrier: A Challenge for Effectual Therapy of Brain Tumors. **BioMed Research International**. . ISSN 2314-6133. (2015). doi: 10.1155/2015/320941.

BORASCHI, Diana; MOEIN MOGHIMI, S.; DUSCHL, Albert - Editorial: Interaction Between the Immune System and Nanomaterials: Safety and Medical Exploitation. **Current Bionanotechnology**. . ISSN 22135294. (2016). doi: 10.2174/2213529402011607181749O4.

BORASCHI, Diana *et al.* - Nanoparticles and innate immunity: new perspectives on host defence. **Seminars in immunology**. . ISSN 1096-3618. (2017). doi: 10.1016/j.smim.2017.08.013.

CAI, Zhixiang; ZHANG, Hongbin - Recent progress on curdlan provided by functionalization strategies. **Food Hydrocolloids**. . ISSN 0268005X. (2017). doi: 10.1016/j.foodhyd.2016.09.014.

CHAN, Godfrey Chi-Fung; CHAN, Wing Keung; SZE, Daniel Man-Yuen - The effects of β - glucan on human immune and cancer cells. (2009) 1–11.

CLOGSTON, Jeffrey D.; PATRI, Anil K. - Zeta Potential Measurement. **Methods in molecular biology (Clifton, N.J.)**. . ISSN 1940-6029. (2011). doi: 10.1007/978-1-60327-198-1_6.

COLMENARES-ROLDAN, Gabriel Jaime *et al.* - Production of bioabsorbible nanoparticles of polycaprolactone by using a tubular recirculating system. **DYNA**. . ISSN 0012-7353. (2018). doi: 10.15446/dyna.v85n204.62292.

CHENG, Christopher J. *et al.* - A holistic approach to targeting disease with polymeric nanoparticles. **Nature Reviews Drug Discovery**. . ISSN 14741784. (2015). doi: 10.1038/nrd4503.

CHIN, Suk Fun; AZMAN, Aressa; PANG, Suh Cem - Size Controlled Synthesis of Starch

Nanoparticles by a Microemulsion Method Size Controlled Synthesis of Starch Nanoparticles by a Microemulsion Method. **Journal of Nanomaterials**. (2014). doi: 10.1155/2014/763736.

CHOI, Jonghoon *et al.* - Physicochemical Characterization and in vitro hemolysis evaluation of silver nanoparticles. **Toxicological Sciences**. ISSN 10966080. 123:1 (2011) 133–143

CROTTY, Shane - A brief history of T cell help to B cells. **Nat Revl Immunol**. 15:3 (2015)185–189.

CRUCHO, Carina I. C.; BARROS, Maria Teresa - Polymeric nanoparticles: A study on the preparation variables and characterization methods. **Materials Science and Engineering C**. . ISSN 09284931. (2017). doi: 10.1016/j.msec.2017.06.004.

DANAFAR, Hossein; SCHUMACHER, Udo - MPEG–PCL copolymeric nanoparticles in drug delivery systems. **Cogent Medicine**. (2016). doi: 10.1080/2331205X.2016.1142411.

DANAFAR, H. - Applications of copolymeric nanoparticles in drug delivery systems. **Drug Research**. ISSN 21949387. (2016). doi: 10.1055/s-0042-109865.

DHANKA, Mukesh; SHETTY, Chaitra; SRIVASTAVA, Rohit - Injectable methotrexate loaded polycaprolactone microspheres: Physicochemical characterization, biocompatibility, and hemocompatibility evaluation. **Materials Science and Engineering C**. ISSN 09284931. (2017). doi: 10.1016/j.msec.2017.08.055.

DOBROVOLSKAIA, Marina A.; MCNEIL, Scott E. - Immunological properties of engineerednanomaterials. **Nature Nanotech.** ISSN 1748-3387. 2:8 (2007) 469–478.

DOBROVOLSKAIA, Marina A.; GERMOLEC, Dori R.; WEAVER, James L. - Evaluation of nanoparticle immunotoxicity. **Nature Nanotechnology**. ISSN 17483395. (2009). doi: 10.1038/nnano.2009.175.

DOBROVOLSKAIA, Marina A. - Pre-clinical immunotoxicity studies of nanotechnologyformulated drugs: challenges, considerations and strategy. HHS Public Access. **J Control Release**. ISSN 1527-5418. 220:0 0 (2016) 571–583.

EVANI, S.J; ANAND, K.- Hemocompatibility of nanopar-ticles. In: Sitharaman B (ed.) **Nanobiomaterials handbook**.Vol. 31, London: Taylor and Francis Group, 2011.

FAROKHZAD, Omid C.; LANGER, Robert - Impact of nanotechnology on drug delivery. **ACS Nano**. ISSN 19360851. (2009). doi: 10.1021/nn900002m.

GIUSTARINI, Daniela *et al.* - Nitrite and Nitrate Measurement by Griess Reagent in Human Plasma: Evaluation of Interferences and Standardization. **Methods in Enzymology**. . ISSN 00766879. (2008). doi: 10.1016/S0076-6879(07)00823-3.

HAGHJOOY JAVANMARD, Shaghayegh *et al.* - In vitro hemocompatibility and cytocompatibility of a three-layered vascular scaffold fabricated by sequential electrospinning of PCL, collagen, and PLLA nanofibers. **Journal of Biomaterials Applications**. . ISSN 15308022. (2016). doi: 10.1177/0885328216652068.

HORAKOVA, Jana *et al.* - Comprehensive assessment of electrospun scaffolds hemocompatibility. **Materials Science and Engineering C**. . ISSN 09284931. (2018). doi: 10.1016/j.msec.2017.05.011.

HUANG, Haibin *et al.* - Distinct patterns of dendritic cell cytokine release stimulated by fungal β-glucans and toll-like receptor agonists. **Infection and Immunity**. . ISSN 00199567. (2009). doi: 10.1128/IAI.00086-09.

HUSSAIN, Salik; VANOIRBEEK, Jeroen A. J.; HOET, Peter H. M. - Interactions of nanomaterials with the immune system. **Wiley Interdisciplinary Reviews: Nanomedicine and Nanobiotechnology**. . ISSN 19395116. (2012). doi: 10.1002/wnan.166.

HWANG, Jangsun *et al.* - Synthesis of Beta-glucan Nanoparticles for the Delivery of Single Strand DNA. **Biotechnology and Bioprocess Engineering**. . ISSN 19763816. (2018). doi: 10.1007/s12257-018-0003-4.

JANEWAY, *et al.* Immunobiology: The Immune System in Health and Disease. 5th edition. New York: Garland Science; 2001. **Immunological memory.** Available from: https://www.ncbi.nlm.nih.gov/books/NBK27158/

JESUS, Sandra *et al.* - The Inclusion of Chitosan in Poly-ε-caprolactone Nanoparticles: Impact on the Delivery System Characteristics and on the Adsorbed Ovalbumin Secondary Structure. **AAPS PharmSciTech**. (2018). doi: 10.1208/s12249-017-0822-1.

JIA, Xuewei *et al.* - Construction of selenium nanoparticles/β-glucan composites for enhancement of the antitumor activity. **Carbohydrate Polymers**. . ISSN 01448617. (2015). doi: 10.1016/j.carbpol.2014.09.088.

JONG, Wim H. DE; BORM, Paul J. A. - Drug delivery and nanoparticles:applications and hazards. **International journal of nanomedicine**. . ISSN 1176-9114. (2008).

JUILLERAT-JEANNERET, Lucienne - Critical Analysis of Cancer Therapy using Nanomaterials. Em **Nanotechnologies for the Life Sciences**

KANKE, M. *et al.* - Application of curdlan-tables controlled drug released. **Pharmaceutical Research**. 9:3 (1992).

KHANDWEKAR, Anand P. *et al.* - Surface engineering of polycaprolactone by biomacromolecules and their blood compatibility. **Journal of Biomaterials Applications**. . ISSN 08853282. (2011). doi: 10.1177/0885328210367442.

KIM, Byung Do; NA, Kun; CHOI, Hoo Kyun - Preparation and characterization of solid lipid nanoparticles (SLN) made of cacao butter and curdlan. **European Journal of Pharmaceutical Sciences**. . ISSN 09280987. (2005). doi: 10.1016/j.ejps.2004.10.008.

KIM, Min Young *et al.* - Prevention of post-surgical peritoneal adhesion in rats using curdlan and gellan gum hydrogels. **Macromolecular Research**. ISSN 15985032. 20:12 (2012)1289–1293.

KOLESKE, J. V. - Blends Containing Poly(ε-caprolactone) and Related Polymers. **Polymer Blends**

LE, Mai Huong *et al.* - The dual effect of curcumin nanoparticles encapsulated by 1-3/1-6 *β* -glucan from medicinal mushrooms *Hericium erinaceus* and *Ganoderma lucidum*. **Advances in Natural Sciences: Nanoscience and Nanotechnology**. ISSN 2043-6262. 7:4 (2016)045019.

LEE, Ji Young *et al.* - Immunostimulatory effect of laminarin on RAW 264.7 mouse macrophages. **Molecules**. ISSN 14203049. 17:5 (2012) 5404–5411.

LEHTOVAARA, Benjamin C.; VERMA, Mohit S.; GU, Frank X. - Synthesis of curdlan-graft-poly(ethylene glycol) and formulation of doxorubicin-loaded core-shell nanoparticles. **Journal**

of Bioactive and Compatible Polymers. . ISSN 08839115. (2012). doi: 10.1177/0883911511432511.

LI, Hongyan *et al.* - Synthesis and cytotoxicity of selenium nanoparticles stabilized by α-D-glucan from Castanea mollissima Blume. **International Journal of Biological Macromolecules**. . ISSN 18790003. (2019). doi: 10.1016/j.ijbiomac.2019.02.085.

LI, Rutian *et al.* - Preparation and evaluation of PEG-PCL nanoparticles for local tetradrine delivery. **International Journal of Pharmaceutics**. . ISSN 03785173. (2009). doi: 10.1016/j.ijpharm.2009.06.007.

LUCIANI, Alessia *et al.* - PCL microspheres based functional scaffolds by bottom-up approach with predefined microstructural properties and release profiles. **Biomaterials**. . ISSN 01429612. (2008). doi: 10.1016/j.biomaterials.2008.09.007.

MAAZ, A. *et al.* - Influence of nanoprecipitation method parameters on nanoparticles loaded with gatifloxacin for ocular drug delivery. **IJASR International Journal of Academic Scientific Research**. . ISSN 1878-5905. (2015).

MASARUDIN, Mas Jaffri *et al.* - Factors determining the stability, size distribution, and cellular accumulation of small, monodisperse chitosan nanoparticles as candidate vectors for anticancer drug delivery: Application to the passive encapsulation of [14C]-doxorubicin. **Nanotechnology, Science and Applications**. . ISSN 11778903. (2015). doi: 10.2147/NSA.S91785.

MAZZARINO, Letícia *et al.* - Nanoparticles made from xyloglucan-block-polycaprolactone copolymers: Safety assessment for drug delivery. **Toxicological Sciences**. . ISSN 10960929. (2015). doi: 10.1093/toxsci/kfv114.

MCINTOSH, M.; STONE, B. A.; STANISICH, V. A. - Curdlan and other bacterial (1→3)-β-D-glucans. **Applied Microbiology and Biotechnology**. . ISSN 01757598. (2005). doi: 10.1007/s00253-005-1959-5.

MEDINA-CÓRDOVA, Noé *et al.* - Immunostimulant effects and potential application of β-glucans derived from marine yeast Debaryomyces hansenii in goat peripheral blood leucocytes. **International Journal of Biological Macromolecules**. . ISSN 18790003. (2018). doi: 10.1016/j.ijbiomac.2018.05.061.

MERLY, Liza; SMITH, Sylvia L. - Murine RAW 264.7 cell line as an immune target: are we missing something? **Immunopharmacology and Immunotoxicology**. . ISSN 15322513. (2017). doi: 10.1080/08923973.2017.1282511.

MOHAMED, Rabiatul Manisah; YUSOH, Kamal - A Review on the Recent Research of Polycaprolactone (PCL). **Advanced Materials Research**. (2015). doi: 10.4028/www.scientific.net/amr.1134.249.

MORA-HUERTAS, C. E.; FESSI, H.; ELAISSARI, A. - Polymer-based nanocapsules for drug delivery. **International Journal of Pharmaceutics**. . ISSN 03785173. (2010). doi: 10.1016/j.ijpharm.2009.10.018.

NASROLLAHI, Zahra *et al.* - Functionalized nanoscale β-1,3-glucan to improve Her2 + breast cancer therapy: In vitro and in vivo study. **Journal of Controlled Release**. . ISSN 18734995. (2015). doi: 10.1016/j.jconrel.2015.01.014.

NG, Kee Woei *et al.* - In vivo evaluation of an ultra-thin polycaprolactone film as a wound dressing. **Journal of Biomaterials Science, Polymer Edition**. . ISSN 09205063. (2007). doi: 10.1163/156856207781367693.

NOSS, Ilka *et al.* - Comparison of the potency of a variety of β-glucans to induce cytokine production in human whole blood. **Innate Immunity**. . ISSN 17534259. (2013). doi: 10.1177/1753425912447129.

NOVAK, M.; VETVICKA, V. - β-glucans, history, and the present: Immunomodulatory aspects and mechanisms of action. **Journal of Immunotoxicology**. . ISSN 1547691X. (2008). doi: 10.1080/15476910802019045.

PACHER, Pál; BECKMAN, Joseph S.; LIAUDET, Lucas - Nitric Oxide and Peroxynitrite in Health and Disease. **Physiological Reviews**..ISSN 0031-9333. (2007). doi:10.1152/physrev.00029.2006.

PRADO, Lucas Bessa *et al.* - Characterization of PCL and Chitosan Nanoparticles as Carriers of Enoxaparin and Its Antithrombotic Effect in Animal Models of Venous Thrombosis. **Journal of Nanotechnology**. . ISSN 16879511. (2017). doi: 10.1155/2017/4925495.

POURAHMAD, Jalal; SALIMI, Ahmad - Isolated human peripheral blood mononuclear cell

(PBMC), a cost effective tool for predicting immunosuppressive effects of drugs and Xenobiotics. **Iranian Journal of Pharmaceutical Research**. (2015). ISSN 17266890.

PORTER, Alan L.; YOUTIE, Jan - Where does nanotechnology belong in the map of science? **Nature Nanotechnology**. . ISSN 1748-3387. (2009). doi: 10.1038/nnano.2009.207.

PUPPI, Dario *et al.* - Additive manufacturing of wet-spun polymeric scaffolds for bone tissue engineering. **Biomedical Microdevices**. . ISSN 13872176. (2012). doi: 10.1007/s10544-012-9677-0.

RAY, Paul D.; HUANG, Bo Wen; TSUJI, Yoshiaki - Reactive oxygen species (ROS) homeostasis and redox regulation in cellular signaling. **Cellular Signalling**. . ISSN 08986568. (2012). doi: 10.1016/j.cellsig.2012.01.008.

REES, Peter Adam *et al.* - Chemokines in Wound Healing and as Potential Therapeutic Targets for Reducing Cutaneous Scarring. **Advances in Wound Care**. . ISSN 2162-1918. (2015). doi: 10.1089/wound.2014.0568.

SANDLE, Tim - Endotoxin and pyrogen testing. Em **Pharmaceutical Microbiology**

SANDLE, Tim - **Sterility, sterilisation and sterility assurance for pharmaceuticals: Technology, validation and current regulations**. ISBN 9781907568381.

SATHYAMOORTHY, Nandhakumar *et al.* - Optimization of paclitaxel loaded poly (ε-caprolactone) nanoparticles using Box Behnken design. **Beni-Suef University Journal of Basic and Applied Sciences**. . ISSN 23148535. (2017). doi: 10.1016/j.bjbas.2017.06.002.

SATZER, Peter *et al.* - Protein adsorption onto nanoparticles induces conformational changes: Particle size dependency, kinetics, and mechanisms. **Engineering in Life Sciences**. . ISSN 16182863. (2016). doi: 10.1002/elsc.201500059.

SENA, Laura A.; CHANDEL, Navdeep S. - Physiological roles of mitochondrial reactive oxygen species. **Molecular Cell**. . ISSN 10974164. (2012). doi: 10.1016/j.molcel.2012.09.025.

SINGH, Raman Preet; RAMARAO, Poduri - Accumulated polymer degradation products as effector molecules in cytotoxicity of polymeric nanoparticles. **Toxicological Sciences**. . ISSN 10966080. (2013). doi: 10.1093/toxsci/kft179.

SINGH, Jasvinder *et al.* - Diphtheria toxoid loaded poly-(ε-caprolactone) nanoparticles as mucosal vaccine delivery systems. **Methods**. . ISSN 10462023. (2006). doi: 10.1016/j.ymeth.2005.11.003.

SINGH, Sushant *et al.* - Biodegradable polycaprolactone (PCL) nanosphere encapsulating superoxide dismutase and catalase enzymes. **Applied Biochemistry and Biotechnology**. . ISSN 02732289. (2013). doi: 10.1007/s12010-013-0427-4.

SINHA, V. R. *et al.* - Poly-ε-caprolactone microspheres and nanospheres: An overview. **International Journal of Pharmaceutics**. . ISSN 03785173. (2004). doi: 10.1016/j.ijpharm.2004.01.044.

SHVEDOVA, Anna A.; KAGAN, Valerian E.; FADEEL, Bengt - Close Encounters of the Small Kind: Adverse Effects of Man-Made Materials Interfacing with the Nano-Cosmos of Biological Systems. **Annual Review of Pharmacology and Toxicology**. . ISSN 0362-1642. (2010). doi: 10.1146/annurev.pharmtox.010909.105819.

SONG, Wen Chao - Crosstalk between Complement and Toll-Like Receptors. **Toxicologic Pathology**. . ISSN 15331601. (2012). doi: 10.1177/0192623311428478.

SUBRAMANIAN, Anand; RODRIGUEZ-SAONA, Luis - Fourier Transform Infrared (FTIR) Spectroscopy. Em **Infrared Spectroscopy for Food Quality Analysis and Control**. ISBN 9780123741363.

SUBEDI, Robhash Kusam; KANG, Keon Wook; CHOI, Hoo Kyun - Preparation and characterization of solid lipid nanoparticles loaded with doxorubicin. **European Journal of Pharmaceutical Sciences**. . ISSN 09280987. (2009). doi: 10.1016/j.ejps.2009.04.008.

SUKHANOVA, Alyona *et al.* - Dependence of Nanoparticle Toxicity on Their Physical and Chemical Properties. **Nanoscale Research Letters**. . ISSN 1556276X. (2018). doi: 10.1186/s11671-018-2457-x.

SUN, Lina; ZHAO, Yong - The biological role of dectin-1 in immune response. **International Reviews of Immunology**. ISSN 08830185. 26:5–6 (2007) 349–364.

SUTHERLAND, Ian W. - Microbial polysaccharides from Gram-negative bacteria. Em **International Dairy Journal**

STOPINŠEK, Sanja *et al.* - Fungal cell wall agents suppress the innate inflammatory cytokine responses of human peripheral blood mononuclear cells challenged with lipopolysaccharide in vitro. **International Immunopharmacology**. ISSN 18781705. 11:8 (2011) 939–947.

TAN, Hor Yue *et al.* - The Reactive Oxygen Species in Macrophage Polarization: Reflecting Its Dual Role in Progression and Treatment of Human Diseases. **Oxidative Medicine and Cellular Longevity**. . ISSN 19420994. (2016). doi: 10.1155/2016/2795090.

TANTRA, Ratna; SCHULZE, Philipp; QUINCEY, Paul - Effect of nanoparticle concentration on zeta-potential measurement results and reproducibility. **Particuology**. ISSN 16742001. 8:3 (2010) 279–285.

TAVARES, Marina Rodrigues *et al.* - Surface-coated polycaprolactone nanoparticles with pharmaceutical application: Structural and molecular mobility evaluation by TD-NMR. **Polymer Testing**. . ISSN 01429418. (2017). doi: 10.1016/j.polymertesting.2017.01.032.

TAYLOR, P. R. *et al.* - The -Glucan Receptor, Dectin-1, Is Predominantly Expressed on the Surface of Cells of the Monocyte/Macrophage and Neutrophil Lineages. **The Journal of Immunology**. . ISSN 0022-1767. (2002). doi: 10.4049/jimmunol.169.7.3876.

TESSARI, Paolo *et al.* - Nitric oxide synthesis is reduced in subjects with type 2 diabetes and nephropathy. **Diabetes**. . ISSN 1939327X. (2010). doi: 10.2337/db09-1772.

TUKULULA, Matshawandile *et al.* - Functionalization of PLGA Nanoparticles with 1,3-β-glucan Enhances the Intracellular Pharmacokinetics of Rifampicin in Macrophages. **Pharmaceutical Research**. . ISSN 1573904X. (2018). doi: 10.1007/s11095-018-2391-8.

TUNCEL, Dönüs; DEMIR, Hilmi Volkan - Conjugated polymer nanoparticles. **Nanoscale**. . ISSN 20403364. (2010). doi: 10.1039/b9nr00374f.

UPADHYAY, Tarun K. *et al.* - Preparation and characterization of beta-glucan particles containing a payload of nanoembedded rifabutin for enhanced targeted delivery to macrophages. **EXCLI Journal**. . ISSN 16112156. (2017). doi: 10.17179/excli2016-804.

VÁSQUEZ MARCANO, Rossana Gabriela Del Jesus *et al.* - Chitosan functionalized poly (ε-caprolactone) nanoparticles for amphotericin B delivery. **Carbohydrate Polymers**. . ISSN 01448617. (2018). doi: 10.1016/j.carbpol.2018.08.142.

VITILIC, Ana *et al.* - Evidence for the Modulation of the Immune Response in Peripheral Blood Mononuclear Cells after Stimulation with a High Molecular Weight β-glucan Isolated from *Lactobacillus fermentum* Lf2. **BioRxiv. (2018).** doi: https://doi.org/10.1101/400267

VU-QUANG, Hieu *et al.* - Immune cell-specific delivery of beta-glucan-coated iron oxide nanoparticles for diagnosing liver metastasis by MR imaging. **Carbohydrate Polymers**. . ISSN 01448617. (2012). doi: 10.1016/j.carbpol.2011.08.091.

WANG, Yichao *et al.* - Microencapsulation of nanoparticles with enhanced drug loading for pH-sensitive oral drug delivery for the treatment of colon cancer. **Journal of Applied Polymer Science**. . ISSN 00218995. (2013). doi: 10.1002/app.38582.

WANG, Yu-Feng *et al.* - Food preservation effects of curcumin microcapsules. **Food Control**. ISSN 0956-7135. 27:1 (2012) 113–117.

WOODRUFF, Maria Ann; HUTMACHER, Dietmar Werner - The return of a forgotten polymer - Polycaprolactone in the 21st century. **Progress in Polymer Science (Oxford)**. . ISSN 00796700. (2010). doi: 10.1016/j.progpolymsci.2010.04.002.

WOJDASIEWICZ, Piotr; PONIATOWSKI, Łukasz A.; SZUKIEWICZ, Dariusz - The role of inflammatory and anti-inflammatory cytokines in the pathogenesis of osteoarthritis. **Mediators of Inflammation**. . ISSN 14661861. (2014). doi: 10.1155/2014/561459.

WU, Chin San; LIAO, Hsin Tzu - Polycaprolactone-based green renewable ecocomposites made from rice straw fiber: Characterization and assessment of mechanical and thermal properties. **Industrial and Engineering Chemistry Research**. . ISSN 08885885. (2012). doi: 10.1021/ie202002p.

WU, Chaoxi *et al.* - Synthesis of β-1,3-glucan esters showing nanosphere formation. **Carbohydrate Polymers**. . ISSN 01448617. (2013). doi: 10.1016/j.carbpol.2013.06.056.

XU, Xiaojuan *et al.* - β-glucan from Lentinus edodes inhibits nitric oxide and tumor necrosis factor-α production and phosphorylation of mitogen-activated protein kinases in lipopolysaccharide-stimulated murine RAW 264.7 macrophages. **Journal of Biological Chemistry**. . ISSN 00219258. (2012). doi: 10.1074/jbc.M111.297887.

YU, Mikyung *et al.* - Nanotechnology for protein delivery: Overview and perspectives. **Journal**

of Controlled Release. . ISSN 18734995. (2016). doi: 10.1016/j.jconrel.2015.10.012.

YU, Min *et al.* - Specifically targeted delivery of protein to phagocytic macrophages. **International Journal of Nanomedicine**. . ISSN 11782013. (2015). doi: 10.2147/IJN.S75950.

ZAKIR HOSSAIN, Majed Halwani; KHIYAMI, Mohammad A. - Liposomal ÃÂ²-Glucan: Preparation, Characterization and Anticancer Activities. **Journal of Nanomedicine & Nanotechnology**. (2015). doi: 10.4172/2157-7439.1000319.

ZHAN, Xiao Bei; LIN, Chi Chung; ZHANG, Hong Tao - Recent advances in curdlan biosynthesis, biotechnological production, and applications. **Applied Microbiology and Biotechnology**. ISSN 01757598. 93:2 (2012) 525–53.

ZHAO, Yannan *et al.* - Interaction of mesoporous silica nanoparticles with human red blood cell membranes: Size and surface effects. **ACS Nano**. . ISSN 19360851. (2011). doi: 10.1021/nn103077k.

ZHANG, Ruoran; EDGAR, Kevin J. - Properties, Chemistry, and Applications of the Bioactive Polysaccharide Curdlan. **BioMacromolecules**. (2014).

ZHANG, Mei; KIM, Julian A.; HUANG, Alex Yee Chen - Optimizing tumor microenvironment for cancer immunotherapy: β-Glucan-based nanoparticles. **Frontiers in Immunology**. . ISSN 16643224. (2018). doi: 10.3389/fimmu.2018.00341.

ZHANG, Xu *et al.* - In situ self-assembly of peptides in glucan particles for macrophage-targeted oral delivery. **Journal of Materials Chemistry B**. . ISSN 2050750X. (2014). doi: 10.1039/c4tb00626g.

ZHOU, Jiang-Ling *et al.* - Electrostatic wrapping of doxorubicin with curdlan to construct an efficient pH- responsive drug delivery system. **Nanotechnology**. 28 (2017).